



Comparative morphology of the feeding apparatus of Staphylinine beetles (Coleoptera: Staphylinidae)

Erich L. Spiessberger¹, Alfred F. Newton², Margaret K. Thayer², Oliver Betz¹

¹ *Evolutionary Biology of Invertebrates, Institute of Evolution and Ecology, University of Tübingen, Auf der Morgenstelle 28E, D-72076, Tübingen, Germany*

² *Field Museum of Natural History, Negaunee Integrative Research Center, Life Sciences, 1400 South DuSable Lake Shore Drive, Chicago, IL 60605, USA*

<https://zoobank.org/C1675EF9-AFA2-4EA1-864B-A58EE980DBB9>

Corresponding author: Erich L. Spiessberger (erich.spiessberger@uni-tuebingen.de)

Received 20 October 2023

Accepted 29 December 2023

Published 17 April 2024

Academic Editors Michael Schmitt, Klaus-Dieter Klass

Citation: Spiessberger EL, Newton AF, Thayer MK, Betz O (2024) Comparative morphology of the feeding apparatus of Staphylinine beetles (Coleoptera: Staphylinidae). *Arthropod Systematics & Phylogeny* 82: 267–303. <https://doi.org/10.3897/asp.82.e114508>

Abstract

The mouthparts and protarsi of adult rove-beetles of the Staphylinine group are examined in detail. We provide descriptions and image plates based on scanning electron micrographs taken from 36 species representing all 10 subfamilies comprising this large staphylinid subunit. We establish groundplan features of the mouthparts for the Staphylinine group and discuss, in detail, aspects and functions of structures that compose the feeding apparatus. A phylogenetic scheme is used to conduct an ancestral character reconstruction of the morphological characters. The potential groundplan features of the characters rendered in our parsimony analysis for the Staphylinine group are: labrum subquadrate or longer than wide; mandible without subapical teeth and retinaculum, with prostheca present, not forming lobe-like projection, and with a mola; maxillary palpomere 4 well-developed, fully sclerotized, similar in width to palpomere 3; ‘glossa’ integrated with prementum plate, sometimes represented by pairs of sensilla basiconica; ‘paraglossa’ with unmodified antero-lateral lobes; labial palpomere 3 from as wide to half as wide as penultimate palpomere. To explain the shape variation of the mandibles, a geometric morphometric analysis was carried out. A character mapping analysis of mandible shapes revealed a trend in the Staphylinine group toward a falcate shape with a narrow base, typically present in some predatory species.

Key words

Character mapping, geometric morphometrics, groundplan, mandible, mouthparts, SEM

1. Introduction

The head is the tagma of insects that is responsible, among other functions such as sensing, for food intake. An understanding of this process leads to an understanding of most of an individual’s biology, especially if an organism that has an active predatory lifestyle is under consideration. The apparatus responsible for feeding

is under constant evolutionary pressure and, therefore, under continuing morphological and functional change across time and taxa. Unsurprisingly, the head and associated structures are regular subjects of biological studies, in addition to being a crucial region used for identifying and distinguishing large taxonomic groups

from each other. Morphological studies focusing on the head capsule and associated structures of single species of insects are abundant (e.g., Chaudonneret 1950; Wenk 1953; Mickoleit 1971; Beutel and Vilhelmsen 2007; Beutel and Baum 2008; Beutel et al. 2010; Schneeberg and Beutel 2011; Wipfler et al. 2011; Kubiak et al. 2015; Randolph et al. 2017; Boudinot et al. 2021; Büsse et al. 2021). Naturally, such studies are of extreme importance for improving knowledge about the investigated species. Moreover, hypotheses can be made or conclusions can be drawn for groups that are closely related or with similar habits. However, a comparative study in which multiple species are analyzed in the same context allows better insights into the evolutionary history of a particular group.

Hyperdiverse groups are optimal choices for a detailed comparative investigation, because phenotypic variations can be explored more thoroughly. They offer a plethora of taxonomic entities for an analysis of the phylogenetic nuances of such groups in more detail. Coleoptera, which are the most diverse order of organisms (Bouchard et al. 2017), meet this prerequisite not only by having a great diversity of species, but also by offering a vast number of morphological and behavioral traits that can be investigated.

Many studies focusing on the head and feeding apparatus of single species of Coleoptera have been conducted recently (e.g., Anton and Beutel 2006; Hörnschemeyer et al. 2006; Beutel et al. 2008; Antunes-Carvalho et al. 2017; Yavorskaya et al. 2018a), some of which focus mainly on the ultrastructure of the sensilla of the mouthparts and some functional aspects (e.g., Liu et al. 2019; Hao et al. 2020; Liu and Tong 2023). Staphylinidae, the most diverse family within Coleoptera with more than 66,928 described species (Newton 2022), is the posterchild of many studies of this kind (e.g., Jałoszyński et al. 2020; Beutel et al. 2021; Luo et al. 2021). However, detailed investigation of the feeding apparatus in a comprehensive comparative context (i.e., containing multiple species in the same study) is not as common (e.g., Dressler and Beutel 2010; Yavorskaya et al. 2017; Antunes-Carvalho et al. 2019). Comparative studies dealing with Staphylinidae head morphology have previously been carried out by focusing mainly on the members of the traditional Omaliinae, Tachyporinae, and Oxytelinae groups (Betz et al. 2003; Weide and Betz 2009, 2014; Weide et al. 2010, 2014) and, particularly, on species that are mainly pollen and/or spore feeders. Herein, we present a comparative study of the feeding apparatus of a mostly predatory assemblage, the Staphylinine group.

The Staphylinine group (sensu Lawrence and Newton 1982; Grebennikov and Newton 2009) is composed of 10 subfamilies: Oxyporinae, Megalopsidiinae, Solieriinae, Steninae, Euaesthetinae, Scydmaeninae, Leptotyphlinae, Pseudopsinae, Paederinae, and Staphylininae. Eight of these subfamilies are considered to be predators, with the only exceptions being the Oxyporinae, which are mycophagous (Newton 1984; Leschen and Allen 1988; Thayer 2016), and the Solieriinae, whose feeding habits are currently unknown (Thayer et al. 2012; Thayer 2016).

Despite the abundance of recent studies about the phylogenetic relationships among the subfamilies and tribes of the Staphylinine and related groups (Clarke and Grebennikov 2009; Grebennikov and Newton 2009; Chatzimanolis et al. 2010; Jałoszyński 2014; McKenna et al. 2015; Brunke et al. 2016; Schomann and Solodovnikov 2017; Chani-Posse et al. 2018; Gusarov 2018; Cai et al. 2019; Lü et al. 2020; Tihelka et al. 2020; Żyła and Solodovnikov 2020; Liu et al. 2021; Żyła et al. 2021), the higher phylogeny of this group and Staphylinidae as a whole is far from being fully understood. Gusarov (2018) concluded in his review of recent molecular phylogenetic studies that “Although a few subfamily-level clades within Staphylinidae have been firmly established, the relationships among staphylinid subfamilies remain largely unknown”, and this still holds true. The monophyly of the Staphylinine group has not been supported by many of these studies, especially the molecular studies. However, these studies neither reach a consensus nor correlate directly with each other in a comprehensive way with the purpose of examining the Staphylinine group as a whole. In the absence of such a consensus, Liu et al. (2021) used the Staphylinine group (sensu Grebennikov and Newton 2009) as the framework for their morphological study of fossils of this group, and we do the same here. Our current study extends the phylogenetic discussion by adding morphological characters that are sometimes neglected and aims at contributing to the debate of the relationships within the Staphylinine group and, in a broader sense, within Coleoptera. Although our intention has not been to perform a phylogenetic analysis based on these characters at this time, our character matrix could provide a fresh impetus for later morphology-based phylogenies.

We have investigated 36 species (Table 1) representing all 10 subfamilies comprising the Staphylinine group. Image plates based on scanning electron microscopy followed by detailed descriptions are provided in order to reveal the main differences of the external morphology of the head and mouthparts of the adult beetles of this group. Moreover, we illustrate and describe the protarsi as they play an important role in the predatory hunting styles observed in some species within the Staphylinine group (e.g., Betz and Mumm 2001; Stocker et al. 2022). In addition, we analyze potential groundplan features of the mouthparts of the Staphylinine group. Finally, a geometric morphometric analysis to explain mandible shape variation is performed, and its phylogenetic significance is evaluated via ancestral character state mapping.

We hypothesize that, because of their predominantly predatory behavior, the representatives of the staphylinine subfamilies possess mouthparts for which both the fine structure and the overall arrangement differ from those previously found in the other (less predominantly predaceous) subfamily groups of Staphylinidae. In potential adaptation to certain prey-capture and extra-oral feeding techniques, specific (and highly derived) mouthpart characters can be established that function in both efficient prey-capture and food processing. Suspected specialists on certain prey types show considerable specializations in their mandibles, maxillae, and labium, as shown in

case studies of Scydmaeninae specialized on heavily sclerotized oribatid or uropodine mites (e.g., Jałoszyński 2018) and of Steninae specialized on elusive prey such as springtails (Collembola) (e.g., Betz et al. 2018). We also expect that several character states are of phylogenetic relevance and form potential autapomorphies for defining certain subfamilies or tribes.

2. Materials and methods

2.1. Selection of taxa

Thirty-six species were selected to represent the 10 subfamilies of the Staphylinine group (sensu Lawrence and Newton 1982; Grebennikov and Newton 2009): Oxyporinae, Megalopsidiinae, Solieriinae, Steninae, Euaesthetinae, Scydmaeninae, Leptotyphlinae, Pseudopsinae, Paederinae, and Staphylininae. Therefore, the reader should consider the species limitation of our study when reading the descriptions that represent each family-group or genus. To facilitate reading, a description is sometimes said to be common for a group (e.g., subfamily or genus), but that may not be true for species not investigated herein, unless otherwise clearly stated. A complete list of the species studied is given in Table 1. All specimens of the Staphylinine group were obtained from the alcohol collection of the Field Museum of Natural History (Chicago, USA). The list of outgroup species was based on available unpublished SEM micrographs of OB.

Although the monophyly of the Staphylinine group has recently been questioned (McKenna et al. 2015; Kypke 2018), we here retain this concept for the following reasons. Regarding molecular phylogenies, the relationships among staphylinid subfamilies remain largely unresolved (Gusarov 2018), i.e., no well-resolved phylogenetic scheme is available for use in our character mapping analyses. For example, in McKenna et al. (2015), a polytomy was obtained that includes part of the Staphylinine group, namely the subfamilies Scydmaeninae + Solieriinae, Euaesthetinae + Steninae, Oxyporinae and Leptotyphlinae (called here “Staphylinine 1”) together with clades that include other subfamilies (not considered as part of the Staphylinine group) such as Aleocharinae as sister of Scydmaeninae + Solieriinae, and Osoriinae (in part) + Neophoninae, Dasysericinae, and Pselaphinae. The only group that seems to be consistently recovered as monophyletic is Paederinae + Staphylininae (called here “Staphylinine 2”) (McKenna et al. 2015; Zhang et al. 2018). These findings, however, do not rule out a possible close relationship of “Staphylinine 1” and “Staphylinine 2”, as this has neither been tested properly, nor been the main goal of such analyses. The relationships among the subfamilies that comprise the Staphylinine group cannot be obtained from these sources, even though they are probably not monophyletic, because of the distance of the clades that include “Staphylinine 1” and “Staphylinine 2” shown in McKenna et al. (2015). Zhang et al. (2018) have

recovered some subfamilies (Scydmaeninae, Steninae, Paederinae and Staphylininae) of the Staphylinine group as monophyletic. However, their taxon sampling does not cover all the taxa that are included in McKenna et al. (2015) and that might split them apart. Kypke (2018) used the data set of Zhang et al. (2018) in one of their analyses, recovering the Staphylinine group (represented by Scydmaeninae, Steninae, Paederinae and Staphylininae) as paraphyletic with respect to *Tachinus* (Tachyporine group) and contradicting the results of Zhang et al. (2018), who have recovered *Tachinus* as a sister group of the Staphylinine group. Other than these higher group phylogenies, the most recent molecular studies only deal specifically with Paederinae + Staphylininae or with (sub)tribal classifications within each of these subfamilies (e.g., Brunke et al. 2016; Żyła and Solodovnikov 2020; Żyła et al. 2021). Therefore, to date, the monophyly of the Staphylinine group remains unclear based on molecular studies alone. The study of Grebennikov and Newton (2009) should, however, be mentioned here as it presents a robust morphological phylogeny based not only on adult, but also on larval characters, plus the 18S rDNA nuclear gene. Nonetheless, we recognize the major flaw of their study, a limited taxon sampling, possibly forcing monophyly of the Staphylinine group. Notwithstanding and regardless of the phylogenetic status of the Staphylinine group as a monophyletic unit, the analyses and hypotheses presented here remain useful for an evaluation of the evolution of mouthpart characters of subordinate clades.

2.2. Scanning electron microscopy (SEM) and dissection protocol

The specimens had previously been preserved in 70% ethanol. The head capsule was separated from the prothorax of each specimen. The mouthparts were dissected in distilled water by using fine insect pins and sharpened tungsten wire (Bolte 1996). In paired mouthparts, the left side was chosen, i.e., potential asymmetries between the sides were not considered in this study. The dissected head capsules and mouthparts were cleaned in hydrogen peroxide (Bolte 1996), then stepwise dehydrated in ethanol, and finally critical-point dried (Polaron 3100). The dried samples were fixed to stubs with silver paint, coated with gold (EmitechK 500X), and viewed using a Scanning Electron Microscope (EVO LS 10). Software GIMP 2.10.32 (GPL) was used to edit micrographs and create image plates (Figs 1–11).

2.3. Terminology

The morphological orientation of the mouthparts and their subsets is here given based on the prognathous design of the staphylinid head. Thus, for instance, the distal parts of mouthparts are categorized as anterior. The morphological terminology for the mandible regarding mola, pseudomola, subapical tooth, retinaculum, and prostheca

Table 1. List of species used to prepare SEM micrographs. The last column “#” corresponds to the species numbers of the dots used in the correlation analyses between PCs and inlever/outlever ratios (Fig. 16 and Fig. S1).

Subfamily	Tribe Subtribe	Genus	Species	Country	#
Oxyporinae		<i>Oxyporus</i>	<i>Oxyporus stygicus</i> Say, 1831	USA	24
		<i>Pseudoxyporus</i>	<i>Pseudoxyporus quinquemaculatus</i> LeConte, 1863	USA	32
Megalopsidiinae		<i>Megalopinus</i>	<i>Megalopinus sanguiniriguttatus</i> (Scheerpeltz, 1972)	Chile	23
Solieriinae		<i>Solierius</i>	<i>Solierius obscurus</i> (Solier, 1849)	Chile	35
Steninae		<i>Dianous</i>	<i>Dianous obliquenotatus</i> Champion, 1921	Thailand	13
		<i>Stenus</i>	<i>Stenus puthzianus</i> Rougemont, 1981	Thailand	37
Euaesthetinae	Austroesthetini	<i>Austroesthetus</i>	<i>Austroesthetus passerculus</i> Oke, 1933	Australia	10
	Euaesthetini	<i>Euaesthetus</i>	<i>Euaesthetus iripennis</i> Casey, 1884	USA	16
	Fenderiini	<i>Fenderia</i>	<i>Fenderia chandleri</i> Puthz, 2003	USA	18
	Stenaesthetini	<i>Agnosthaetus</i>	<i>Agnosthaetus cariniceps</i> Bernhauer, 1939	New Zealand	7
Scydmaeninae	Cephenniini	<i>Cephennodes</i>	<i>Cephennodes clavatus</i> (Marsh, 1957)	USA	12
	Eutheini	<i>Veraphis</i>	<i>Veraphis</i> sp.	USA	40
	Mastigini	<i>Palaeostigus</i>	<i>Palaeostigus bifoveolatus</i> (Boheman, 1851)	South Africa	26
	Scydmaenini	<i>Scydmaenus</i>	<i>Scydmaenus</i> sp.	Panama	34
	Stenichnini	<i>Stenichnus</i>	<i>Stenichnus</i> sp.	USA	36
Leptotyphlinae	Neotyphlini	<i>Eutyphlops</i>	<i>Eutyphlops</i> sp.	Chile	17
	Neotyphlini	<i>Homeotyphlus</i>	<i>Homeotyphlus</i> sp.	USA	6
Pseudopsinae		<i>Pseudopsis</i>	<i>Pseudopsis subulata</i> Herman, 1975	USA	31
		<i>Zalobius</i>	<i>Zalobius nancyae</i> Herman, 1977	USA	41
Paederinae	Lathrobiini Astenina	<i>Astenus</i>	<i>Astenus</i> sp.	Mexico	8
	Lathrobiini Lathrobiina	<i>Lathrobium</i>	<i>Lathrobium</i> sp.	USA	21
	Lathrobiini Medonina	<i>Medon</i>	<i>Medon vittatipennis</i> (Fairmaire & Germain, 1862)	Chile	22
	Lathrobiini Stilicina	<i>Stilicoderus</i>	<i>Stilicoderus woodwardi</i> (Rougemont, 1986)	Australia	38
	Paederini Dicaxina	<i>Baryopsis</i>	<i>Baryopsis</i> sp.	Chile	11
	Paederini Dolicaonina	<i>Gnathymenus</i>	<i>Gnathymenus</i> sp.	Chile	19
	Paederini Cryptobiina	<i>Homaeotarsus</i>	<i>Homaeotarsus bicolor</i> (Gravenhorst, 1802)	USA	20
	Paederini Paederina	<i>Paederus</i>	<i>Paederus littoralis</i> Gravenhorst, 1802	USA	25
	Pinophilini Pinophilina	<i>Pinophilus</i>	<i>Pinophilus parvus</i> LeConte, 1863	USA	28
Staphylininae	Diochini	<i>Diochus</i>	<i>Diochus schaumii</i> Kraatz, 1860	USA	14
	Othiini	<i>Atrecus</i>	<i>Atrecus punctiventris</i> (Fall, 1901)	USA	9
	Platyprosopini	<i>Platyprosopus</i>	<i>Platyprosopus</i> sp.	South Africa	30
	Staphylinini Erichsoniina	<i>Erichsonius</i>	<i>Erichsonius patella</i> (Horn, 1884)	USA	15
	Staphylinini Philonthina	<i>Philonthus</i>	<i>Philonthus politus</i> (Linnaeus, 1758)	USA	27
	Staphylinini Quediina	<i>Quedius</i>	<i>Quedius capucinus</i> (Gravenhorst, 1806)	USA	33
	Staphylinini Staphylinina	<i>Platydracus</i>	<i>Platydracus femoratus</i> (Fabricius, 1801)	Belize	29
	Xantholinini	<i>Thyrecephalus</i>	<i>Thyrecephalus albertisi</i> (Fauvel, 1877)	USA	39
Outgroup taxa					
Tachyporinae		<i>Tachinus</i>	<i>Tachinus fumipennis</i> (Say, 1832)	USA	5
Oxytelinae		<i>Anotylus</i>	<i>Anotylus</i> sp.	USA	2
Omaliinae		<i>Eusphalerum</i>	<i>Eusphalerum pothos</i> (Mannerheim, 1843)	USA	3
Agryrtidae		<i>Necrophilus</i>	<i>Necrophilus hydrophiloides</i> Guérin-Méneville, 1835	USA	4
Leiodidae		<i>Agathidium</i>	<i>Agathidium oniscoides</i> Palisot de Beauvois, 1805	USA	1

follows the definitions provided in Betz et al. (2003). The incisor area of mandible (cf. prosthema, retinaculum, and subapical tooth in Betz et al. 2003) is the inner continuous curvature from the apex (incisor) to its end or change of course, usually attributable to the presence of a retinaculum or a prosthema. It is also the region in which the subapical tooth (if present) is located. The labium-hypopharynx complex is mainly formed by the prementum distally and the hypopharynx posterodorsally, usually more proximally; a membranous joint is present between these two parts, enabling different degrees of movement, depending on the species (cf. Weide and Betz 2009). The

labium is composed of submentum, mentum (neither investigated in the present study) and prementum, the latter bearing distally a pair of labial palps (Snodgrass 1993). The paired ‘glossae’ lie between the palps, and the paired ‘paraglossae’ are located lateral to the ‘glossae’ (cf. Böving and Craighead 1931; Blackwelder 1936; Betz 1996). The ‘glossae’ can be modified into lobes that are usually covered with sensilla coeloconica or are integrated with the prementum and represented externally only by pairs of sensilla basiconica. The ‘paraglossae’ can be represented by (1) unmodified antero-lateral lobes of the prementum, (2) anterior digitiform lobes, or (3) adhesive pads.

Since many authors consider the ‘glossa’ and ‘paraglossa’ to be lacking or completely reduced in Coleoptera (e.g., Crowson 1981; Beutel and Lawrence 2016), we use these terms in quotation marks throughout the text; see more in the Discussion section. The hypopharynx is integrated into the dorsal face of the mentum and submentum posterior to (= proximal to) the prementum. In most cases, a clear delimitation is caused by the anterior part of the hypopharynx being less sclerotized than the prementum, by its bearing of different kinds of trichomes, or by being clearly more membranous when it is glabrous.

In the description of the protarsus below we also include the propretarsus (to which, e.g., the claws belong), while acknowledging that the pretarsus is a podomere separate from the tarsus.

2.4. Homologizing substructures of the mandible

Some substructures of the mandible are problematic to homologize across different taxa when many different studies from a wide variety of groups are considered. The inconsistent use of the terms prostheca and mola or the teeth occurring at the incisor area of the mandible or further proximal to it (here treated as subapical tooth and retinaculum, respectively) causes potential problems in how to correctly homologize these substructures. Indeed, a great variation in the form and position of such substructures is present across clades, one possible reason being as follows, with the maxilla being used as an example from an embryological perspective. Whereas the embryonic development of the maxilla supports the division of true distinct endite regions (lacinia and galea) (Coulcher and Telford 2013), the developmental biology of the mandible does not. Both the incisor and the mola (or the molar region in cases when a proper mola is absent) are derived from only one endite (Coulcher and Telford 2013), some substructures between those such as the mandibular teeth or the prostheca are then less obvious to homologize across different taxa. The maxilla, on the other hand, bears two endites that can be more easily homologized with the lacinia and the galea in different taxa (Coulcher and Telford 2013). Nevertheless, although evolutionary developmental biology does not yet provide clues for homologizing the specific structures found at the medial (cutting) edge of the mandible, structures such as the incisor, subapical tooth, prostheca, and mola might be homologizable across staphylinine group members according to their position and specific quality. Only in some species (i.e., Paederinae and Staphylininae) is a distinction between subapical tooth and retinaculum doubtful, and hence, we have treated a structure as a subapical tooth only if it is integrated with the incisor cutting surface (e.g., Fig. 3E). Once such a tooth is positioned beyond this area (usually originating from a more basal region of the mandible (e.g., Fig. 3G)) and more separated from the mandibular apex, we have treated it as a retinaculum. Prostheca and retinaculum have been distinguished via their appearance, i.e., a (semi-)membranous region covered by a row or a brush of

trichomes versus a well-sclerotized tooth-like structure, although they might be developmentally homologous, representing two facets of the same structure, and sometimes co-occurring in one mandible. Further studies to establish the homology of prostheca-like structures across Pterygota are required (Richter et al. 2002).

2.5. Character mapping analysis

To illustrate the evolutionary history of discrete mouthpart characters, we created a phylogenetic scheme (used in Figs 12, 14 and 15) based on previously published studies. Since the relationships within the Staphylinidae are far from being resolved, we chose the classic definition of the Staphylinine group based on the work of Lawrence and Newton (1982), with the additions made by Grebennikov and Newton (2009). For the relationships within the Staphylinine group at the subfamily level, we used mainly Grebennikov and Newton (2009) as a reference, despite the Solieriinae relationships presented being unresolved, and therefore we followed Żyła et al. (2017) who placed the Solieriinae as a sister group to the Scydmaeninae + (Steninae + Euaesthetinae). For relationships within the subfamilies, we used the following references: Euaesthetinae (Clarke and Grebennikov 2009), Scydmaeninae (Yin et al. 2019), Paederinae (Żyła et al. 2021), and Staphylininae (Tihelka et al. 2020, also see Boudinot et al. 2023 for analytical flaws on this study). As outgroup taxa, we chose the following species from Betz et al. (2003): *Anotylus* sp. (Oxytelinae, Staphylinidae), *Eusphalerum pothos* (Mannerheim, 1843) (Omaliinae, Staphylinidae), *Tachinus fumipennis* (Say, 1832) (Tachyporinae, Staphylinidae), *Agathidium oniscoides* Palisot de Beauvois, 1805 (Leiodidae), and *Necrophilus hydrophiloides* Guérin-Méneville, 1835 (Agyrtidae). To score the character states of the outgroup taxa, we used as source literature mainly Betz et al. (2003), plus Wheeler and Miller (2005) for *A. oniscoides* and Grebennikov and Newton (2009) for *N. hydrophiloides*.

The ancestral character mapping for discrete (Fig. 12) and continuous character states (Figs 14, 15) based on maximum parsimony was prepared using the software Mesquite 3.61 (Maddison and Maddison 2019). The character matrix (Table S1) used in the analysis displayed in Fig. 12 was prepared based on a set of characters and their states derived from the morphological findings and listed in section 3.2. All schemes (Figs 12, 14, 15) were edited on Inkscape 1.2. (GPL) (Fig. 12 was first imported to FigTree v1.4.4 (Rambaut and Drummond 2016) and then exported to Inkscape 1.2.).

2.6. Geometric morphometrics

For the recording of (semi-)landmarks with tpsDig2 2.32 (Rohlf 2015), we followed the protocol of Stocker et al. (2022), which we adapted to our data (see landmarks added to the consensus shape in Fig. 13). Whereas the data generated herein were used for landmark placement

for the ingroup, we used unpublished SEM data from OB for the outgroup; one specimen per species was used in this analysis (Table 1). As the data presented here are morphologically diverse, the homology of some sites was not possible to establish. We therefore discarded landmarks 3–5 used by Stocker et al. (2022), and hence, their landmark number 6 corresponds to our landmark number 3 and so on up until their landmark number 9, which corresponds to our landmark number 6. Following this adaptation, our semilandmarks are then placed between 3 and 4 and between 4 and 5. Mandible shapes were compared using tpsRelw 1.75 (Rohlf 2015). A principal component analysis (PCA) was carried out using tpsRelw from which the deformation grid presented in Fig. 13 was obtained. Another PCA was performed using the software PAST 4.03 (Hammer et al. 2001) to obtain the morphospace and convex hulls presented in Fig. 13. A list showing the values of the principal components (PC) 1 and 2 of each species is shown in Table S2. The final image montage (Fig. 13) was created using Inkscape 1.2, the data obtained from both tpsRelw and PAST being combined therein. The Eigenvalues and explained percentage of variance of principal components 1 and 2 are shown in Table S3.

In addition, we analyzed the PCA scores as a continuous variable in Mesquite 3.61 (Maddison and Maddison 2019) and performed an ancestral character mapping analysis. The analyses of PC 1 and 2 that are illustrated in Figs 14 and 15 show the distribution of the mandible shapes across taxa and the evolutionary history of this character based on the phylogenetic scheme created for the current study. The hypothetical mandible shapes were obtained from tpsRelw 1.75. The final image montages (Figs 14, 15) were created using Inkscape 1.2, the data obtained from both tpsRelw and Mesquite being combined therein.

Mahalanobis distances (Table 2) were calculated using a canonical variate analysis (CVA) with 1,000,000 permutations in MorphoJ 1.07a (Klingenberg 2011) to quantify the separation between the subfamilies.

2.7. Lever calculations

Lever arm lengths were measured using distances between landmarks. Two levers were measured: the inlever, which is defined as the shortest distance between the ventral mandibular condyle (landmark 1, see Fig. 13) and the insertion region of the mandibular adductor muscle (*Musculus craniomandibularis internus*) (landmark 2, see Fig. 13), and the outlever, defined as the shortest distance between the ventral mandibular condyle (landmark 1, see Fig. 13) and the mandibular apex (landmark 4, see Fig. 13). The ratio between the in- and the outlever can be used to interpret the relative force output at the tip of the mandible, i.e., smaller ratios between in- and outlever mean smaller force outputs, whereas larger ratios mean larger outputs. This ratio is also referred to as the “mechanical advantage” by some authors (e.g., Weihmann et al. 2015; Blanke 2019). According to the general force-velocity

trade-off inherent to lever systems, this quotient is also indicative of the kinematic transmission, i.e., lower values correlate with relatively fast-closing mandibles and vice versa (e.g., Weihmann et al. 2015).

A list with the ratio between the in- and outlever can be found in Table S4. Measurements were taken using tpsDig2 2.32 (Rohlf 2015) and with the same landmarks as those in the geometric morphometrics analysis being employed as a reference. For the ingroup, the data generated herein were used as a reference for landmark placement and measurements, whereas for the outgroup, we employed unpublished data from OB; one specimen per species was used in this analysis (Table 1).

2.8. Statistics

Two statistical correlation analyses were performed to test for any relationship between the log-transformed mandibular shape variables (PC 1, PC 2) and the inlever/outlever ratio of the mandibles. The numerical value of 2 was added to each PC value before logarithmization to avoid negative values. These analyses were performed in SPSS (IBM SPSS Statistics; Version 28 (IBM, Armonk, NY, USA)). To take into account phylogenetic non-independence of the data points, these analyses were repeated using phylogenetic independent contrasts that were calculated using the “ape” package (version 5.7-1). In this case, Pearson correlations were calculated using the “Hmisc” package (version 5.0-1) in RStudio (version 2023.3.0.386, Posit team 2023) using R (version 4.3.0, R Core Team 2023).

3. Results

The following results are given as descriptions and image plates based on SEM micrographs of the: labrum-epipharynx (Figs 1, 2), mandible (Figs 3, 4), maxilla (Figs 5–7), labium-hypopharynx (Figs 8, 9), and protarsus (Figs 10, 11).

The protarsus is considered in the present study, in addition to the mouthparts, because of its observed importance in the predatory feeding systems of some *Philonthus* spp. and other genera (Betz and Mumm 2001; Barthold and Betz 2020; Stocker et al. 2022). However, we did not study other parts of the legs or other tarsi, because the protarsus is more likely to be the one used (if used at all) to capture and / or manipulate prey. Additionally, as we did not record the sex of the specimens, we could not establish possible sexual dimorphism such as occurs in related groups, e.g., the Leiodidae (Gnaspini et al. 2017).

The descriptions below relate only to the material analyzed in this study (Table 1) and therefore should not be considered a general description of the respective taxa. The genera used in this study are given below, within each subtopic, between parentheses (for the full scientific names of the taxa, see Table 1).

3.1. Mouthparts and protarsi description of the Staphylinine group

3.1.1. Staphylinine group

Labrum. Variable, asymmetrical, bifurcate, subquadrate, or transverse. Epipharynx glabrous to densely covered with trichomes, forming bristle-trough or not, sometimes covered with sensilla.

Mandible. Variable in shape; subapical tooth, retinaculum and prosthema absent or present, forming lobe-like structure or not; mola-like structure usually absent, present only in a few groups (*Oxyporinae*, *Solieriinae*, *Scydmaeninae*, *Pseudopsis*, and *Diochus*).

Maxilla. With cardo transverse. Stipes subdivided into basi- and mediostipes, the latter forming the base for both galea and lacinia. Lacinia fused with mediostipes. Galea inserted at mediostipes between lacinia and palpifer. Palpifer distinct, at base of maxillary palps, or also at base of galea (*Megalopinus*). Palpi consisting of 4 palpomeres.

Labium-hypopharynx. Prementum covered laterally with spine- or hair-like trichomes, glabrous medially or covered with sensilla. Distally with pair of ‘glossae’, ‘paraglossae’, and labial palpi consisting of 3 palpomeres. ‘Glossae’ usually reduced and integrated into prementum (*Oxyporinae*, *Megalopsidiinae*, *Solieriinae*, *Steninae*, *Euaesthetinae*, *Scydmaeninae*, *Zalobius*) and represented by sensilla trichodea or basiconica, or ‘glossae’ modified into medial lobes (*Leptotyphlinae*, *Pseudopsis*, *Paederinae*, and *Staphylininae*) that vary in form, usually covered with sensilla coeloconica. ‘Paraglossae’ unmodified antero-lateral lobes or modified into anterior digitiform lobes (*Agnosthaetus* and *Austroesthetus*) or modified into adhesive pads (*Stenus*). The base of the prementum is connected to the distal hypopharynx, with a transverse suture separating them.

Protarsus. Usually consisting of 5 tarsomeres (except in *Leptotyphlinae*, consisting of 3, and the *Euaesthetinae* genera *Austroesthetus* and *Euaesthetus*, consisting of 4), always with symmetrical pair of claws on pretarsus. Tarsal setae present on the ventral region can be divided into two major groups, i.e., unmodified hair-like (sometimes spine-like, a difference not taken into consideration in this context) or modified into a widened adhesive pad, covered by tenent setae. There is a great variety of tarsal setae with potential phylogenetic value; however, this is not within the scope of this study (for more information about tarsal seta types, see, for example, Stork 1980, Betz 2003, and Gnaspini et al. 2017). The overall width of each tarsomere is considered, and two main kinds are given: (1) slender, bearing spine- and/or hair-like setae, and (2) widened bilobed, bearing distally widened (tenent) setae, usually spatulate and/or discoid in shape.

3.1.2. *Oxyporinae* (*Oxyporus*, *Pseudoxyporus*)

Labrum (Fig. 1A, B). Asymmetrical, longer than wide, and strongly emarginate. Epipharynx flat, without furrow, covered by mesally directed hair- and scale-like

trichomes; prominent dense medial tuft of posteriorly directed hair-like trichomes.

Mandible (Fig. 3A, B). Somewhat broadened at base, blade-like shape, only slightly curved. Subapical tooth absent, incisor area smooth. Retinaculum absent. Small tooth-like projection (with unclear homology) present at outer rim of mandible. Prosthema present, not forming lobe-like projection, arising from elongate ledge-like inner margin, composed of brush-like fringe of fimbriate hair-like trichomes along medial margin. Mola present, forming a broad surface provided with grinding surface resembling a nipple-carpet (*Pseudoxyporus*) or an almost flat surface studded with faint ridges (*Oxyporus*); partially surrounded by trichomes of prosthema.

Maxilla (Fig. 5A). Lacinia extending toward half the length of galea; from base nearly to apex densely covered with anteriorly directed short straight hair-like trichomes. In apical region, meso-posteriorly directed curved bristle-like trichomes present. Galea elongated, subequal to lacinia, reaching more than half length of second palpomere and bearing robust brush of posteriorly curved bristle-like trichomes. Apical palpomere longer than and similar in width to preceding one.

Labium-hypopharynx (Fig. 8A). Prementum strongly bilobed and dorsally, along lateral margins, with prominent dense fringe of mesally directed hair-like trichomes; without spine-like trichomes, densely covered medially with carpet of cone-shaped trichomes. Palps directed distad, palpomere 3 distinctly enlarged, flattened and strongly securiform. Ligula consisting of paired ‘glossae’ and ‘paraglossae’; ‘glossae’ represented by two pairs of sensilla trichodea; ‘paraglossae’ represented by well-developed antero-lateral lobes of prementum. Hypopharynx distally covered with arrays of mesally directed hair-like trichomes. Proximally, antero-lateral directed hair-like trichomes, forming a medial tuft.

Protarsus (Fig. 10A, B): Consisting of 5 tarsomeres, all slender and subequal in width. Tarsomeres bearing spine-like setae laterally and medially glabrous in *Oxyporus* or hair-like setae completely covering tarsomeres 1–4 ventrally and 5 laterally in *Pseudoxyporus*.

3.1.3. *Megalopsidiinae* (*Megalopinus*)

Labrum (Fig. 1C). Longer than wide, strongly bifurcate, bearing row of long hair-like setae anteriorly and along inner margins of labral lobes. Lateral lobes bearing longer hair-like setae at tips. Epipharynx flat, without furrow, glabrous, except for margins of lateral lobes.

Mandible (Fig. 3C). Broad at base and acute at apex, strongly curved medially near apex. Incisor area without subapical teeth. Retinaculum present with only weakly developed teeth-like protrusions. Prosthema absent. Mola absent. Distinct concave area covered with proprioceptive setae near ventral mandibular condyle.

Maxilla (Fig. 5B). Lacinia reaching to apical part of galea, bearing few rows of hair- and bristle-like trichomes, basal half with straight trichomes antero-medially directed, apical half with curved trichomes medially directed, unarticulated spine present apically. Galea elongated,

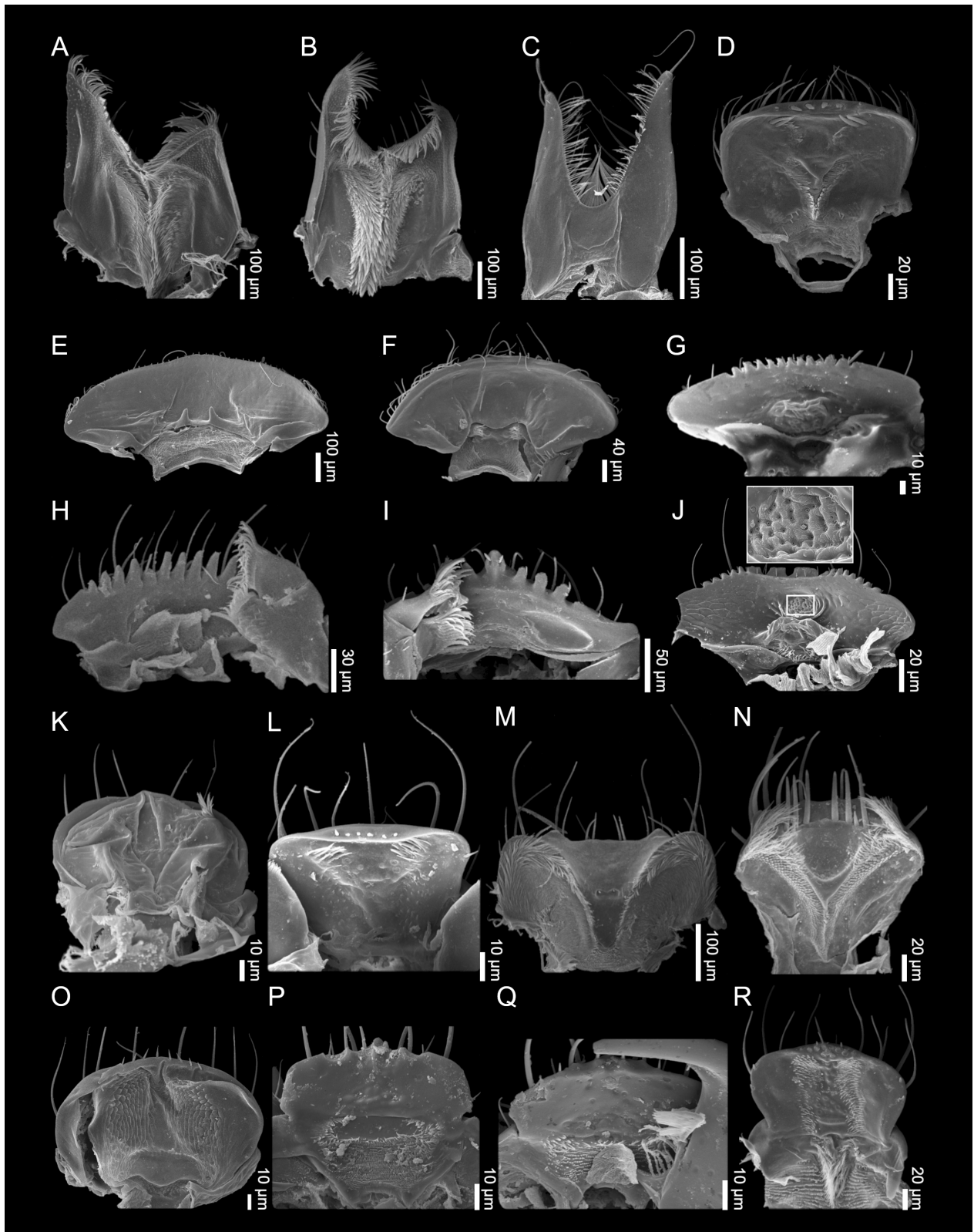


Figure 1. Labrum-epipharynx (ventral aspect), SEM micrographs: **A** *Oxyporus stygicus*, **B** *Pseudoxyporus quinquemaculatus*, **C** *Megalopinus sanguiniriguttatus*, **D** *Solierius obscurus*, **E** *Dianous obliquenotatus*, **F** *Stenus puthzianus*, **G** *Austroesthetus passerculus*, **H** *Euaesthetus iripennis*, **I** *Fenderia chandleri*, **J** *Agnosthaetus cariniceps*, **K** *Cephennodes clavatus*, **L** *Veraphis* sp., **M** *Palaeostigus bifoveolatus*, **N** *Scydmaenus* sp., **O** *Stenichnus* sp., **P** *Eutyphlops* sp., **Q** *Homeotyphlus* sp., **R** *Pseudopsis subulata*.

more than half of lacinia length, reaching base of third maxillary palpomere; bearing brush of antero-mesally directed hair- and bristle-like trichomes. Apical palpomere longer than and similar in width to preceding one.

Labium-hypopharynx (Fig. 8B). Prementum dorsally along lateral margins with dense fringe of mesally directed hair-like trichomes; innermost row of these lateral fringes differentiated into spine-like trichomes, me-

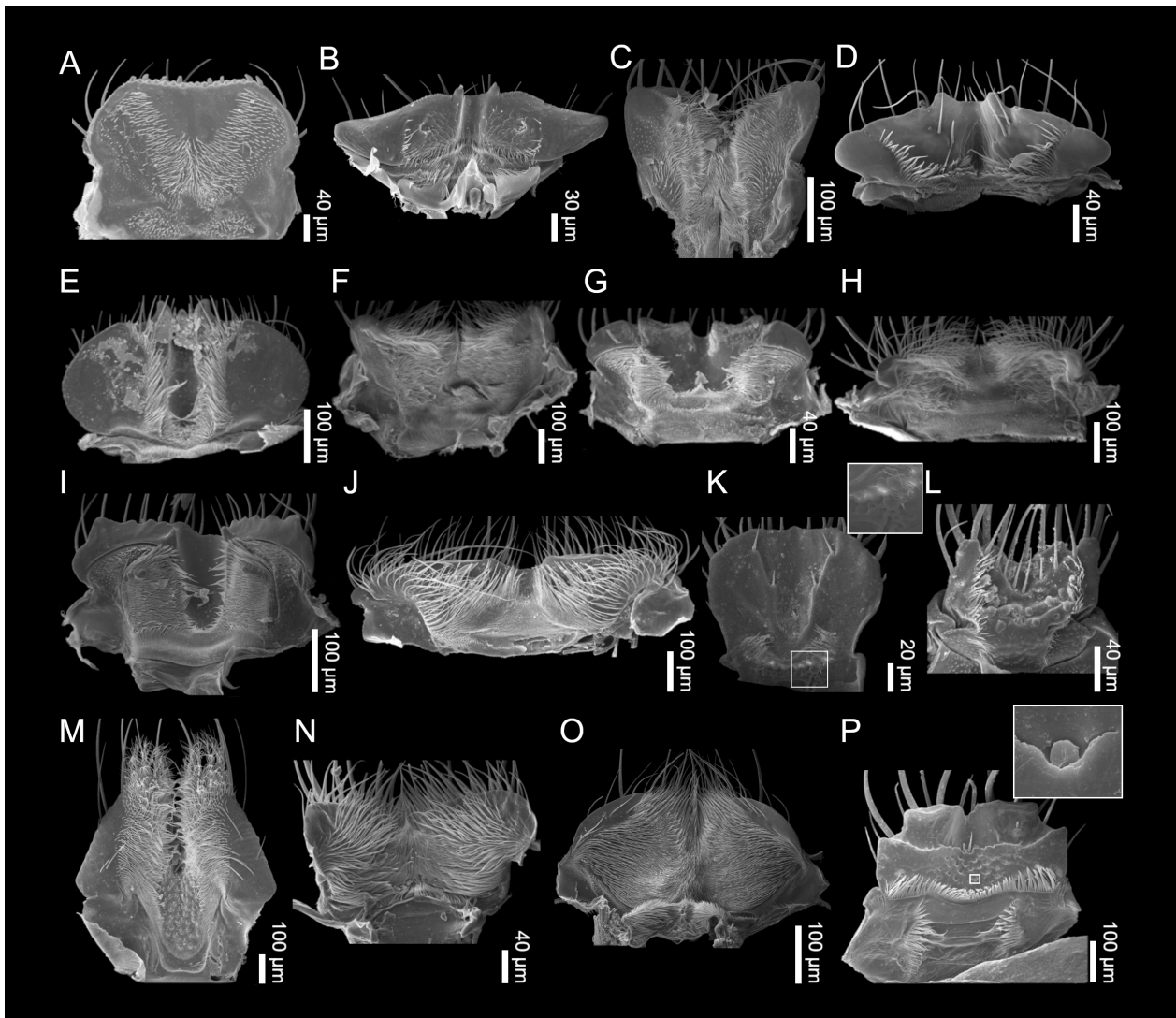


Figure 2. Labrum-epipharynx (ventral aspect), SEM micrographs: **A** *Zalobius nancyae*, **B** *Astenus* sp., **C** *Lathrobium* sp., **D** *Medon vittatipennis*, **E** *Stillicoderus woodwardi*, **F** *Baryopsis* sp., **G** *Gnathymenus* sp., **H** *Homaeotarsus bicolor*, **I** *Paederus littoralis*, **J** *Pinophilus parvus*, **K** *Diochus schaumii*, **L** *Atrecus punctiventris*, **M** *Platyprosopus* sp., **N** *Erichsonius patella*, **O** *Philonthus politus*, **P** *Thyrecephalus albertisi*.

dial surface glabrous. Palpomere 3 slightly wider than palpomere 2. Ligula consisting of paired ‘glossae’ and ‘paraglossae’; ‘glossae’ represented by pairs of sensilla basiconica; ‘paraglossae’ represented by well-developed antero-lateral lobes of prementum. Hypopharynx dorsally along lateral margins with short mesally directed hair-like trichomes. Medially glabrous, but distally covered with loose series of proximally directed bristle-like trichomes. **Protarsus** (Fig. 10C). Consisting of 5 tarsomeres, all slender and subequal in width. Tarsomeres loosely covered with spine- and hair-like setae, more densely so toward basal tarsomeres.

3.1.4. Solieriinae (*Solierius*)

Labrum (Fig. 1D). Subquadrate with anterior margin not bilobed. Epipharynx flat without furrow, mostly glabrous, but with two pairs of obliquely anteriorly directed prominent bristle-like sensilla distally. With larger two pairs of sensilla at anterior rim. Mesally directed hair-

like trichomes medially forming loose rows and small brush toward base. Rows of posteriad-directed hair-like trichomes proximally.

Mandible (Fig. 3D). Strongly broadened at base, acute at apex. Incisor area with subapical tooth. Retinaculum absent. Prostheca present, not forming lobe-like projection, short, bearing brush-like fringe of fimbriate hair-like trichomes. Mola present, forming smooth flat surface.

Maxilla (Fig. 5C). Lacinia reaching to apical part of galea; bearing rows of antero-medially directed bristle-like trichomes, restricted to apical half of lacinia, multi-branched unarticulated structure present apically. Galea length subequal to lacinia, reaching second palpomere; apex bearing rows of anteriorly directed bristle-like trichomes. Apical palpomere reduced and conical.

Labium-hypopharynx (Fig. 8C). Prementum slightly bilobed and dorsally along lateral margins with parallel continuous fringes of mesally directed comb-like trichomes; without spine-like trichomes, medially glabrous. Palpomere 3 distinctly thinner than palpomere 2. Ligula

consisting of paired ‘glossae’ and ‘paraglossae’; ‘glossae’ represented by pair of sensilla trichodea; ‘paraglossae’ represented by antero-lateral lobes of prementum. Hypopharynx dorsally covered with mesally directed hair-like trichomes forming a medial tuft.

Protarsus (Fig. 10D). Consisting of 5 tarsomeres, all slender and subequal in width. Tarsomeres covered with hair-like setae.

3.1.5. Steninae (*Dianous*, *Stenus*)

Labrum (Fig. 1E, F). Strongly transverse, with anterior margin not bilobed. Epipharynx flat, without furrow, mainly glabrous with two thorn-like projections at proximal margin (*Dianous*). Distinct separate plate proximally covered with campaniform sensilla, with antierad-directed hair-like trichomes (*Dianous*), or with only few lateral patches of hair-like trichomes (*Stenus*).

Mandible (Fig. 3E, F). Slender and of falciform shape. Incisor area with subapical tooth with serrate inner margin (*Stenus*) or not (*Dianous*). Retinaculum, prosthema and mola absent.

Maxilla (Fig. 5D). Lacinia reaching to nearly the apical part of galea; bearing a brush of curved bristle- and hair-like trichomes, ventral fringe anteriorly directed and dorsal fringe postero-medially directed (*Dianous*) or basal half with straight antero-medially directed trichomes and apical half of curved postero-medially directed trichomes (*Stenus*). Galea length subequal to lacinia, reaching first palpomere; bearing dense brush of curved bristle- and hair-like posteriorly directed trichomes. Apical palpomere vestigial and peg-like.

Labium-hypopharynx (Fig. 8D). In *Dianous*, prementum dorsally along lateral margins with dense fringe of meso-anteriorly directed hair-like trichomes, without lateral spine-like trichomes; medially covered with anteriorly directed spine-like setae. Palpomere 3 distinctly thinner than palpomere 2. In *Stenus* (the typical strikingly distinct elongated rod-like prementum is present, the distal part is however similar and comparable to the other investigated genera), prementum dorsally along lateral margins with rows of short bristle-like trichomes, becoming longer on the innermost margin, without lateral spine-like trichomes; single longitudinal row of spine-like setae is present medially. Ligula consisting of paired ‘glossae’ and ‘paraglossae’; ‘glossae’ represented by two pairs of sensilla trichodea; ‘paraglossae’ represented by antero-lateral lobes of prementum, more prominently so in *Stenus*, which bears ventrally specialized sticky pads covered with adhesive trichomes. Hypopharynx in *Dianous* dorsally along lateral margins with mesally directed hair-like trichomes. Medially provided with dense vestiture of antierad-directed hair-like trichomes forming medial tuft and glabrous proximally or with only few scattered short hair-like trichomes. In *Stenus*, the hypopharynx sits on the base of the membranous arthroal membrane of the elongated labium, forming a roof-shaped fold directed away from the mouth opening and covered by antero-mesally directed scale-like trichomes. Distally, it runs out into two folds that border the recess of the hypopharynx laterally

and that are also occupied by anteriorly directed scale-like trichomes. SEM images of different species of *Stenus* labium and hypopharynx are presented in Betz (1996).

Protarsus (Fig. 10E, F). Consisting of 5 tarsomeres; tarsomeres (especially the antepenultimate and the penultimate ones), apart from the tarsi shown here, can vary from slender and weakly bilobed to wide and bilobed. Great species-specific diversity in number and shape of tarsal tenent setae has been recorded (Betz 2003; Betz et al. 2018).

3.1.6. Euaesthetinae (*Austroesthetus*, *Euaesthetus*, *Fenderia*, *Agnosthaetus*)

Labrum (Fig. 1G–J). Strongly transverse, anterior margin denticulate with prominent teeth. Epipharynx flat, without furrow, glabrous. Medial membranous field bearing sensilla and / or gland openings present. Pair of concavely dented fields present proximally in *Fenderia*.

Mandible (Fig. 3G–J). Slender and moderately curved. Incisor area without subapical tooth. Retinaculum present, with (*Euaesthetus*) or without serrate inner margin (*Austroesthetus*, *Agnosthaetus*, *Fenderia*). Prosthema and mola absent.

Maxilla (Fig. 5E, F). Lacinia with corrugated ventral surface, almost completely divided from mediostipes; reaching half-length of galea; bearing brush of posteriorly curved bristle-like trichomes. Galea length subequal to lacinia, reaching second palpomere; apico-mesally covered by posteriorly directed curved bristle-like trichomes; distinct spine on lateral margin in *Agnosthaetus*. Apical palpomere vestigial and peg-like.

Labium-hypopharynx (Fig. 8E–H). Prementum deeply emarginate anteriorly (*Austroesthetus*, *Agnosthaetus*, and *Fenderia*) or not (*Euaesthetus*), and dorsally along lateral margins with dense fringe of mesally directed hair- and spine-like trichomes (*Austroesthetus*, *Agnosthaetus*, *Euaesthetus*) or with non-continuous fringe of mesally directed comb-like trichomes (*Fenderia*); medially glabrous. Palpomere 3 peg-like, distinctly thinner than palpomere 2. Ligula consisting of paired ‘glossae’ and ‘paraglossae’; ‘glossae’ represented by pair of sensilla trichodea, present medially (*Euaesthetus* and *Fenderia*) or shifted laterad toward inner margins of ‘paraglossal’ digitiform lobes (*Austroesthetus* and *Agnosthaetus*); ‘paraglossae’ represented by unmodified antero-lateral lobes of prementum (*Euaesthetus* and *Fenderia*) or sometimes modified into digitiform lobes (*Austroesthetus* and *Agnosthaetus*). Hypopharynx dorsally along lateral margins with mesally directed hair-like trichomes. Medially glabrous.

Protarsus (Fig. 10G–J). Consisting of 5 tarsomeres in *Agnosthaetus* and *Fenderia*, and 4 in *Austroesthetus* and *Euaesthetus*; all tarsomeres slender and subequal in width. Tarsomeres covered with spine- and hair-like setae in *Euaesthetus* and *Agnosthaetus*. In *Austroesthetus* and *Fenderia*, tarsomeres are glabrous medially and bear lateral rows of spine- and hair-like setae. In *Fenderia*, the first two tarsomeres are covered medially with distinct discoid tenent setae. *Austroesthetus* and *Fenderia* have

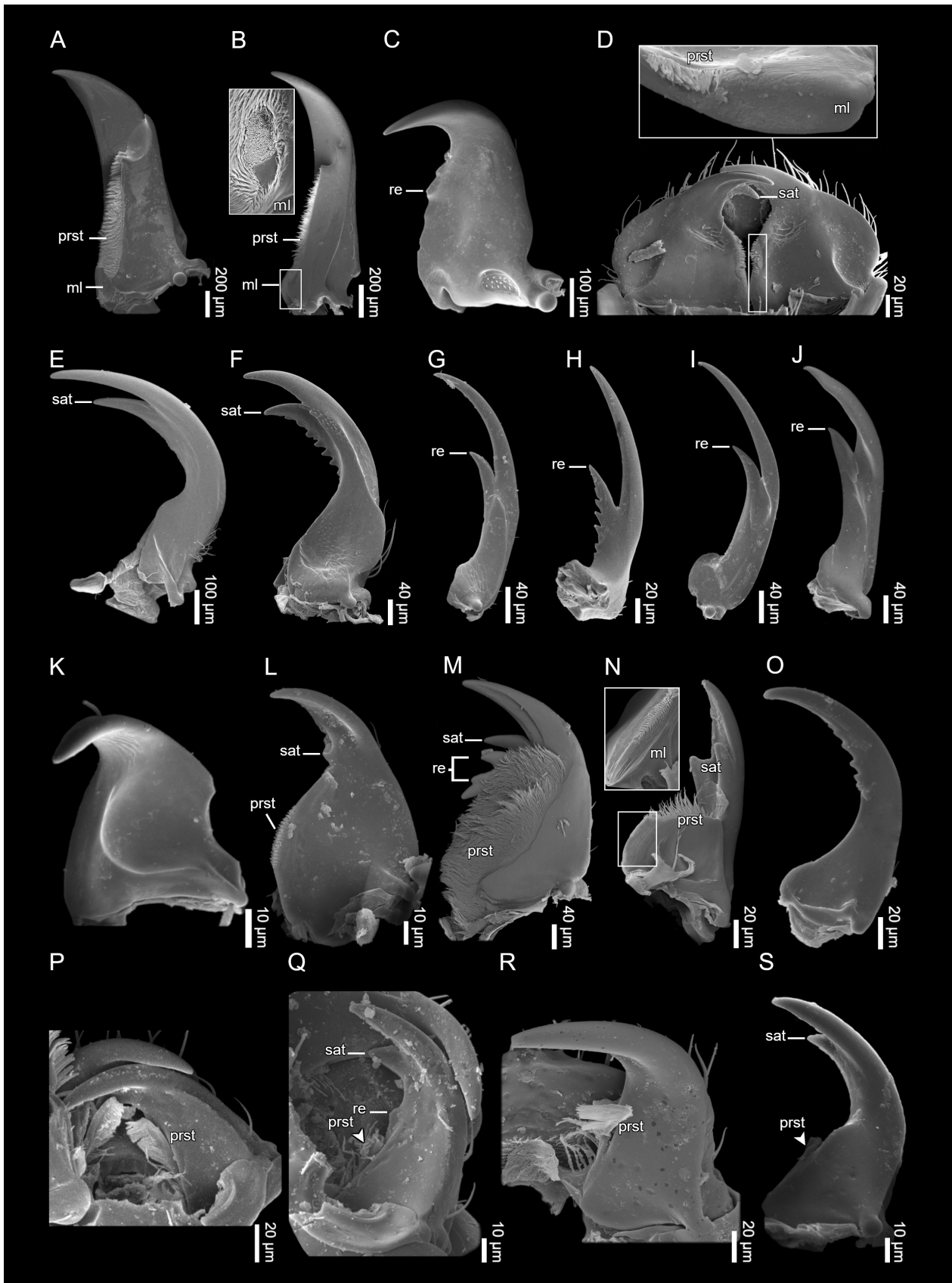


Figure 3. Left mandible (ventral aspect), SEM micrographs: **A** *Oxyporus stygicus*, **B** *Pseudoxyporus quinquemaculatus*, **C** *Megalopinus sanguiniriguttatus*, **D** *Solierius obscurus* (left and right mandibles), **E** *Dianous obliquenotatus*, **F** *Stenus puthzianus*, **G** *Austroesthetus passerculus*, **H** *Euaesthetus iripennis*, **I** *Fenderia chandleri*, **J** *Agnosthaetus cariniceps*, **K** *Cephennodes clavatus*, **L** *Veraphis* sp., **M** *Palaeostigus bifoveolatus*, **N** *Scydmaenus* sp., **O** *Stenichnus* sp., **P** *Eutyphlops* sp., mandibular teeth hidden by prostheca of right mandible, **Q** *Eutyphlops* sp. (prostheca damaged, indicated by arrow), mandibular teeth exposed, **R** *Homeotyphlus* sp. subapical tooth hidden because of the direction of view, **S** *Homeotyphlus* sp. (prostheca damaged, indicated by arrow), subapical tooth exposed. — Abbreviations: ml = mola, prst = prostheca, re = retinaculum, sat = subapical tooth.

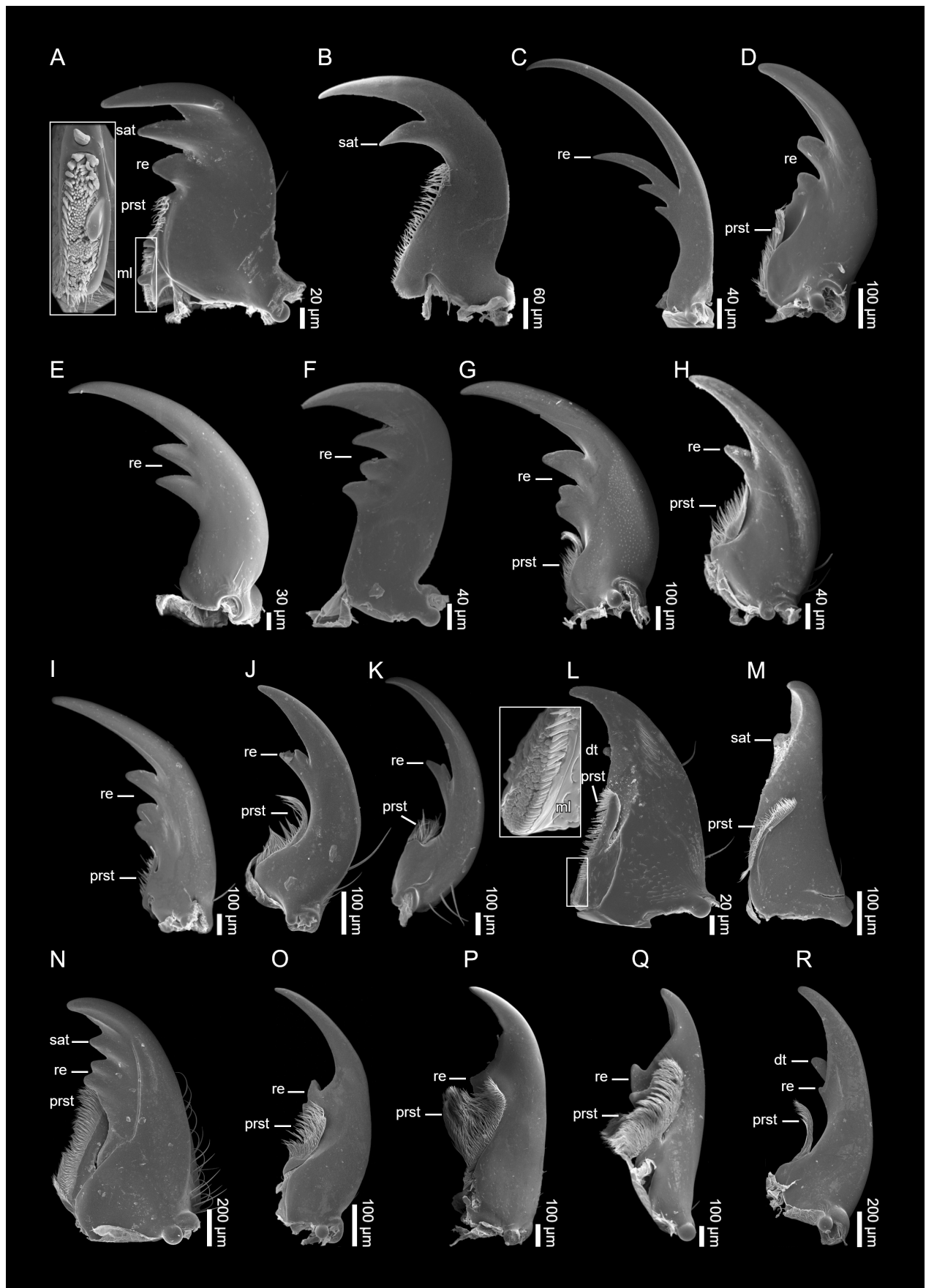


Figure 4. Left mandible (ventral aspect), SEM micrographs: **A** *Pseudopsis subulata*, **B** *Zalobius nancyae*, **C** *Astenus* sp., **D** *Lathrobium* sp., **E** *Medon vittatipennis*, **F** *Stilicoderus woodwardi*, **G** *Baryopsis* sp., **H** *Gnathymenus* sp., **I** *Homaeotarsus bicolor*, **J** *Paederus littoralis*, **K** *Pinophilus parvus*, **L** *Diochus schaumii*, **M** *Atrecus punctiventris*, **N** *Platyprosopus* sp., **O** *Erichsonius patella*, **P** *Philonthus politus*, **Q** *Platydracus femoratus*, **R** *Thyreocephalus albertisi*. — Abbreviations: dt = dorsal tooth, ml = mola, prst = prosthema, re = retinaculum, sat = subapical tooth.

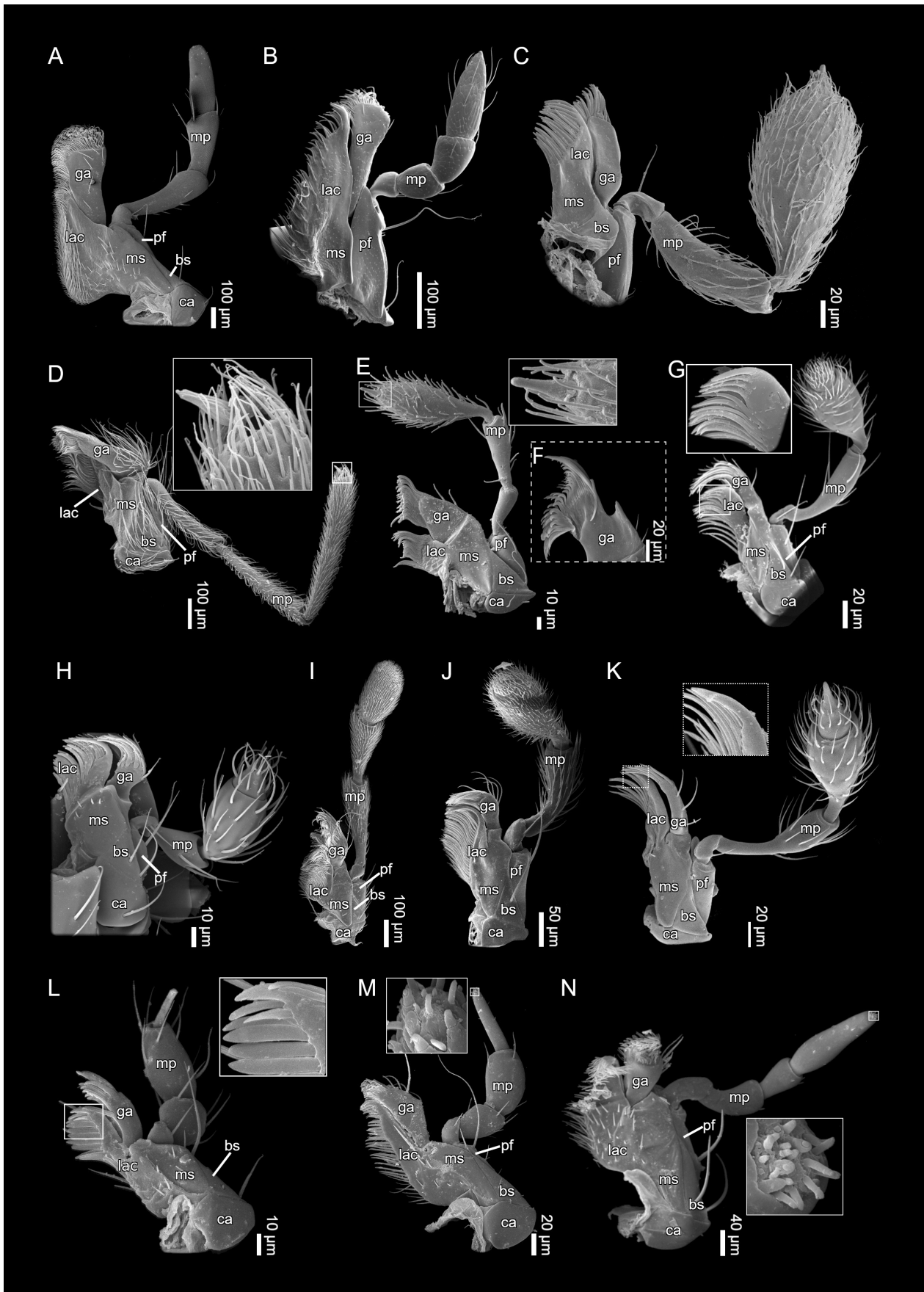


Figure 5. Left maxilla (ventral aspect), SEM micrographs: **A** *Oxyporus stygicus*, **B** *Megalopinus sanguinitriguttatus*, **C** *Solierius obscurus*, **D** *Dianous obliquenotatus*, **E** *Euaesthetus iripennis*, **F** *Agnosthaetus cariniceps*, **G** *Cephenodes clavatus*, **H** *Veraphis* sp., **I** *Palaeostigus bifoveolatus*, **J** *Scydmaenus* sp., **K** *Stenichmus* sp., **L** *Eutyphlops* sp., **M** *Pseudopsis subulata*, **N** *Zalobius nancyae*. — Abbreviations: bs = basistipes, ca = cardo, ga = galea, lac = lacinia, mp = maxillary palp, ms = mediostipes, pf = palpifer.

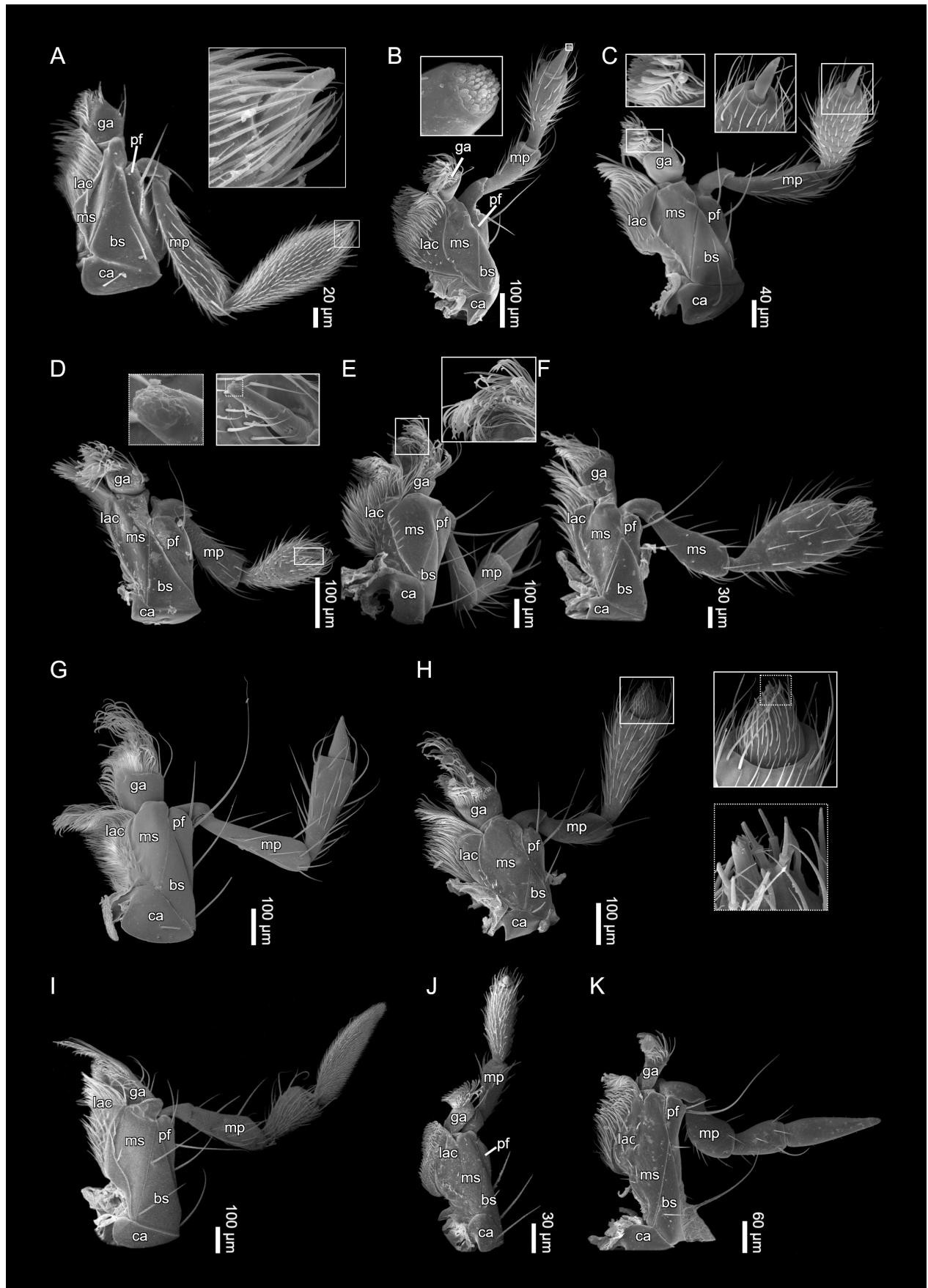


Figure 6. Left maxilla (ventral aspect), SEM micrographs: **A** *Astenus* sp., **B** *Lathrobium* sp., **C** *Medon vittatipennis*, **D** *Stilicoderus woodwardi*, **E** *Baryopsis* sp., **F** *Gnathymenus* sp., **G** *Homaeotarsus bicolor*, **H** *Paederus littoralis*, **I** *Pinophilus parvus*, **J** *Diochus schaumii*, **K** *Atrecus punctiventris*. — Abbreviations: bs = basistipes, ca = cardo, ga = galea, lac = lacinia, mp = maxillary palp, ms = mediostipes, pf = palpifer.

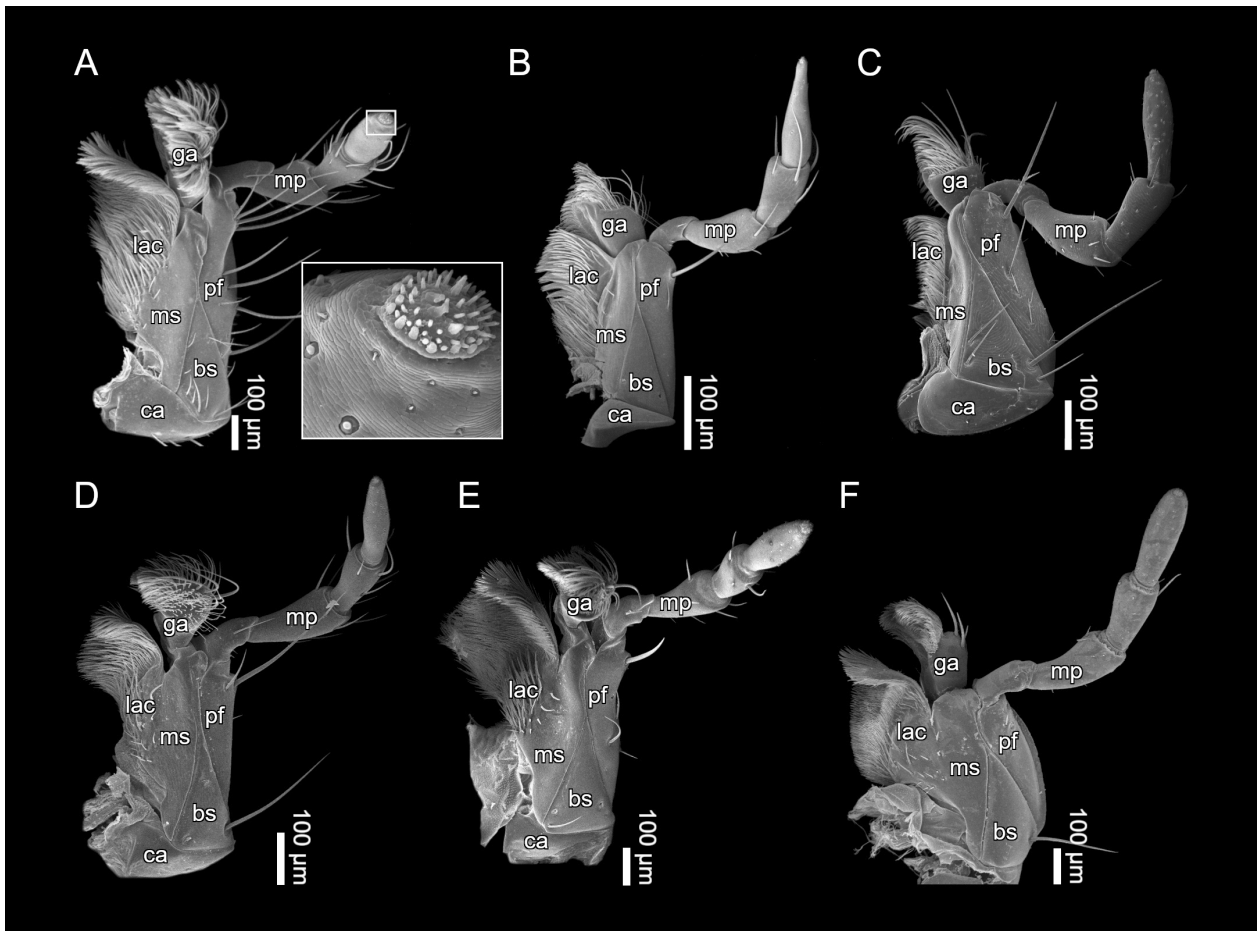


Figure 7. Left maxilla (ventral aspect), SEM micrographs: **A** *Platyprosopus* sp., **B** *Erichsonius patella*, **C** *Philonthus politus*, **D** *Quedius capucinus*, **E** *Platydracus femoratus*, **F** *Thyreocephalus albertisi*. — Abbreviations: bs = basistipes, ca = cardo, ga = galea, lac = lacinia, mp = maxillary palp, ms = mediostipes, pf = palpifer.

distinctly elongated tarsomere 5 when compared with *Euaesthetus* and *Agnosthaetus*.

3.1.7. Scydmaeninae (*Cephennodes*, *Veraphis*, *Palaeostigus*, *Scydmaenus*, *Stenichnus*)

Labrum (Fig. 1K–O). Subquadrate (*Scydmaenus*, *Cephennodes*, and *Veraphis*) or transverse (*Stenichnus*, *Palaeostigus*). Anterior margin not bilobed, with single pair of short and broad tooth-like projections in *Palaeostigus*. Epipharynx flat, without furrow, mostly covered by mesally directed hair-like (*Palaeostigus*), scale-like (*Stenichnus*), or both (*Scydmaenus*) trichomes, glabrous medially. *Scydmaenus* forming tuft medio-posteriad, and *Scydmaenus* and *Veraphis* forming pair of tufts apico-laterally. Proximal patch of hair-like trichomes anteriorly-directed in *Palaeostigus*. In *Cephennodes*, the epipharynx has semi-membranous surface showing irregular folds.

Mandible (Fig. 3K–O). Broad at base, curved, and acute at apex (*Cephennodes*, *Veraphis*, *Palaeostigus*, *Scydmaenus*), or slender and falciform (*Stenichnus*). Incisor area with (*Veraphis*, *Palaeostigus*, and *Scydmaenus*) or without (*Cephennodes* and *Stenichnus*) subapical tooth. Retinaculum absent (*Cephennodes*, *Veraphis*, *Scydmae-*

nus, *Stenichnus*) or present (*Palaeostigus*). *Stenichnus*, however, have a serrated inner edge of the mandible. Prostheca well-developed as dense brush of hair-like trichomes covering nearly half of the ventral surface (*Palaeostigus*), limited to only medial inner margin (*Scydmaenus*), or close to base of inner margin (*Veraphis*); in *Veraphis*, prostheca is broader than usual and bears tooth-like structures. Prostheca is absent in *Cephennodes* and *Stenichnus*. Mola present in *Scydmaenus*, mesal edge flattened surface composed of small rows of bristle-like trichomes with ridge-studded surface just lateral to them.

Maxilla (Fig. 5G–K). Lacinia reaching basal (*Palaeostigus*) or meso-apical (*Stenichnus*, *Cephennodes*, *Veraphis*, *Scydmaenus*) part of galea; bearing curved bristle-like trichomes directed postero-medially and with unarticulated spine apically (*Stenichnus*, *Cephennodes*, *Veraphis*, *Scydmaenus*) or curved hair-like trichomes directed posteriorly without unarticulated spine (*Palaeostigus*). Galea length subequal to lacinia, reaching second palpomere; bearing mesally directed curved bristle- (*Stenichnus*, *Cephennodes*, *Veraphis*, *Scydmaenus*) or hair-like (*Palaeostigus*) trichomes. Apical palpomere subequal to preceding one (*Palaeostigus*) or much shorter (*Stenichnus*, *Cephennodes*, *Veraphis*, *Scydmaenus*).

Labium-hypopharynx (Fig. 8I–M). Prementum¹ dorsally along lateral margins with dense fringe of mesally directed hair- or spine-like trichomes. Palpomere 3 somewhat (*Cephenodes*, *Veraphis*, *Stenichnus*) to distinctly (*Palaeostigus*, *Scydmaenus*) thinner than palpomere 2. Ligula consisting of paired ‘glossae’ and ‘paraglossae’; ‘glossae’ represented by pair(s) of sensilla basiconica (*Palaeostigus* and *Scydmaenus*) or trichodea (*Veraphis*); ‘paraglossae’ represented by antero-lateral lobes of prementum. Hypopharynx dorsally along lateral margins with mesally directed hair-like trichomes, medially glabrous or with only one single pair of trichomes. More proximally, dense fringe of antero-lateral directed hair-like trichomes (*Palaeostigus* and *Veraphis*). For the genera *Cephenodes*, *Stenichnus*, and *Scydmaenus*, in which the hypopharynx overlaps the prementum, the hypopharynx has a different appearance as follows. Hypopharynx dorsally along lateral margin with short thorn-like trichomes (*Cephenodes* and *Scydmaenus*) and, innermost to these, longitudinal striae, continuing medially (*Stenichnus*) or not (*Cephenodes* and *Scydmaenus*). More proximally with dense tuft of hair-like trichomes (*Scydmaenus*), or glabrous (*Cephenodes* and *Stenichnus*).

Protarsus (Fig. 10K–O). Consisting of 5 tarsomeres, all slender and subequal in width. Tarsomeres are ventrally covered with spine- and hair-like setae. *Palaeostigus* with pairs of distinct spines laterally on tarsomeres 1–3.

3.1.8. Leptotyphlinae (*Eutyphlops*, *Homeotyphlus*)

Labrum (Fig. 1P, Q). Transverse, anterior margin slightly denticulate. Epipharynx flat, without furrow, mainly glabrous. Antero-lateral directed hair-like trichomes proximally, and mesally directed hair-like trichomes lateroproximally. With few campaniform sensilla medially.

Mandible (Fig. 3P–S). Slightly broadened at base, becoming acute toward apex, falciform. Incisor area with subapical tooth. Retinaculum absent (*Homeotyphlus*) or present (*Eutyphlops*). Prosthema present, forming prominent, robust, sclerotized lobe-like projection with brush-like fringe of fimbriate hair-like trichomes along medial margin. Mola absent.

Maxilla (Fig. 5L). Lacinia reaching to apical part of galea; bearing row of straight mesally directed bristle-like trichomes, unarticulated spine present apically. Galea length subequal to lacinia, reaching third palpomere (*Eutyphlops*) or about half of lacinia length, reaching only base of second palpomere (*Homeotyphlus*); bearing antero-medially directed slightly curved bristle-like trichomes. Apical palpomere distinctly shorter and thinner (peg-like) than preceding one.

¹ The prementum of some scydmaenines can be covered by the hypopharynx dorsally after dissection (such a case is exemplified here by the representatives of *Scydmaenus*, *Cephenodes*, and *Stenichnus*), preventing a clear view of its surface structures (i.e., trichomes and sensilla types and their distribution). The prementum of *Scydmaenus* is described, because we had many specimens at our disposal enabling us to remove the hypopharynx to obtain a clear view of the covered region of the prementum.

Labium-hypopharynx (Fig. 8N). Prementum dorsally along lateral margins with parallel continuous fringes of mesally directed comb-like trichomes; without spine-like trichomes, medially glabrous. Palpomere 3 somewhat thinner than palpomere 2. Ligula consisting of paired ‘glossae’ and ‘paraglossae’; ‘glossae’ modified into spatulate meso-lateral lobes, projecting antero-lateral, bearing few sensilla coeloconica at tip; ‘paraglossae’ represented by antero-lateral lobes of prementum. Hypopharynx dorsally with arrays of mesally directed hair-like trichomes distally and antero-lateral directed hair-like trichomes proximally.

Protarsus (Fig. 10P, Q): Consisting of 3 tarsomeres, all slender and subequal in width. Tarsomeres glabrous medially. *Eutyphlops* with spine-like setae and *Homeotyphlus* with spoon-like tenent setae with distinctly enlarged adhesive pads.

3.1.9. Pseudopsinae (*Pseudopsis*, *Zalobius*)

Labrum (Figs 1R, 2A). Subquadrate, not bilobed. Epipharynx without furrow, with sparsely distributed vestiture, with medio-lateral region covered by rows of mesally directed hair-like trichomes, forming bristle-trough. Campaniform sensilla present medially (*Pseudopsis*) or absent (*Zalobius*). Posteriorly with patches of hair- or scale-like anteriorly directed trichomes (*Zalobius*) or a tuft of hair-like trichomes (*Pseudopsis*). Short basiconic (*Zalobius*) or disc-like (*Pseudopsis*) sensilla distally.

Mandible (Fig. 4A, B). Broad, abruptly curved at incisor (*Pseudopsis*) or only slightly broad at base and falciform in shape (*Zalobius*). Incisor area with subapical tooth. Retinaculum absent (*Zalobius*) or present (*Pseudopsis*). Prosthema well-developed, without lobe-like projection but with only short extension distally; bearing row of branched hair-like trichomes along medial margin, extending anteriorly. Mola present in *Pseudopsis*, somewhat broad, covered by teeth- and bristle-like trichomes, thicker on edges and finer on inner region.

Maxilla (Fig. 5M, N). Lacinia reaching to apical part of galea; bearing few rows of straight bristle- and hair-like trichomes directed mesally; unarticulated spine present apically. Galea about half of lacinia length, reaching only to base of second palpomere (*Zalobius*) or more than half length of lacinia, reaching third palpomere (*Pseudopsis*); bearing brush of curved hair- and bristle-like trichomes directed postero-medially. Apical palpomere slightly longer and thinner (*Pseudopsis*) than preceding one or distinctly longer than and same width as preceding one, tapering apically (*Zalobius*).

Labium-hypopharynx (Fig. 9A, B). Prementum dorsally along lateral margins with fringe of mesally directed hair-like trichomes; innermost row of lateral fringes differentiated into spine-like trichomes (*Pseudopsis*) or spine-like trichomes still present (but not on innermost row) and prementum medially covered with hair-like setae (*Zalobius*). Palpomere 3 somewhat thinner than palpomere 2. Ligula consisting of paired ‘glossae’ and ‘paraglossae’; ‘glossae’ spatulate, modified dorsally into medial lobes, projecting antero-lateral and covered apically with sensilla coeloconica in *Pseudopsis*. In *Zalobius*, the ‘glossae’

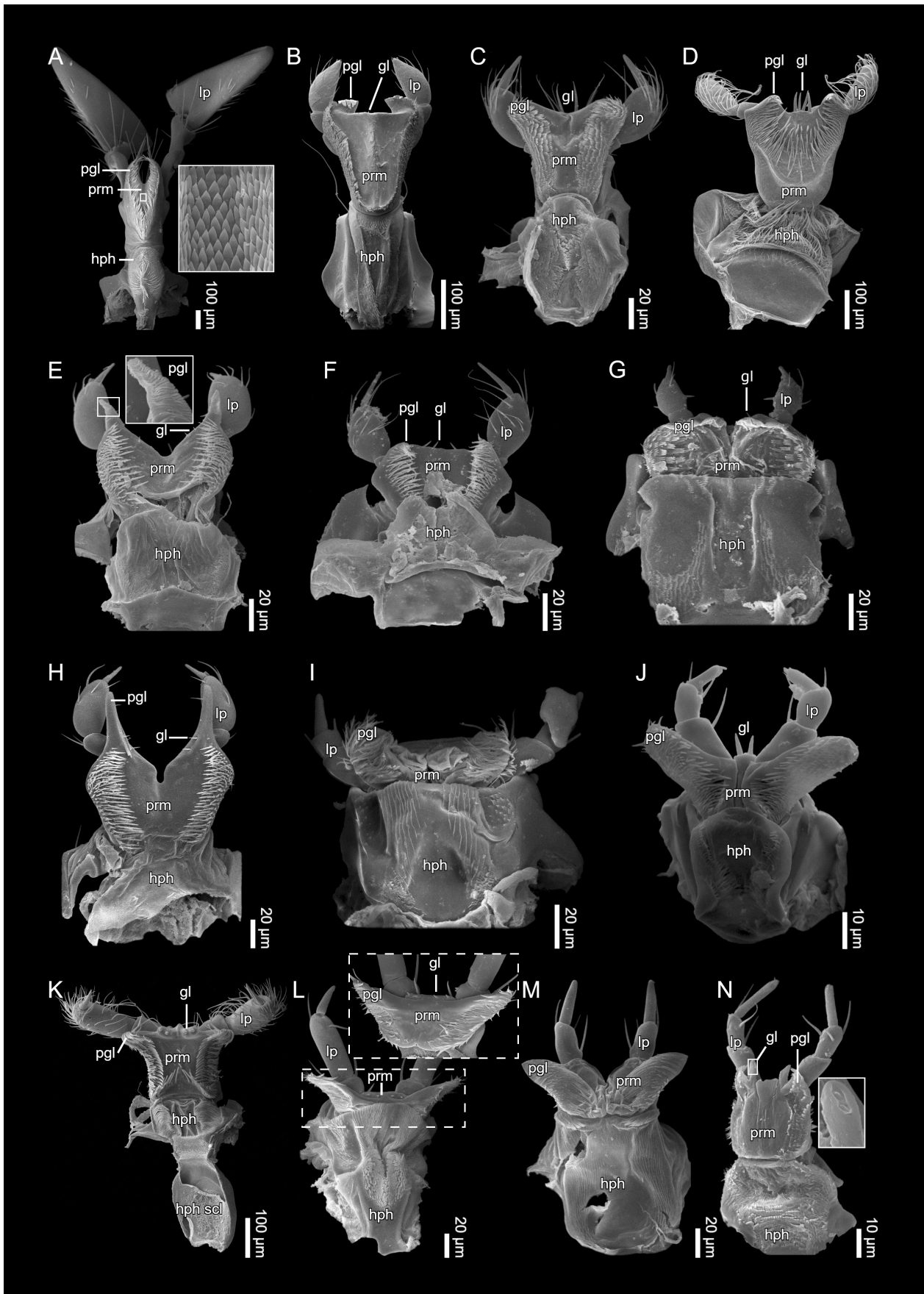


Figure 8. Labium-hypopharynx (dorsal aspect), SEM micrographs: **A** *Oxyporus stygicus*, **B** *Megalopinus sanguiniriguttatus*, **C** *Solierius obscurus*, **D** *Dianous obliquenotatus*, **E** *Austroesthetus passerculus*, **F** *Euaesthetus iripennis*, **G** *Fenderia chandleri*, **H** *Agnostaetus cariniceps*, **I** *Cephennodes clavatus*, **J** *Veraphis* sp., **K** *Palaeostigus bifoveolatus*, **L** *Scydmaenus* sp., **M** *Stenichnus* sp., **N** *Eutyphlops* sp. — Abbreviations: gl = ‘glossa’, hph = hypopharynx, hph scl = hypopharynx sclerite, lp = labial palp, pgl = ‘paraglossa’, prm = prementum.

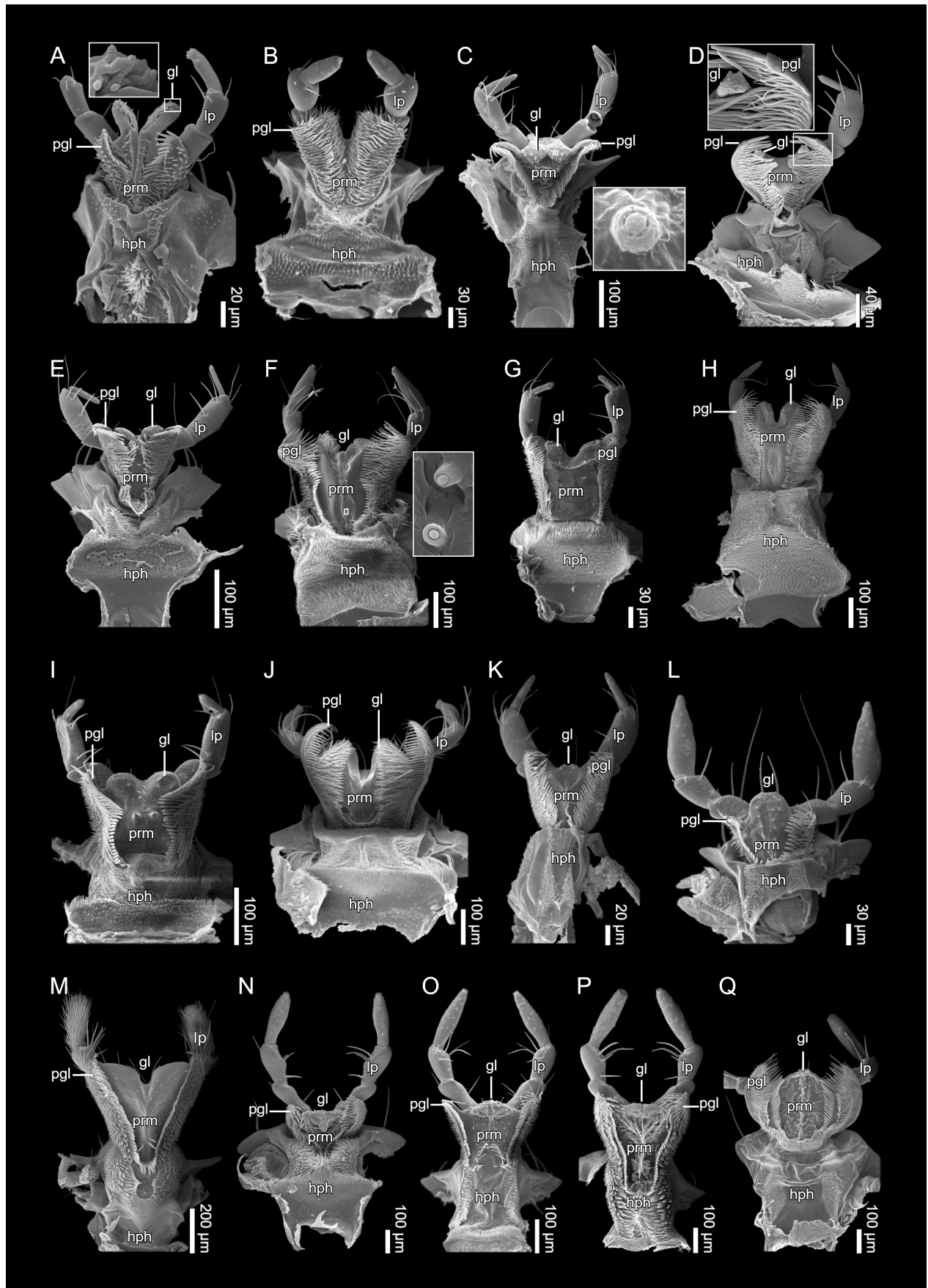


Figure 9. Labium-hypopharynx (dorsal aspect), SEM micrographs: **A** *Pseudopsis subulata*, **B** *Zalobius nancyae*, **C** *Lathrobium* sp., **D** *Medon vittatipennis*, **E** *Stilicoderus woodwardi*, **F** *Baryopsis* sp., **G** *Gnathymenus* sp., **H** *Homaeotarsus bicolor*, **I** *Paederus littoralis*, **J** *Pinophilus parvus*, **K** *Diachus schaumii*, **L** *Atrecus punctiventris*, **M** *Platyprosopus* sp., **N** *Philonthus politus*, **O** *Quedius capucinus*, **P** *Platydracus femoratus*, **Q** *Thyreocephalus albertisi*. — Abbreviations: gl = 'glossa', hph = hypopharynx, lp = labial palp, pgl = 'paraglossa', prm = prementum.

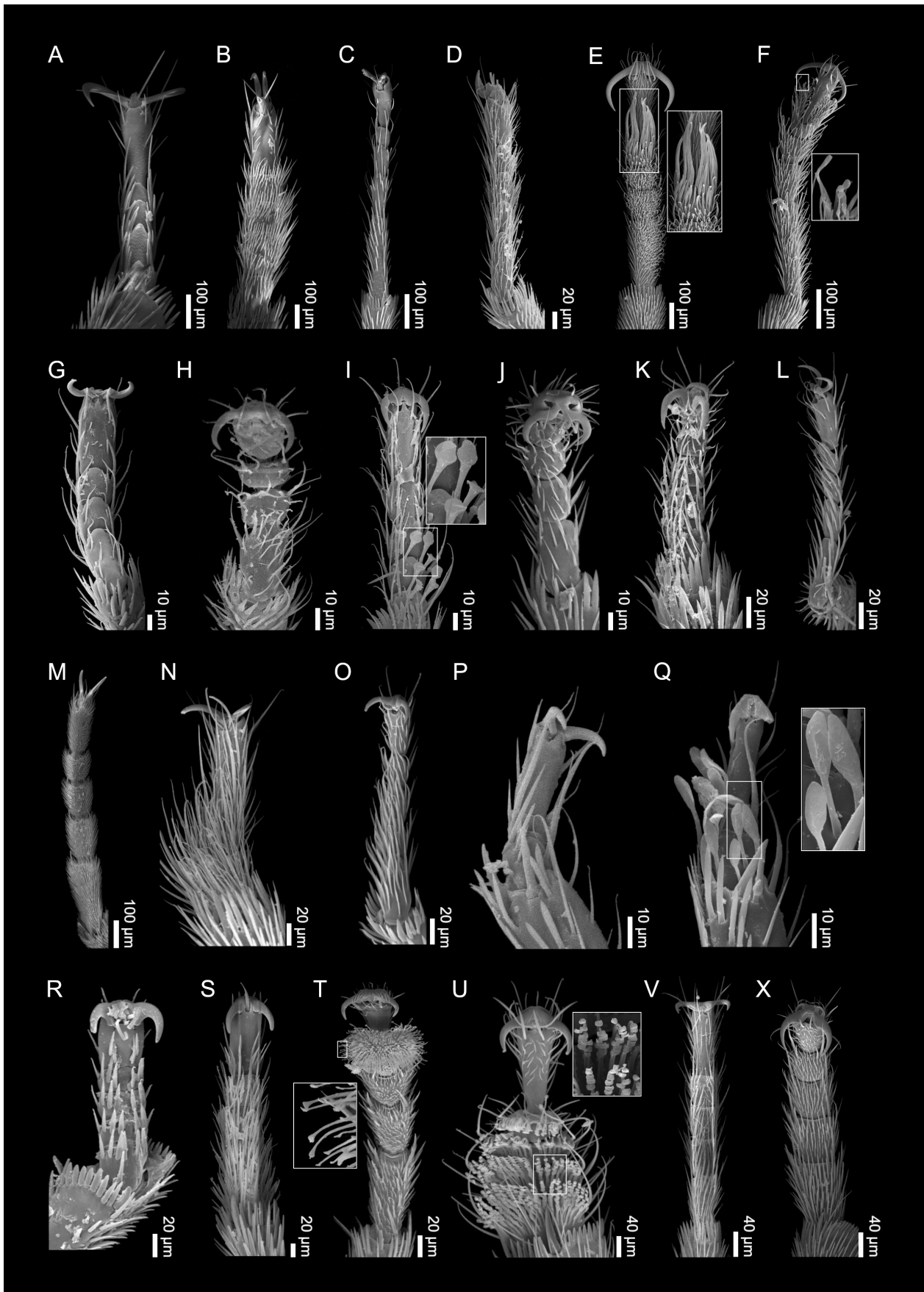


Figure 10. Left protarsi (ventral aspect), SEM micrographs: **A** *Oxyporus stygicus*, **B** *Pseudoxyporus quinquemaculatus*, **C** *Megalopinus sanguinigruttatus*, **D** *Solierius obscurus*, **E** *Dianous obliquenotatus*, **F** *Stenus puthzianus*, **G** *Austroesthetus passerculus*, **H** *Euaesthetus iripennis*, **I** *Fenderia chandleri*, **J** *Agnosthaetus cariniceps*, **K** *Cephennodes clavatus*, **L** *Veraphis* sp., **M** *Palaeostigus bifoveolatus*, **N** *Scydmaenus* sp., **O** *Stenichnus* sp., **P** *Eutyphlops* sp., **Q** *Homeotyphlus* sp., **R** *Pseudopsis subulata*, **S** *Zalobius nancyae*, **T** *Astenus* sp., **U** *Lathrobium* sp., **V** *Medon vittatipennis*, **X** *Stillicoderus woodwardi*.

are integrated with the prementum plate and probably represented by hair-like setae, but we were not able to distinguish these clearly as this area of the prementum is densely covered by other hair-like setae; ‘paraglossae’ represented by antero-lateral lobes of prementum. Hypopharynx covered dorsally with antero-lateral directed hair-like trichomes, forming small tuft more distally (*Zalobius*) or along lateral margins with mesally directed hair-like trichomes and medially mainly glabrous, forming a dense brush proximally (*Pseudopsis*).

Protarsus (Fig. 10R, S). Consisting of 5 tarsomeres, all slender and subequal in width. Tarsomeres in *Pseudopsis* with distinct rows of spine-like setae and in *Zalobius* densely covered with spine- and hair-like setae, somewhat longer than *Pseudopsis*.

3.1.10. Paederinae (*Astenus*, *Lathrobium*, *Medon*, *Stilicoderus*, *Baryopsis*, *Gnathymenus*, *Homaeotarsus*, *Paederus*, *Pinophilus*)

Labrum (Fig. 2B–J). Transverse, not or only slightly bilobed; subquadrate and strongly bilobed in *Lathrobium*. Epipharynx extensively and densely covered by mesally directed hair- or scale-like trichomes combined with dense medial tuft of anteriorly directed hair-like trichomes (*Lathrobium*, *Baryopsis*, *Homaeotarsus*, and *Pinophilus*), or with some regions covered by mesally directed hair- or scale-like trichomes and glabrous furrow medially (*Astenus*, *Medon*, *Stilicoderus*, *Gnathymenus*, and *Paederus*); medially directed trichomes forming bristle-trough in all species, except *Astenus* and *Medon*. Longitudinal furrow is also present in *Pinophilus*, but mainly covered with anteriorly directed hair-like trichomes medially.

Mandible (Fig. 4C–K). Robust at base and falciform in shape at apical half (*Lathrobium*, *Medon*, *Baryopsis*, *Gnathymenus*, *Homaeotarsus*, *Paederus*, *Pinophilus*), or slender and strongly falciform (*Astenus*), or overall broad with incisor angled almost 90° in relation to base (*Stilicoderus*). Incisor area without subapical tooth. Retinaculum present, with one or two teeth; retinaculum in *Astenus* has one tooth with three cusps (tricuspid). Prosthema well-developed, forming prominent sclerotized lobe-like projection, which bears brush-like fringe of fimbriate hair-like trichomes along medial margin, sometimes extending anteriorly toward most proximal tooth of retinaculum. Prosthema absent in *Astenus*, *Medon*, and *Stilicoderus*. Mola absent.

Maxilla (Fig. 6A–I). Lacinia reaching to just basal part of galea; bearing robust brush of hair-like trichomes, basal region consisting of straight antero-mesally directed trichomes and apical region of curved trichomes (antero-) mesally directed. Galea about half length of lacinia, reaching first palpomere or only to base of second palpomere; bearing robust brush of curved hair-like trichomes curved mesally, trichomes sometimes with spatulate tip (*Medon*, *Stilicoderus*, *Baryopsis*, *Homaeotarsus*, *Paederus*). Apical palpomere subequal to longer (*Pinophilus*), or much shorter than preceding one (*Paederini*) or vestigial and peg-like (*Lathrobiini*).

Labium-hypopharynx (Fig. 9C–J). Prementum dorsally along lateral margins with prominent and dense fringe of mesally directed hair-like trichomes; innermost row of lateral fringes differentiated into spine-like trichomes, medially with sensilla coeloconica (*Lathrobium*, *Baryopsis*, *Homaeotarsus*), with spine-like erect setae (*Stilicoderus*) or glabrous (*Medon*, *Gnathymenus*, *Paederus*, *Pinophilus*); pair of prominent peg-like protuberances are visible in *Paederus*. Palpomere 3 about as wide to half as wide as, or distinctly (*Medon*, *Stilicoderus*) thinner than palpomere 2. Ligula consisting of paired ‘glossae’ and ‘paraglossae’; ‘glossae’ dorsally modified into anterior lobes, sometimes bulbous, covered with sensilla coeloconica; ‘paraglossae’ represented by antero-lateral lobes of prementum. Hypopharynx dorsally mainly with dense homogeneous array of antero-lateral directed hair-like trichomes (*Baryopsis*, *Gnathymenus*). Alternatively, along lateral margins with mesally directed hair-like trichomes and medially with dense vestiture of hair-like trichomes converging to form medial tuft (*Stilicoderus*, *Homaeotarsus*, *Paederus*, *Pinophilus*). *Lathrobium* with such vestiture, but with distinct glabrous furrow medially. In *Lathrobiini*, the hypopharynx is narrowed distally and suddenly enlarged proximally where most of hypopharynx sclerite is present (the connection between these regions is fragile and susceptible to tearing during dissection).

Protarsus (Figs 10T–X, 11A–E). Consisting of 5 tarsomeres, tarsomeres covered by tenent setae are widened and bilobed. Tarsomeres 1–4 of *Lathrobium*, *Baryopsis*, *Gnathymenus*, *Paederus*, and *Pinophilus* ventrally densely covered by distally widened spatulate (tenent) setae. *Pinophilus* is much more densely covered by distally widened spatulate (tenent) setae than the other genera. In *Astenus*, the only tarsomere that bears tenent setae is 4, whereas 1–3 are covered by rows of unmodified prominent spine-like setae. In *Medon*, *Stilicoderus*, and *Homaeotarsus*, tarsomeres 1–5 are mainly covered by spine- and hair-like setae, and all tarsomeres are subequal in width.

3.1.11. Staphylininae (*Diochus*, *Atrecus*, *Platyprosopus*, *Erichsonius*, *Philonthus*, *Quedius*, *Platydracus*, *Thyrecephalus*)

Labrum (Fig. 2K–P). Transverse, but subquadrate in *Diochus* and *Thyrecephalus*, and in *Platyprosopus* rhomboidal, longer than wide including hidden part beneath clypeus, or, for only externally exposed part, gradually widening toward exposed base; anterior margin not or only slightly bilobed. Epipharynx flat, without furrow (except *Platyprosopus*), covered by mesally directed hair-like trichomes, forming dense medial tuft of antero-lateral directed trichomes medially (*Erichsonius*, *Philonthus*, *Platydracus*, *Quedius*). *Platyprosopus* distinctly longitudinally furrowed, with ramified trichomes distally and antero-lateral directed cone-shaped trichomes medially. In *Diochus* and *Thyrecephalus*, epipharynx is mainly glabrous, *Thyrecephalus* with transverse row of anteriorly directed hair-like trichomes, and grooved peg-like sen-

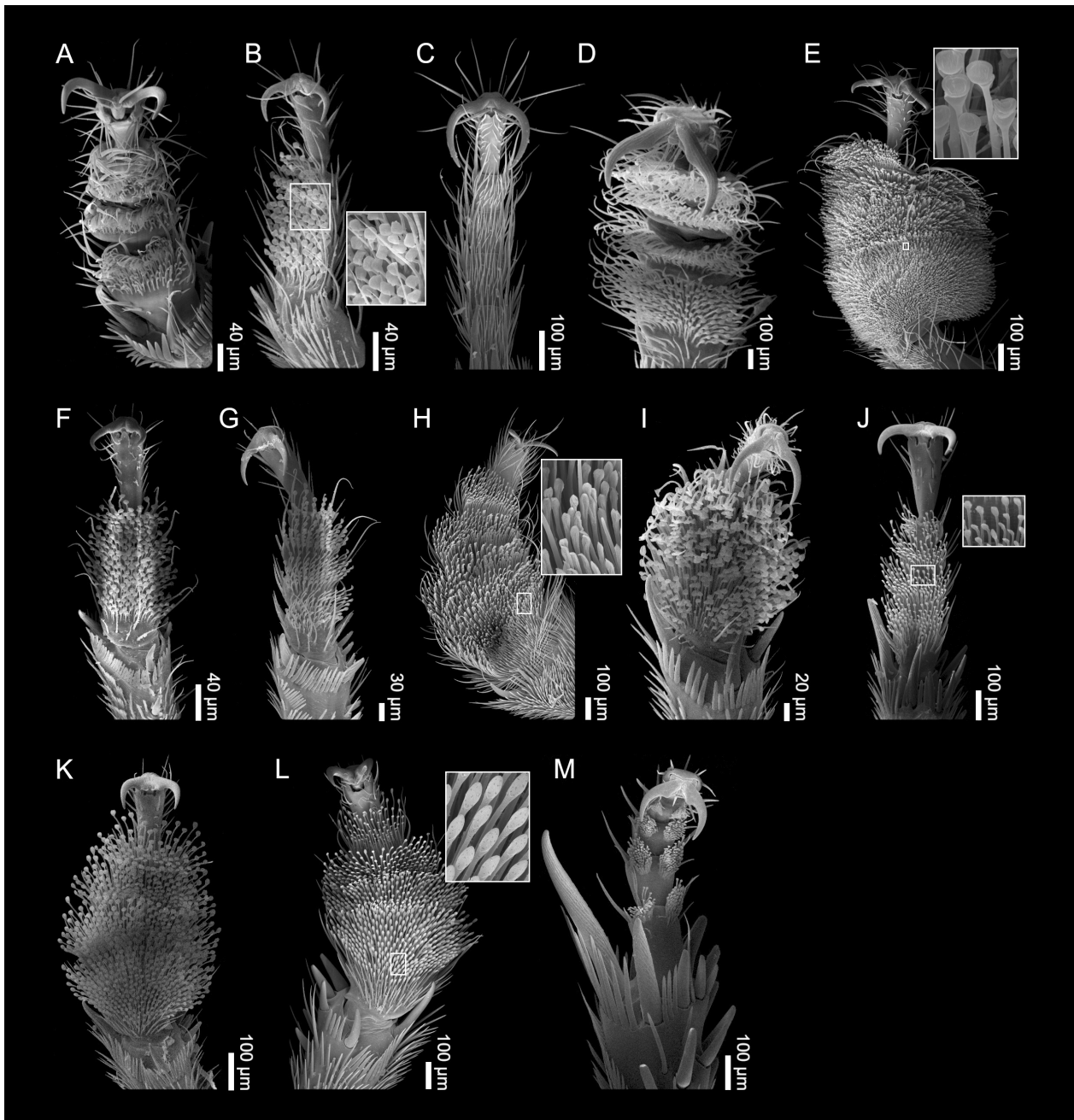


Figure 11. Left protarsi (ventral aspect), SEM micrographs: **A** *Baryopsis* sp., **B** *Gnathymenus* sp., **C** *Homaeotarsus bicolor*, **D** *Paederus littoralis*, **E** *Pinophilus parvus*, **F** *Diochus schaumii*, **G** *Atrecus punctiventris*, **H** *Platyprosopus* sp., **I** *Erichsonius pattella*, **J** *Philonthus politus*, **K** *Quedius capucinus*, **L** *Platydracus femoratus*, **M** *Thyreoecephalus albertisi*.

silla medially, distal to transverse row; and *Diochus* with paired patches of anteriad-directed hair-like trichomes proximally and row of bowl-like (campaniform?) sensilla proximally and row of prominent peg-like sensilla just distal to that. *Atrecus* with loose row of mesally directed hair-like trichomes laterally, row of anteriad-directed thorn-like setae distally, and few rows of prominent peg-like sensilla meso-proximally; medially directed trichomes forming bristle-trough in all species, except *Diochus*, *Atrecus* and *Thyreoecephalus*.

Mandible (Fig. 4L–R). Somewhat broadened at base, acute at apex, falciform (*Erichsonius*, *Philonthus*, *Quedius*, *Platydracus*, *Thyreoecephalus*.); *Diochus* and *Platyprosopus* with broader base, only slightly falciform and

with blunt incisor; *Atrecus* with broad base but not falciform shape and more robust than other genera studied; incisor blunt. Incisor area with (*Atrecus* and *Platyprosopus*) or without (*Diochus*, *Erichsonius*, *Quedius*, *Philonthus*, *Platydracus*, *Thyreoecephalus*) subapical tooth. Retinaculum absent (*Diochus*, *Atrecus*, *Platyprosopus*) or present (*Erichsonius*, *Philonthus*, *Quedius*, *Platydracus*, *Thyreoecephalus*), usually partially covered by more posterior or prostheca; *Diochus* and *Thyreoecephalus* bearing one dorsal mesal tooth. Prostheca well-developed, forming prominent sclerotized lobe-like projection bearing brush-like fringe of fimbriate hair-like trichomes along medial margin, sometimes extending anteriorly toward most proximal tooth of retinaculum. Mola present only in *Di-*

ochus, forming broader region covered with bristle-like trichomes.

Maxilla (Figs 6J, K, 7A–F). Lacinia reaching to just base or half-length of galea; bearing brush-like structure with bristle-like trichomes on basal region directed straight anteriorly and on apical region curved and directed postero-medially (*Diachus*), or hair-like trichomes, basal region consisting of straight anteriorly directed (*Atrecus*, *Platyprosopus*, *Erichsonius*, *Thyrecephalus*), or mesally directed (*Philonthus*, *Quedius*, *Platydracus*) directed trichomes and apical region with curved mesally directed trichomes; brush especially dense and long in *Platydracus* and *Platyprosopus* and significantly shorter in *Diachus*. Galea about half lacinia length, reaching first or second palpomere; apex bearing brush of curved bristle (*Diachus*) or hair-like trichomes (*Atrecus*, *Platyprosopus*, *Philonthus*, *Quedius*, *Platydracus*, *Thyrecephalus*) or curved hair- and bristle-like trichomes (*Erichsonius*); brush especially dense and long in *Platydracus* and *Platyprosopus*. Apical palpomere subequal to or slightly longer than preceding one, or vestigial (*Diachus*).

Labium-hypopharynx (Fig. 9K–Q). Prementum dorsally along lateral margins with dense fringe of mesally directed hair-like trichomes; innermost row differentiated into spine-like trichomes, medially covered with sensilla coeloconica (*Atrecus*, *Platyprosopus*, *Quedius*, *Thyrecephalus*), with hair-like setae (*Philonthus* and *Platydracus*) or glabrous (*Diachus* and *Erichsonius*). Palpomere 3 about as wide to half as wide as palpomere 2. Ligula consisting of paired ‘glossae’ and ‘paraglossae’; ‘glossae’ dorsally modified into anterior lobes (*Platyprosopus* and Staphylinini) covered with sensilla coeloconica, sometimes bulbous, or modified into single medial projection covered with sensilla coeloconica (*Diachus*, *Atrecus*, and *Thyrecephalus*); ‘paraglossae’ represented by antero-lateral lobes of prementum. Hypopharynx dorsally along lateral margins with mesally directed hair-like trichomes. Medially provided with dense vestiture of hair-like trichomes forming medial tuft (*Erichsonius*, *Philonthus*, *Platydracus*), medially glabrous or with only few scattered short hair-like trichomes (*Diachus*, *Atrecus*, *Platyprosopus*, *Quedius*, *Thyrecephalus*).

Protarsus (Fig. 11F–M). Consisting of 5 tarsomeres, tarsomeres covered by tenent setae are widened and bilobed (except in *Thyrecephalus*). Tarsomeres 1–4 of all investigated Staphylininae are covered by distally widened (tenent) setae of various shapes (depending on species). Although *Thyrecephalus* bears tenent setae like the other genera, they have a different arrangement, forming a pair of setal patches on each tarsomere.

3.2. Analysis of potential groundplan patterns of the mouthparts in staphylinines

The character mapping analysis (Fig. 12) was performed using the taxa in Table 1 and the character matrix in Table S1. The following 13 characters and their states were defined and mapped:

Labrum-epipharynx

- 1 Labrum, width vs length: (0) subquadrate or longer than wide; (1) wider than long, transverse.
- 2 Anterior margin of labrum: (0) not or only slightly bilobed, not denticulate or serrate; (1) strongly bilobed, not denticulate or serrate; (2) not bilobed, denticulate or serrate.
- 3 Medial surface of epipharynx: (0) with medially positioned prominent hair tuft of posteriorly directed long hair- or bristle-like trichomes; (1) without any rows of medially directed hair- or bristle-like trichomes; (2) with loose rows of medially directed hair- or bristle-like trichomes; (3) with medially and/or anteriorly directed hair- bristle-like trichomes, forming a bristle-trough.

Mandible

- 4 Subapical tooth: (0) absent; (1) present.
- 5 Retinaculum: (0) absent; (1) present.
- 6 Prosthema: (0) absent; (1) present, not forming lobe-like projection; (2) present, forming lobe-like projection.
- 7 Mola: (0) absent; (1) present.

Maxilla

- 8 Apical unarticulated structure (spine or multibranching structure) of lacinia: (0) absent; (1) present.
- 9 Maxillary palpomere 4: (0) well-developed, fully sclerotized, similar in width to palpomere 3; (1) about half the width of palpomere 3 or much shorter but similar width, fully sclerotized; (2) less than half the width of palpomere 3, fully sclerotized; (3) not more than 1/4 width of palpomere 3, conical or vestigial and peg-like.

Labium-hypopharynx

- 10 ‘Glossa’: (0) integrated with prementum plate, sometimes represented by pairs of sensilla basiconica or trichodea; (1) represented by paired spatulate lobes, projected anteriorly; (2) represented by paired anterior lobes, sometimes bulbous and covered by sensilla coeloconica.
- 11 ‘Paraglossa’: (0) represented by inconspicuous antero-lateral lobes; (1) represented by prominent anterior digitiform lobes; (2) represented by pads bearing multiple (adhesive) outgrowths.
- 12 Trichomes on prementum lateral margin: (0) hair-like; (1) conspicuous spine-like; (2) comb-like.
- 13 Labial palpomere 3: (0) about as wide to half as wide as penultimate palpomere; (1) about third or less as wide as penultimate palpomere, vestigial; (2) moderately to strongly expanded apically.

3.3. Mandible shape analysis

The first two relative warps or principal components (PC), PC 1 and PC 2 explain 53.6% and 22.9% of the total shape variation, respectively. In the morphospace (Fig. 13), convex hulls are used to cluster the subfamilies (or

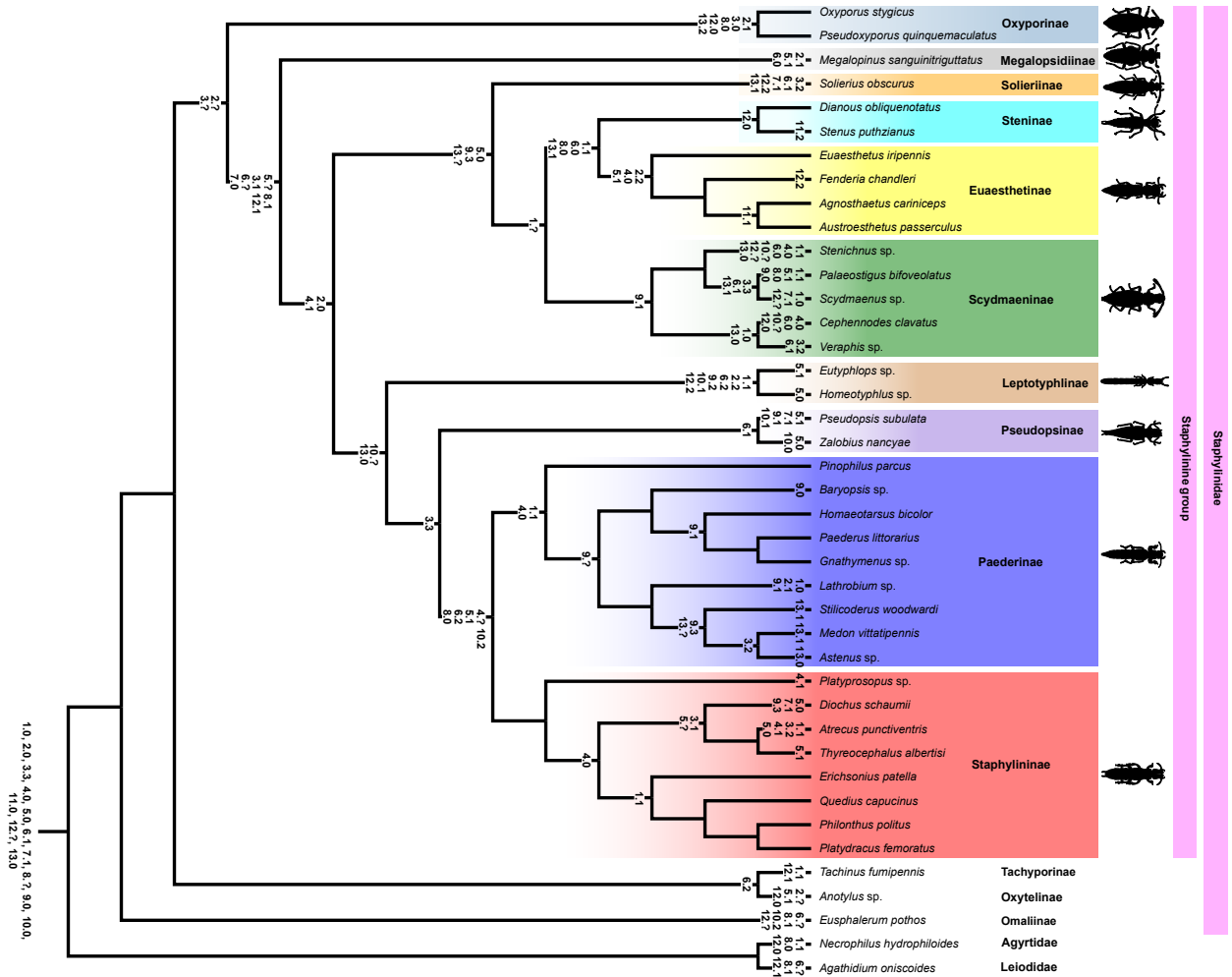


Figure 12. Ancestral character state reconstruction of categorical data based on maximum parsimony performed in Mesquite 3.61 (Maddison and Maddison 2019). The characters are mapped on a phylogenetic scheme based on multiple studies cited in the Materials and Methods section. The numbers on the branches of the tree indicate the character and the state, respectively, according to list in section 3.2. Each color corresponds to a subfamily as labelled. Pink bars span the members of the Staphylinine group and the Staphylinidae.

the outgroup species as its own group) that possess more than three species. The consensus shape of all species is illustrated in the center (at zero), and a shape at each extremity of the two axes is provided to achieve a better understanding of the deformation of the shape depending on the position of the species in the morphospace.

Shape changes according to PC 1 mainly involve the inner edge of the mandible with the tip becoming increasingly blunter and the base becoming broader toward the left side of this axis, whereas higher PC 1 values are associated with the mandibles becoming laterally compressed, resulting in increasingly slender and falcate mandible shapes with a narrow base (Fig. 13). Shape changes along PC 2 mainly affect the outer edge of the mandible, which becomes increasingly straight and oblong and with a slightly narrow base toward lower PC values, but more strongly curved and with a relatively large base in the opposite direction (Fig. 13).

The character mapping analysis of PC 1 is shown in Fig. 14. Hypothetical mandible shapes are given according to the generated color scheme. A tendency to a mandible with a blunt apex and broad base is seen among the

species of the outgroup, represented by a lower PC 1. This finding, together with the most basal groups not having a high PC 1, leads to the hypothetical ancestral group of the Staphylinines having a PC 1 between -0.11 and -0.06, meaning a comparatively blunter apex and broader base than most of the staphylinines investigated. The same range of PC 1 of hypothetical ancestral staphylinines has secondarily evolved in a few other groups independently (*Cephennodes*, *Veraphis*, *Leptotyphlinae*, *Diochus*, *Platydacus*). However, in most groups, the mandibles have become more slender with especially falcate mandibles in *Euaesthetus* and *Astenus*.

The character mapping analysis of PC 2 is shown in Fig. 15. The outgroup taxa plus the majority of the in-group species possess intermediate PC 2 values (ranging from -0.04 to 0.62, represented by the green colors). Whereas in several groups, the mandibles have become straighter (with a less curved outer edge), in some other cases such as *Stillicoderus* and *Medon*, the mandibles have become strongly curved and sickle-shaped, with the special case of *Cephennodes*, whose mandible tips are curved inward.

Table 2. Mahalanobis distances between groups. Euae = Euaesthetinae, Lept = Leptotyphlinae, Mega = Megalopsidiinae, Outg = Outgroup, Oxy = Oxyporinae, Paed = Paederinae, Pseu = Pseudopsinae, Scyd = Scydmaeninae, Soli = Solieriinae, Stap = Staphylininae, Sten = Steninae. Significance values (in parentheses) are included after the distance values: * = $p < 0.05$, ** = $p < 0.005$, *** = $p < 0.001$, and n.s. = not significant.

	Euae	Lept	Mega	Outg	Oxyp	Paed	Pseu	Scyd	Soli	Stap
Lept	10.34 (*)									
Mega	12.18 (*)	14.54 (***)								
Outg	11.16 (*)	13.01 (*)	9.89 (n.s.)							
Oxyp	14.47 (n.s.)	17.78 (n.s.)	10.61 (***)	9.77 (*)						
Paed	5.80 (**)	9.55 (*)	10.38 (n.s.)	9.54 (***)	12.41 (**)					
Pseu	6.23 (*)	9.93 (n.s.)	10.80 (n.s.)	10.93 (*)	14.98 (***)	6.52 (*)				
Scyd	7.18 (**)	7.34 (*)	12.21 (*)	10.59 (**)	15.56 (**)	7.52 (***)	8.11 (*)			
Soli	14.02 (n.s.)	11.40 (***)	19.12 (n.s.)	14.85 (*)	21.61 (***)	14.63 (*)	13.45 (n.s.)	11.47 (n.s.)		
Stap	10.29 (***)	14.76 (**)	11.12 (**)	9.03 (***)	10.73 (*)	9.29 (***)	12.13 (**)	11.23 (***)	17.52 (*)	
Sten	7.94 (n.s.)	9.89 (***)	12.67 (***)	10.15 (*)	15.06 (n.s.)	6.42 (*)	6.85 (***)	8.69 (*)	12.51 (n.s.)	12.24 (**)

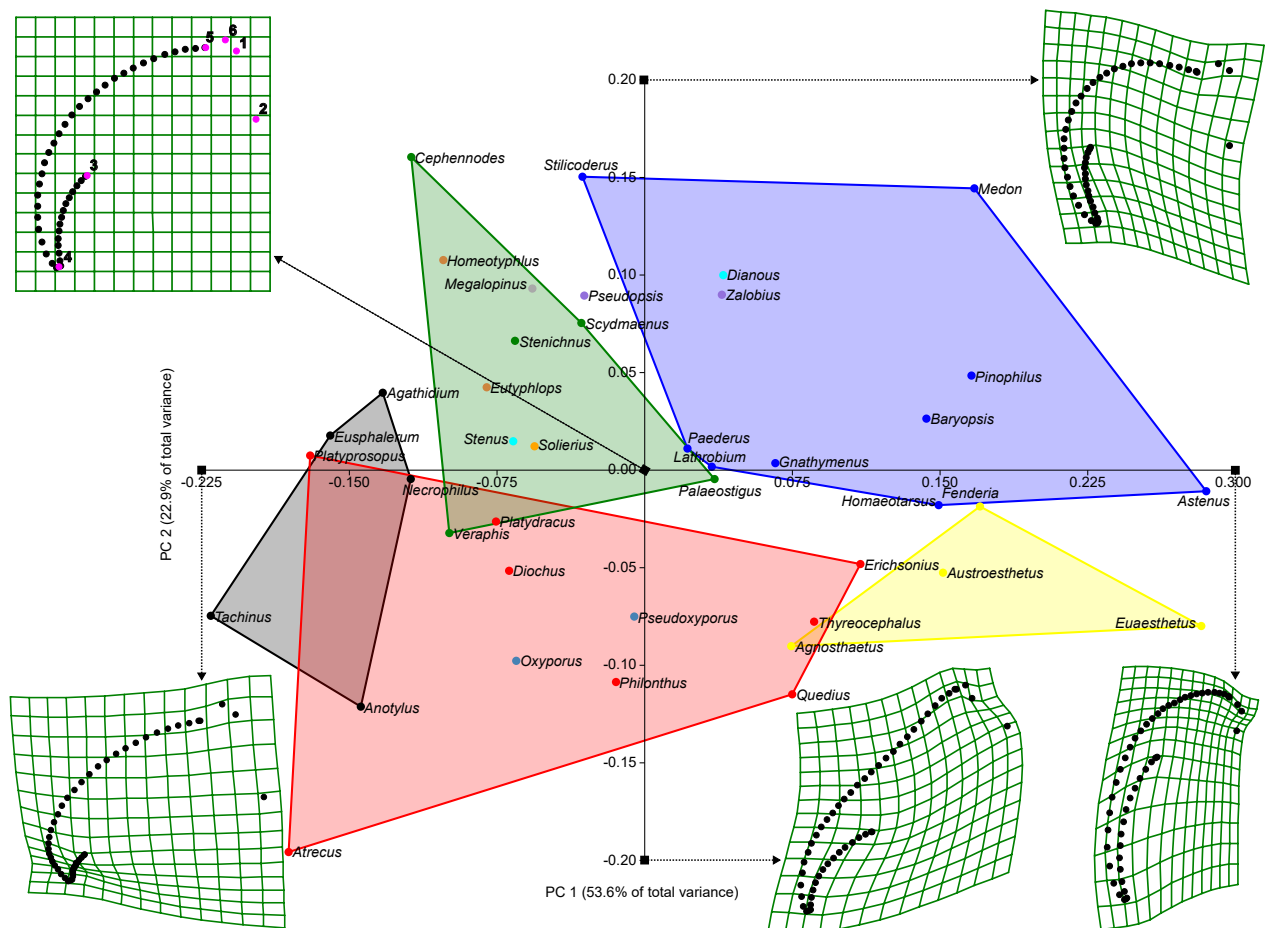


Figure 13. Principal component analysis of mandible shapes. Deformation grids are assigned to the maximum and minimum values of each axis, and in the center, the deformation grid (upper left) of the consensus shape of all species, with pink dots representing the landmarks and black dots the semilandmarks. Convex hulls are displayed for subfamilies (and the outgroup) with more than three species studied. Each dot or convex hull color in the plot corresponds to a subfamily or outgroup species as follows: Oxyporinae = blue-gray, Megalopsidiinae = gray, Solieriinae = orange, Steninae = aqua, Euaesthetinae = yellow, Scydmaeninae = green, Leptotyphlinae = brown, Pseudopsinae = purple, Paederinae = blue, Staphylininae = red, Outgroup = black.

Mahalanobis distances based on canonical variate analysis were calculated between the subfamilies and the outgroup species as a distinct group (Table 2).

Two correlation analyses were performed, between PC 1 and the inlever/outlever quotient (Fig. 16), and be-

tween PC 2 and the inlever/outlever quotient (Fig. S1). They show that falciform mandibles with a narrow base (i.e., high PC 1 values) tend to correlate with relatively fast-closing mandibles (i.e., a low inlever/outlever quotient), such as in *Astenus* and *Euaesthetus*; and that falciform

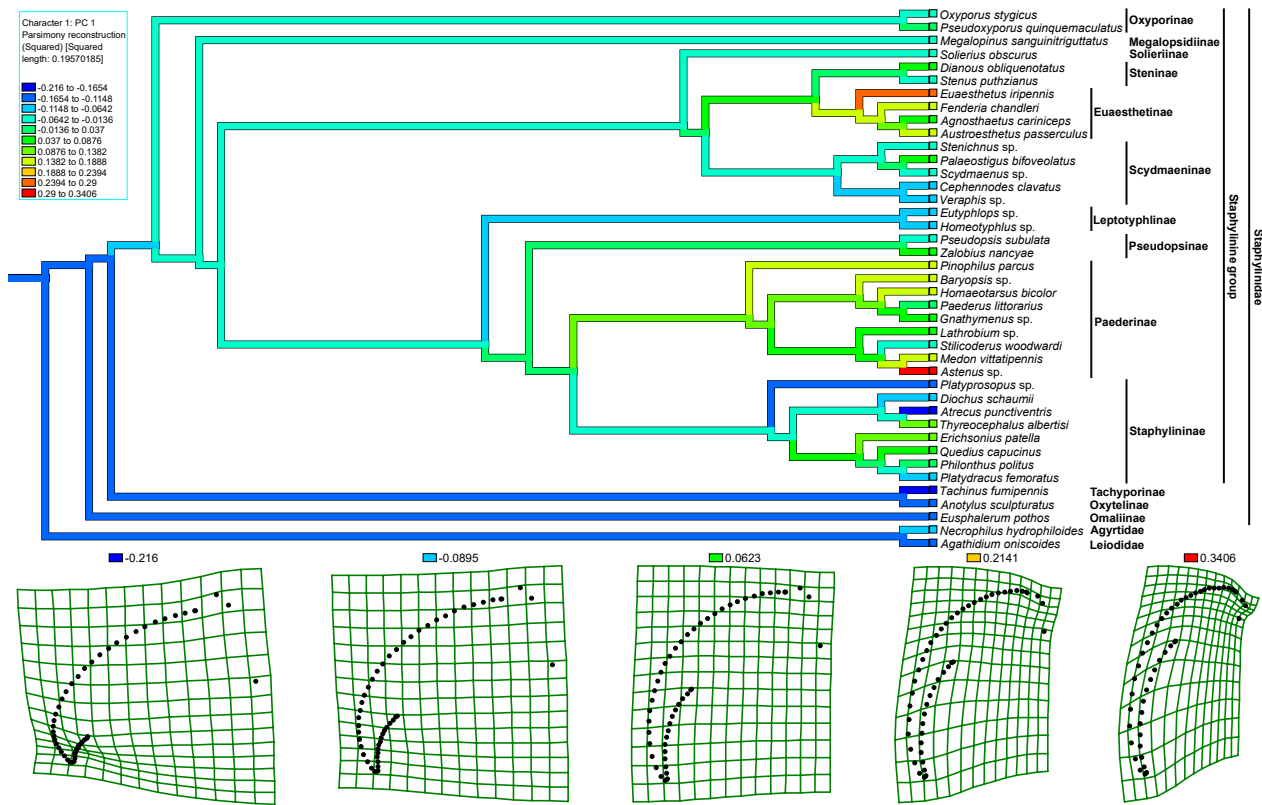


Figure 14. Ancestral character state reconstruction of PC 1 (cf. Fig. 13) as continuous data based on the maximum parsimony method. Color gradient automatically generated by Mesquite ranging from the smallest to the largest PC 1 values, with colder colors representing lower PC 1 values and warmer colors higher PC 1 values. Deformation grids below show mandibular shapes represented by different values of PC1 (small colored squares).

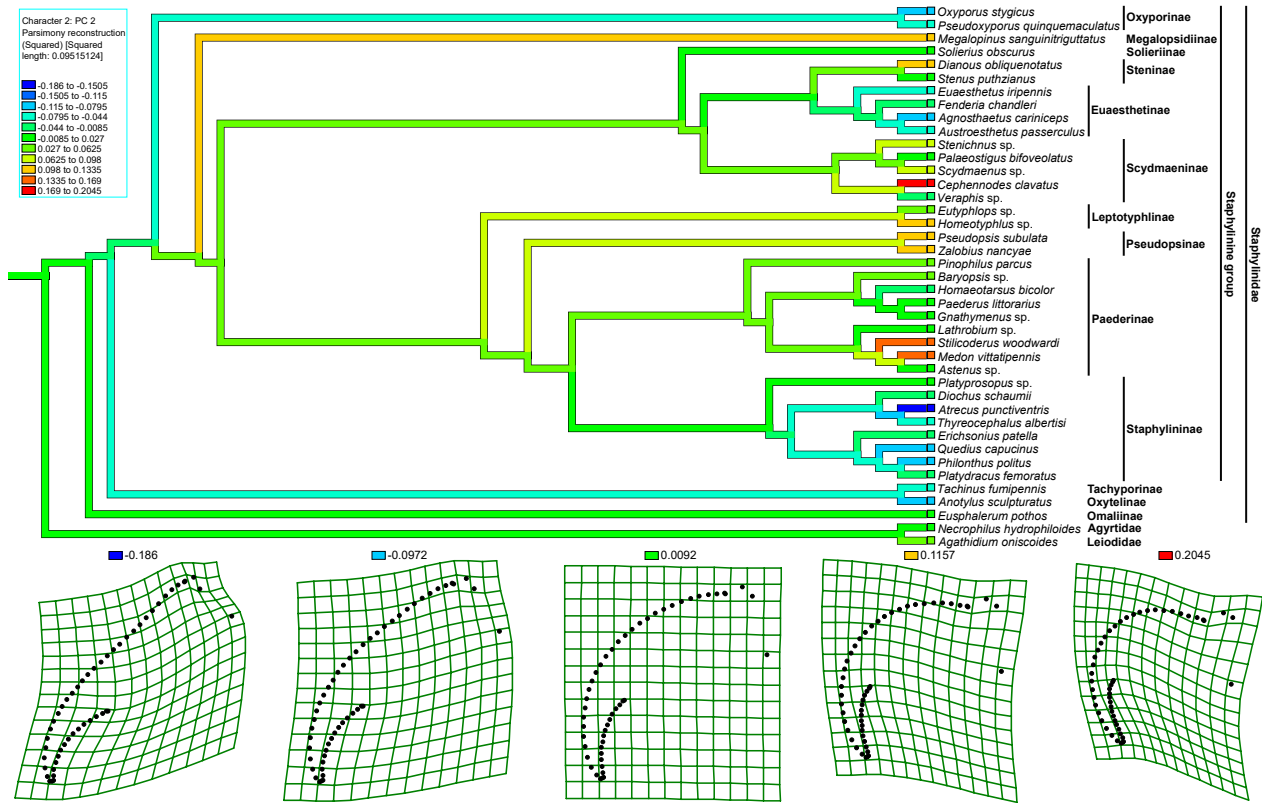


Figure 15. Ancestral character state reconstruction of PC 2 (cf. Fig. 13) as continuous data based on maximum parsimony method. Color gradient automatically generated by Mesquite ranging from the smallest to the largest PC 2 values, with colder colors representing lower PC 2 values and warmer colors higher PC 2 values. Deformation grids below show mandibular shapes represented by different values of PC2 (small colored squares).

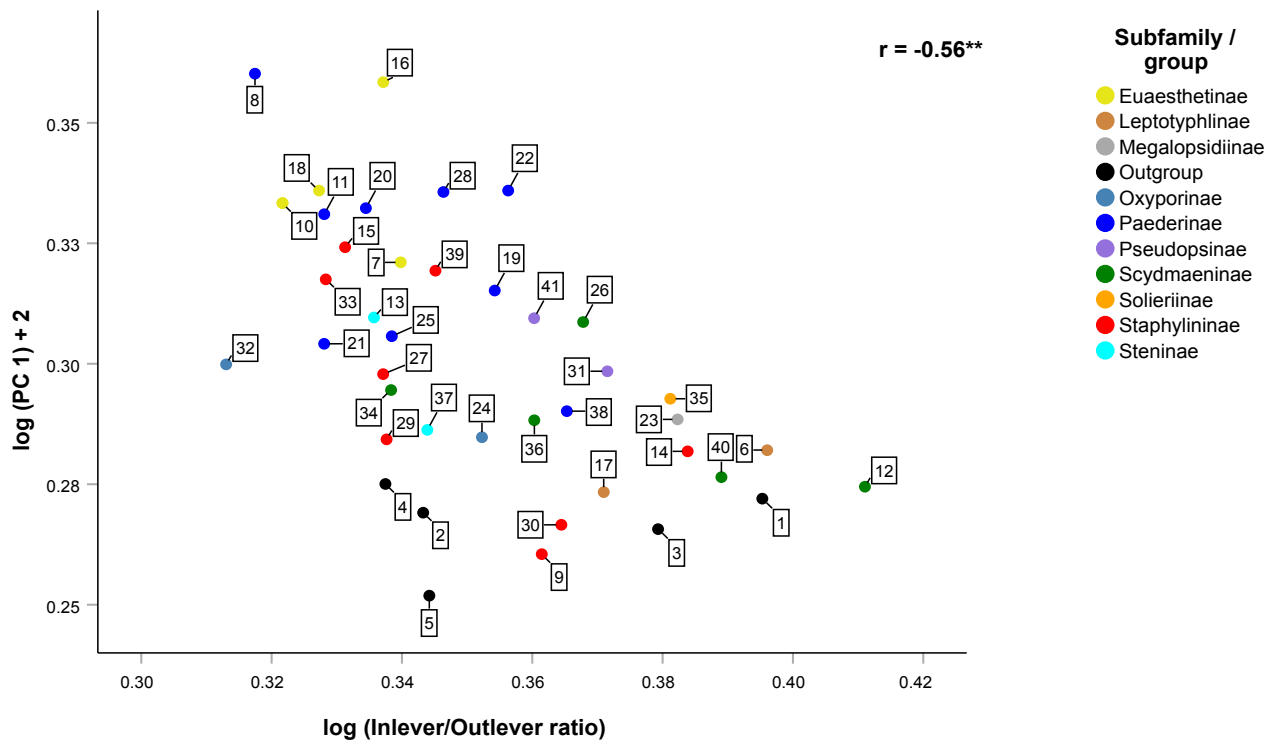


Figure 16. Correlation between log-transformed PC 1 as obtained from the geometric morphometric shape analysis of the mandibles (cf. Fig. 13) and the log-transformed inlever/outlever ratio of the mandible (cf. Table S4). Each dot represents a different species, color-coded by subfamily or group. Species numbers are explained in Table 1. r = Pearson's correlation coefficient. $^{**} = p < 0.01$. The negative correlation also holds true for an analysis using phylogenetic independent contrasts ($r = -0.46^{**}$).

form mandibles with a broad base (i.e., high PC 2 values) tend to correlate with high relative output forces (i.e., a high inlever/outlever quotient), such as in *Cephenmodes* and *Homeotyphlus*. As explained above, the in-lever/out-lever ratio is indicative of both relative mandible force output and relative kinematic transmission. Smaller ratios mean a lower force and faster closure, whereas larger ratios mean a higher force and slower closure (e.g., Weihmann et al. 2015; Blanke 2019). However, we need to consider that the values of the PCs are related to the overall shape, and not only to the inlever/outlever ratio, and that, therefore, the pattern described above is not always true; nonetheless, this trend is seen.

4. Discussion

In the current study, we focus on the various subfamilies traditionally assigned to the Staphylinine group, because their head and mouthpart morphology in the context of feeding has been neglected so far, despite these clades contributing significantly to the vast diversity of Staphylinidae (26,480 species worldwide, placed in 63 higher taxa ((sub)tribes): AFN unpublished data). Stocker et al. (2022) have recently performed an ecomorphological analysis of selected species of Staphylininae and Paederinae; however, this is an exception, and such studies are rare. Our comprehensive comparison of the head morphology of representatives of the Staphylinine

group is a contribution to an understanding of mouthpart divergence across subfamilies within Staphylinidae. Both adults and larvae of the selected subfamilies are predators, many having evolved complex mouthpart modifications that are correlated with their highly specialized feeding and extra-oral digestion (e.g., Evans 1964; Betz 1996; Beutel and Molenda 1997; Betz et al. 2003; Leschen and Newton 2003; Jałoszyński and Beutel 2012; Beutel et al. 2021). They include not only predators (both generalists and specialists), but also obligate feeders on fungal hyphae and fruit and nectar feeders (Thayer 2016).

The Staphylinine group is included in the superfamily Staphylininoidea, one of the most diverse insect groups on Earth. This superfamily has a relatively basal phylogenetic position among the Polyphaga (Hunt et al. 2007; Zhang et al. 2018; McKenna et al. 2019), and therefore, such comparative studies are of great importance for our understanding of the evolution of this suborder. As justified in the Introduction, although the monophyly of the Staphylinine group and some of its subfamilies has recently been questioned by molecular studies (McKenna et al. 2015; Kypke 2018), we retain this morphology-based concept here because recent studies did not yield a conclusive solution yet (Gusarov 2018; also see Zhang et al. 2018 for a contradictory result regarding the Staphylinine group compared with that of Kypke 2018).

Below, we discuss the functional aspects of the feeding apparatus and the possible morphological groundplan features of the Staphylinine group based on the species studied herein and compare them with the complex of

groundplan features previously assumed to constitute the groundplan of microphagous mouthparts in basal staphylinoids (Betz et al. 2003). We also discuss the diversity of mouthpart and protarsus morphologies found in the members of the Staphylinine group and further elaborate some details regarding the form and function of the mandibles.

4.1. Morphofunctional and groundplan features of the feeding apparatus

4.1.1. Labrum-epipharynx

In Staphyloidea, the groundplan condition is the form that also occurs most often within the Staphylinine group, with a transverse labrum (Blackwelder 1936; Naomi 1988a). Our analysis regarding the anterior margin of the labrum and the medial surface of the epipharynx has yielded the groundplan condition of these characters for Staphylinine as ambiguous (Fig. 12). On the other hand, our analysis has shown that the groundplan state of the epipharyngeal surface in Staphyloidea is the same as found in Betz et al. (2003), i.e., bearing a bristle-trough bordered by hairs or spines involved in concentrating and directing the food stream in the median line. Half of the Staphylinine species that we studied possess the character state of the epipharyngeal surface with a bristle-trough. This fact supports the view that bristle-troughs in staphylinoids are functionally connected not only to a microphagous feeding style but might also have an important role in the context of predation in some members of the Staphylinine group. The rows of trichomes forming the bristle-trough have also been described by other authors in Ptiliidae (Yavorskaya et al. 2017) and Leiodidae (e.g., Wheeler and Miller 2005; Antunes-Carvalho et al. 2017), but also in non-staphylinoid polyphagans (e.g., Anton and Beutel 2004, 2012), and in Myxophaga (e.g., Anton and Beutel 2006; Yavorskaya et al. 2018b).

The rotary mill behavior as described for *Philonthus* by Evans (1964) is closely associated with the labrum-epipharynx complex. The shape of the labrum might give hints as to the performance of this behavior among the staphylinines. Evans (1964) provided an illustration and described how a food item passes through the medial notch of the labrum during the rotary mill process. Leschen and Newton (2003) suggested that the mill might serve as a filter for larger indigestible particles for fluid feeders. The feature of additional filtering would therefore only be possible in groups that have such a notch present in the labrum. Such filtering has been observed in Megalopsidiinae (Leschen and Newton 2003) and some Staphylininae (*Philonthus*, Evans 1964). The Oxyporinae possess a notch in the labrum, although the rotary mill behavior has never been observed in this group, despite studies in which their feeding behavior has been closely observed (Newton 1984; Leschen and Allen 1988; Lipkow 1997). The rotary mill behavior has also been reported in Steninae (Betz 1999); however, their labrum shape (Fig. 1E, F) is differ-

ent from that of Megalopsidiinae and Staphylininae in that the medial notch is missing. The absence of the medial notch prevents the movement of pushing the food dorsally as in *Megalopinus* (as shown in Leschen and Newton 2003) and *Philonthus* (as shown in Evans 1964). Therefore, a special additional filtering feature of the rotary mill is unlikely to be present in the Steninae.

The orientation of the trichomes present on the surface of the epipharynx can be associated with the function of directing solid food particles, either by preventing the ingestion of solid food when they are anteriorly directed (Evans 1964) or by directing food particles toward the pharynx when they are posteriorly directed (Yavorskaya et al. 2017; Antunes-Carvalho et al. 2017), the latter case being the groundplan condition in Staphyloidea (Betz et al. 2003). As shown by our results (Figs 1, 2), the orientation or even presence of the trichomes varies quite substantially among members of the Staphylinine group. For example, in Oxyporinae, the epipharynx trichomes are directed posteriorly (Fig. 1A, B), contradicting its hypothesized function of preventing the ingestion of solid food. Even though the diet of these beetles consists of fluid via extra-oral digestion (Newton 1984; Leschen and Allen 1988; Thayer 2016), when the trichome orientation is considered, the function of the epipharynx apparently deviates from the other members of the group regarding at least the way in which the food is directed to the mouth opening. The high variability found in this character leads to the hypothesis of the Staphylinine group members showing a great diversity of feeding styles, the direction of the trichomes of the epipharyngeal (together with the hypopharyngeal) tuft being the main indication for determining whether larger food particles are directed toward (i.e., trichomes posteriorly directed) or away from (i.e., trichomes anteriorly directed) the mouth opening. Megalopsidiinae, Steninae, Euaesthetinae, some Scydmaeninae, Leptotyphlinae, and some Staphylininae have an epipharynx that is completely or mainly devoid of trichomes, so such a function of directing food items seems to be absent in these species.

4.1.2. Mandibles

The potential groundplan condition of the mandibles in the staphylinine group according to our character mapping analysis based on maximum parsimony (Fig. 12) is the following: subapical tooth absent; retinaculum absent; prostheca present, not forming a lobe-like projection; mola present. Subapical tooth and retinaculum are terms usually used to refer to mandibular teeth present in Coleoptera larvae (Böving and Craighead 1931; Lawrence et al. 2011). In adult beetles, they were consistently used and clearly differentiated by Betz et al. (2003) in their study on Staphyloidea and are similarly interpreted and used herein. Nevertheless, the term retinaculum has also been used by Ball et al. (2011) in Carabidae but is not homologous to our usage. Luo et al. (2021), in their anatomical study of a pselaphine (Staphylinidae) species, state that it is difficult to interpret the phylogenetic significance of series of subapical mandibular teeth. Many au-

thors in their descriptions refer only to “mandibular teeth” while disregarding their positions (as being on the incisor area of the mandible or not), thereby making it difficult to homologize their designation with our current interpretation (sensu Betz et al. 2003). Notwithstanding, Naomi (1988a) proposed that the likely groundplan condition for the mandible of staphylinoids is without any teeth, i.e., the absence of both subapical teeth and retinaculum. On the other hand, Betz et al. (2003) found retinacula widespread among adult sporophagous staphylinoids. Two other groundplan aspects of the assumed microphagous primitive staphylinoid are the well-developed prostheca and mola (Naomi 1988a; Betz et al. 2003; Beutel and Yavorskaya 2019). The Staphylinine group typically lacks the mola, with few exceptions (Thayer 2016). Our data show the presence of a mola in the Oxyporinae, Solieriinae, Scydmaeninae (*Scydmaenus*), Pseudopsinae (*Pseudopsis*), and Staphylininae (*Diachus*). According to our tree, the only group to possess a “true” plesiomorphic mola is the Oxyporinae, the other groups having a secondarily evolved (pseudo)mola. This hypothesis is however difficult to establish, as the relationships of these groups remain doubtful (Hansen 1997; Grebennikov and Newton 2009; McKenna et al. 2015). Since the absence of a mola is usually associated with predators (Hansen 1997; Beutel and Yavorskaya 2019; Krenn 2019) (see discussion further below), the secondary evolution of a (pseudo)mola in these beetles might indicate feeding strategies that differ from the specialized extra-oral digestion feeding type that is markedly present in the Staphylinine group.

Steninae have been the subject of several ecomorphological studies and investigations into feeding behavior (e.g., Jenkins 1960; Betz 1996, 1998, 1999, 2002, 2003; Kölsch and Betz 1998), whereas the Euaesthetinae have largely been neglected in this respect. The only records known to us are from Remillet (1969) who fed diplurans to a specimen of *Octavius massatensis* Coiffait, 1959 and from Orousset (1988) who reported the presence of a specimen of oribatid mite attached to the mouthparts of a dead specimen of *Tyrannomastax* Orousset, 1988. We can, however, infer, based on their morphology, that the Euaesthetinae are predators that feed on small arthropods, because their mandibles are slender and falcate (Clarke 2018), similar to those of Steninae, which are optimized for hunting agile prey. The retinaculum in the Euaesthetinae might function similarly to the subapical tooth present in the Steninae for holding prey after capture, but more closely to the body. The size of the lacinia and galea are notably shorter in Euaesthetinae when compared with its sister group Steninae. This might also be an adaptation toward handling food items that are more proximally located, as is the retinaculum.

The prostheca can be interpreted as a tool for gathering and transporting food particles toward the mouth, as stated by Betz et al. (2003), although the taxa that they studied were microphagous spore feeders. In contrast, the taxa examined herein are predators that feed on fluids, and therefore, the prostheca might have evolved a different function. Evans (1964) suggests that the prostheca (referred to as “penicillus”) of *Philonthus* assists with

both the fluid intake and extrusion of digestive fluids. Stocker et al. (2022) have also proposed that the presence of the prostheca in staphylinines allows a “mixed-feeding strategy”, and that its lack represents a specialized predatory morphology. *Veraphis* possesses a distinct type of prostheca (Fig. 3L) that might be used as a pseudomola because of its morphology and position.

Only six species of the ingroup studied here possess a developed molar region: the two oxyporine species, which are interpreted as having retained its plesiomorphic form as stated previously, and four other species (*Solierius*, *Scydmaenus*, *Pseudopsis*, and *Diachus*) that evolved it secondarily. Therefore, the feeding conditions that can be linked to the secondary evolution of a pseudomola are worthy of discussion. *Solierius* is a rare group, and nothing is known about its feeding behavior (Thayer et al. 2012; Thayer 2016). Scydmaeninae feeding habits have been reviewed in Jałoszyński (2018). According to Jałoszyński (2012a, 2012b), two species of *Scydmaenus* have been shown to prefer Collembola or soft-bodied Acari and display no interest in specimens of Oribatida under controlled laboratory conditions. Additionally, that author has reported the scavenging of dead arthropods and cannibalistic behavior exhibited by these species. Jałoszyński (pers. comm.) has however pointed out the difficulties in observing precisely the way that such small beetles use the specific parts of their mandible. Therefore, we currently lack information concerning the employment of the pseudomola of *Scydmaenus* or the pseudomola-like prostheca of *Veraphis* during the feeding process. Regarding the feeding habits of *Pseudopsis*, Klimaszewski et al. (2013) found that the gut of these beetles contains traces of yeast, but no arthropod cuticle. The authors have nevertheless concomitantly determined the presence of eight unidentified DNA strands indicating that an extra-oral digestion feeding strategy is a plausible explanation for the missing cuticle particles in the examined gut. Little is known about the biology of *Diachus*.

As the shape of the mandible might not fit precisely into a categorical description, we performed a 2D geometric morphometric analysis based on (semi-)landmarks. The value of PC 1 in this analysis (Figs 13, 14) refers mainly to the extent to which the mandibles are sickle-shaped and their apices are pointed. The value of PC 2 (Figs 13, 15) refers to their overall curvature, ranging from straight toward strongly curved. Whether the investigated subfamilies have diverged with regard to their mandibular morphology and their connected feeding ecology (as indicated by their partly exclusive occupation of certain regions of the morphospace in Fig. 13) needs to be substantiated in future studies by examining more representatives per subfamily. The shape corresponding to lower PC 1 might be functionally associated with: (1) non-predatory staphylinoids (e.g., *Tachinus* (Klimaszewski et al. 2013) and *Anotylus* (Thayer 2016; Okuzono and Tokuda 2022)), or (2) more generalist feeders (including predators) possibly using their mandibles for a wide variety of food items and using strong force against certain food types, for example, *Platydracus* beetles have a relatively robust mandible (Figs 4Q, 13) used to feed on various kinds of

prey, ranging from soft and lightly sclerotized dipteran maggots to hard and heavily sclerotized oribatid mites (ELS unpublished observations), or (3) more specialized predators of heavily sclerotized organisms such as some Scydmaeninae that are specialized for feeding on sclerotized mites (Jałoszyński 2018). The more robust shapes corresponding to lower PC 1 also correspond to high in-lever/outlever ratios (Fig. 16) because of the increased length of the inlever and shortened outlever length (see, for example, the hypothetical model in Fig. 13 at -0.225 along the x-axis), which translate into higher force output but lower velocities to close the mandibles (see Table S3). The slender falcate and curved shapes corresponding to higher PC 1 values are characterized by low in-lever/outlever ratios because of the narrow base (small in-lever length) and long length (large outlever length) allowing faster closing movements and can be considered as adaptations by predators specialized on elusive prey that are not heavily sclerotized (Betz et al. 2018; Stocker et al. 2022). *Astenus* (Paederinae) is a good representative of such a specialized predatory mandible shape, and indeed, members of this genus feed on entomobryid springtails (Collembola) (Assing 2015). Stocker et al. (2022) suggested that the paederine genus *Rugilus*, which is closely related to *Astenus* (Żyła et al. 2021) and which possesses falcate mandibles, is also adapted toward feeding on elusive springtails. Other representatives of the Staphylinine group that fall in the regions of the morphospace of falcate mandibles (e.g., *Pinophilus* or *Medon*) might also represent predators that are capable of preying upon especially vigilant prey. In the ancestral character reconstruction of PC 1 (Fig. 14), the Staphylinine group exhibits lower PC values, suggesting a tendency towards mandibles with a predatory shape when compared to the outgroup.

The functional consequences and feeding types that are related to the shape changes associated with PC 2 (straight versus curved mandibles) remain to be clarified. Future comparative studies on the feeding ecology of rove beetles should help to improve our understanding of relationships between morphology and ecology.

Mahalanobis distances between the subfamilies (and outgroup species) with resulting *p* values of the CVA to quantify the separations between the subfamilies (and the outgroup species) are shown in Table 2.

4.1.3. Maxillae

For a definition of the groundplan aspects of the maxilla in Staphylinoidea, Naomi (1988b) considered the major parts of the maxilla, i.e., cardo, stipes, palpifer, lacinia, and galea. Blackwelder (1936) stated that the cardo, stipes, galea and lacinia are subject to much variation and Hansen (1997) suggested that the lacinia was probably not a particularly informative character at higher taxonomic levels because of its high variability. Betz et al. (2003), however, focused on the functional parts of the maxilla, i.e., the lacinia and galea, and showed that the groundplan condition in Staphylinoidea was most likely a microphagous maxilla with brush-, rake-, or comb-like structures for sweeping in diffuse food material. Yavorskaya et al.

(2017) also paid close attention to some structures of the maxilla regarding the fimbriate galea and the curved rows of trichomes. Such features were interpreted by them to be present in the ancestor of Staphyliniformia and related to a microphagous feeding style. Our data confirm that the lacinia and galea are diverse among staphylinines, and therefore, we follow Hansen's (1997) interpretation that these characters are uninformative at higher taxonomic levels and ignore them in our character mapping analysis. The high variability reflects the strong selective demands on these structures, as they probably serve as important tools in the context of feeding (Betz et al. 2003). Hansen (1997) nonetheless considered maxillary palpomere 4 to be informative for higher taxonomic levels, and we also have included it in our character mapping analysis. In addition, Betz et al. (2003) pointed out that the palpifer may serve as a mechanical support for the galea, which can also be seen in *Megalopinus* (Fig. 5B).

For the character mapping analysis, we investigated the apical unarticulated spine of the lacinia and maxillary palpomere 4. The apical unarticulated spine of the lacinia, even though it was rendered as ambiguous for the groundplan of the Staphylinine group, was identified as a groundplan feature of the hypothetical ancestor between the split of Oxyporinae + the rest of the staphylinines (Fig. 12). Maxillary palpomere 4, on the other hand, was unambiguously rendered as “well developed, fully sclerotized, similar in width to palpomere 3”, as the groundplan state for the Staphylinine group. Hansen (1997) interpreted this state as being basal to most of the Staphyliniformia families and subfamilies. A spine on the lateral margin of the galea was present in *Agnosthaetus*, but we did not score it on our character mapping analysis since it is an autapomorphic character for this genus and therefore not informative for our purposes. Nonetheless, this character was used by Clarke and Grebennikov (2009) as they had analyzed another genus that also possessed this feature.

No suggestions have been made in the aforementioned literature that the maxillae are used for fluid uptake. However, Wilhelmi and Krenn (2012) reported that the maxillary palps, together with the galea and lacinia, might be adapted in some groups of beetles to feed on nectar. In Scarabaeidae, the maxillae have been described as being moistened with nectar, enabling the adherence of pollen grains (Karolyi et al. 2009). The maxillary brushes of the highly specialized leiodid *Platypsyllus castoris* Ritsema, 1869 were considered a tool for transferring fluid to the mouth by capillary forces (Yavorskaya et al. 2023). The feeding behavior of *Philonthus* was closely studied by Evans (1964), whose findings confirmed the occurrence of extra-oral digestion involving a fluid feeding technique. In addition to these behavioral observations, an analysis of the gut has revealed the presence of finely divided solid content (Evans 1964). Such information (together with the maxilla's dense brushes present on both lacinia and galea) sustain a hypothesis that in *Philonthus* and closely related groups the dense brushes aid the ingestion of a fluid diet, probably via capillarity, as described in *Platypsyllus*. The combination of dense brushes on the maxillae together with an epipharynx with anteriorly directed

trichomes might help to determine whether a beetle is an exclusive fluid feeder. Interestingly, *Diochus* is the only member of the Staphylininae that we have studied that possesses a developed molar region and is the only one to have a lacinia bearing significantly short trichomes. This suggests that *Diochus* does not feed exclusively on fluids.

4.1.4. Labium-hypopharynx

The most phylogenetically informative characters of the labium-hypopharynx complex probably concern the labial palpomeres. In this study, we have focused on the apical palpomere, which serves as a diagnostic feature of some groups, such as the Oxyporinae in which it is strongly expanded, whereas the Solieriinae and the clade Steninae + Euaesthetinae have a distinctly reduced type. According to our results, the most likely hypothesis is that the staphylinine ancestor would have had a labial palpomere 3 “about as wide to half as wide as penultimate palpomere”. Naomi (1988b) also considered the labial palpomere 3 when establishing the groundplan conditions of Staphylinoida, considering it as “about as long and a little thinner than the 2nd”, which does not agree with our description model but might overlap our definition. Hansen (1997), however, considered this to be an informative character only at lower taxonomic levels.

Another character that has some phylogenetic potential is the ‘glossa’, which has not previously been explored in such a context. Our interpretation suggests that it is a good character for separating the clade Paederinae + Staphylininae from the other groups. These subfamilies share mainly a ‘glossa’ that is dorsally modified into anterior lobes, which are sometimes bulbous and covered with sensilla coeloconica. Naomi (1988b) states that most staphylinoids have ‘glossae’ and ‘paraglossae’ fused (ligula) in various degrees, characterizing the ligula as synglossa or hologlossa according to its degree of fusion. Betz et al. (2003) refrained from using the terms ‘glossa’ or ‘paraglossa’ and instead referred to ligula, e.g., by saying: “Ligula represented by antero-lateral lobes of prementum plus anteriorly directed setae in different numbers and arrangements at distal margin of prementum.” However, in the present work on the Staphylinine group, we have not followed this terminology any longer, because, at the distal margin of the prementum, we can often clearly distinguish between lateral lobe (i.e., the ‘paraglossae’) and a median assemblage of paired sensilla or differentiated lobes (i.e., the ‘glossae’) as separate structures. However, since many authors consider the ‘glossa’, together with the ‘paraglossa’, to be lacking or completely reduced in Coleoptera (e.g., Crowson 1981; Beutel and Lawrence 2016), we have put these terms in quotation marks throughout the text.

A notable feature in the genus *Stenus* is the ‘paraglossae’ on which the sticky pads of its highly specialized adhesion-capture apparatus are located (Betz 1996; Betz et al. 2018). Few studies have been carried out on the function of this region in other staphylinids. Indeed, the morphological definition of the ‘paraglossae’ as a distinct structure is not clear in Coleoptera, it being usually con-

sidered as completely reduced or fused with the ‘glossae’, forming a ligula (Crowson 1981; Beutel and Lawrence 2016). Clarke and Grebennikov (2009) discussed the potential presence of sticky pads also being present in an undescribed genus originally suspected of being a member of the Euaesthetinae (Leschen and Newton 2003; Betz and Kölsch 2004). However, following a phylogenetic analysis, the genus has ended up being considered a member of the Steninae, as the potential sister group of *Stenus*. In the same study, Clarke and Grebennikov (2009) pointed out the difficulties of the term ‘paraglossa’ and ‘glossa’ being treated as distinct and cited studies reinforcing the idea that they are probably fused with the ‘glossa’ as a ligula. Nonetheless, as explained in the last paragraph we refer to both ‘glossa’ and ‘paraglossa’ between quotation marks as there are no accepted terms at the moment for these distinct structures. We score our character matrix with three distinct states for the ‘paraglossa’: the highly specialized type present in *Stenus*, the type with inconspicuous antero-lateral lobes, and the type in which the lobes are represented by prominent anterior or digitiform lobes. Most members of the Staphylinine group have the potential groundplan condition of inconspicuous antero-lateral lobes (e.g., Figs 8B, 9O), whereas in Euaesthetinae, the genera *Austroesthetus* and *Agnosthaetus* possess the third type represented as anterior digitiform lobes (Fig. 8E, H), whose specific function (e.g., during prey-capture) needs to be elucidated.

The dorsal part of the prementum has been poorly documented in morphological studies. We have explored it here, as we consider this region to be closely involved in the food intake process as this is the side that the food item will first pass through while being directed to the mouth opening via the hypopharynx. A glabrous prementum surface is the trend that most repeats within the Staphylinine group, but it varies considerably in the presence of setae or sensilla, or both. We have characterized the lateral margin with regard to the types of trichomes present: hair-like, conspicuous spine-like, or comb-like. These types have been used in our character mapping analysis (Fig. 12), however for the establishment of the groundplan feature of the Staphylinine group, it was rendered ambiguous.

Betz et al. (2003) designated the groundplan of the staphylinoid hypopharynx as having a tuft of posteriorly directed trichomes working together with the epipharynx to direct food toward the pharynx. In the investigated staphylinines, hair-like trichomes are usually present on its surface, but not always forming a tuft. Great variation has been found in this area within the Staphylinine group. A comparison of *Quedius* (Fig. 9O) with *Platydracus* (Fig. 9P) illustrates its high variability. Even though these two groups are both members of the same tribe, namely the Staphylinini, *Quedius* is medially glabrous, whereas *Platydracus* is provided with a dense vestiture, forming a tuft. We have not included this character in our trait mapping analysis because of its being a highly variable (apparently evolutionarily labile) character and therefore uninformative for higher taxonomic level analysis.

The function of the labium-hypopharynx has been extensively studied in the extreme case of *Stenus* (e.g., Betz

1996, 1998; Kölsch and Betz 1998; Koerner et al. 2012), which has an elongated labium type with the addition of adhesive pads at the tip, adapted for sticking to elusive prey such as collembolans. Another case of a highly modified labium is found in the scydmaenine *Cephenodes*, with labial discs adapted for suction (Jałoszyński and Beutel (2012). Similarly to the state in some other species within Scydmaeninae in our study, this region was entirely covered by the hypopharynx, which prevented us from more closely describing these structures. The functional aspect of this region in other Staphylinidae has been poorly studied. Weide et al. (2010) explored its potential protrusibility and retractability in species of Aleocharinae and the way in which the hypopharynx serves as a receptacle for receiving spores, which are subsequently ground by the mola or pseudomola. To infer the degree of protrusibility and retractability, they used microCT data. We cannot infer this motility with such precision from our data, but there are examples of at least potential movements of the prementum-hypopharynx complex in Scydmaeninae, as some of the specimens that we studied had their premental dorsal surface covered by the hypopharynx (see Fig. 8L for both covered/uncovered views in the same species). Interestingly, *Scydmaenus* is one of the few members of the Staphylinine group studied herein to possess a mola that could potentially work together with the retractability of the prementum. In Ptiliidae and Leiodidae (Staphyliinoidea), the longitudinal arrangement of abundant trichomes on the dorsal surface of the prementum and the hypopharynx has been interpreted to work in combination with the epipharyngeal trichomes, gathering and directing the food flow in the midline (Betz et al. 2003; Antunes-Carvalho et al. 2017; Yavorskaya et al. 2017).

Functional studies of the ‘glossa’ and ‘paraglossa’ in beetles are also lacking, as they are usually reduced and sometimes even considered lost in many groups of Coleoptera (Crowson 1981; Beutel and Lawrence 2016). In Coleoptera, the ‘glossa’ and ‘paraglossa’ are usually fused forming a ligula, which has been reported to be involved, for example, in fluid (nectar) uptake in Scarabaeidae (Karolyi et al. 2016) and Lucanidae (Krenn et al. 2002). Evans (1964) described the function of the labium-hypopharynx complex in *Philonthus*. He mostly referred to the hairs present on the hypopharyngeal surface, suggesting that they help prevent large pieces of food from being directed to the mouth. He also mentioned the prominent lateral spine-like trichomes on the dorsal region of the prementum, assuming that their function is to hold the food item between the mandibles and maxillae while it is being processed.

4.1.5. Protarsi

The groundplan tarsal formula for Staphyliinoidea is 5-5-5 (Naomi 1989). Several deviations from this can be found within the family, but, as we have investigated only the protarsi, we will not explore this character in depth, only listing the subfamilies that show some variation on the pretarsus regarding the setal type. In the species of Euaesthetinae that we studied, the tarsomeres vary, ranging

from five to four. Both species of Leptotyphlinae analyzed possess three tarsomeres. In Leptotyphlinae, this reduction is associated with an endogean lifestyle that leads to several reductions, such as body miniaturization, eye reduction, and pigmentation loss (Andújar and Grebennikov 2021). This character has been studied in depth in Steninae (Betz 2003) in which the multiple (currently 14 recognized) types of tenent setae might also have potential for within-genus phylogenetic analyses. However, the presence or absence of spatulate and/or discoid tenent setae is not an informative character for higher level taxonomic analysis as this can be variable among the species of a same genus (see Betz 2003 as an example for the genus *Stenus*). Therefore, we did not include this character in our character mapping analysis. Another character system of phylogenetic value for Staphyliinoidea that we have not explored, is the pretarsus and distal margin of the terminal tarsomere (Antunes-Carvalho and Gnaspini 2016).

While the setal type is not significant at higher taxonomic levels for a character mapping analysis, it is a valuable character that should be considered when the functional morphology of some species is studied. Some Staphylinine group species have been reported to use the first pair of legs to capture prey (Betz and Mumm 2001; Barthold and Betz 2020; Stocker et al. 2022), and the presence of tenent setae might be a cue for a more recurrent usage of this prey capturing and handling method. Another important function associated with the tenent setae in the Staphylinine group is the ability of the beetles to climb plants, as observed in the genus *Stenus* (Betz 2003). In addition, some tenent setae show sexual dimorphism and are probably used for mating (Gnaspini et al. 2017). Therefore, the presence of tenent setae in both sexes might be indicative of active usage in prey capturing behavior.

5. Conclusion

In our study we compared 36 species representing all 10 subfamilies assigned to the traditional Staphylinine group. Together with previous findings from the literature (e.g., Naomi 1988a, 1988b; Hansen 1997; Betz et al. 2003; Jałoszyński and Beutel 2012; Antunes-Carvalho et al. 2017; Yavorskaya et al. 2017), our investigation permits us to suggest potential groundplan features in the mouthparts of the Staphylinine group: labrum subquadrate or longer than wide; mandible without subapical teeth and retinaculum, with prostheca present, not forming lobe-like projection, and with a mola, even though, in the split between Oxyporinae from the rest of the Staphylinine group, the mola was lost, and its absence is ultimately shared by most of the Staphylinine group; maxillary palpomere 4 well-developed, fully sclerotized, similar in width to palpomere 3; ‘glossa’ integrated with prementum plate, sometimes represented by pairs of sensilla basiconica; ‘paraglossa’ represented by inconspicuous

antero-lateral lobes, projected antieriad; labial palpomere 3 about as wide to half as wide as penultimate palpomere. Because of their seeming evolutionary lability, the setal types of the protarsi have not been included in our analyses, but their predatory function has been discussed, and the presence of non-sexually dimorphic tenent setae might be indicative of its usage for prey-capture in a few Staphylinine group members, or other functions such as walking on foliage or flowers (e.g., Stork 1980).

A geometric morphometric analysis was performed to explain the shape of the mandibles of Staphylinine group members, a method previously performed for this group only by Stocker et al. (2022), for members of the Staphylininae and Paederinae. Our results confirm that the last common ancestor of the Staphylinine group was likely a predator as previously hypothesized (Lawrence and Newton 1982; Thayer 2016), based on our mandible shape analysis (Fig. 14). In light of the results shown herein and the hypotheses that can be raised concerning the mandible shape and feeding preferences, we highlight the value of this method and the ease with which it can be applied to future studies of the group. For instance, our data have been used herein to connect the morphology to the behavioral data of *Astenus* and have allowed us to predict or hypothesize that *Medon* and *Pinophilus* are also probably adapted to feed on elusive prey items such as springtails. The method also serves as a viable alternative or additional means for analyzing and describing mandible shapes, as previously published descriptions are often ambiguous and/or imprecise.

6. Acknowledgements

This research was funded by the German Research Foundation (DFG project BE-2233/13-1) as part of the PhD studies of ELS. We thank Monika Meinert for assisting ELS while operating the scanning electron microscope; Benjamin Eggs, Margarita Yavorskaya, Mario Schädel, Benedict Stocker, Michael Csader and Lea von Berg for useful discussions and suggestions; Rolf Beutel and an anonymous reviewer for their helpful comments; Theresa Jones for correcting the English of the manuscript.

The authors gratefully acknowledge the Tübingen Structural Microscopy Core Facility (funded by the Excellence Strategy of the German Federal and State Governments) for its support.

7. References

- Andújar C, Grebennikov VV (2021) Endogean beetles (Coleoptera) of Madagascar: Deep soil sampling and illustrated overview. *Zootaxa* 4963(2): 317–334. <https://doi.org/10.11646/zootaxa.4963.2.4>
- Anton E, Beutel RG (2004) On the head morphology and systematic position of *Helophorus* (Coleoptera: Hydrophiloidea: Helophoridae). *Zoologischer Anzeiger* 242: 313–346. <https://doi.org/10.1078/0044-5231-00107>
- Anton E, Beutel RG (2006) On the head morphology of Lepiceridae (Coleoptera: Myxophaga) and the systematic position of the family and suborder. *European Journal of Entomology* 103(1): 85–95. <https://doi.org/10.14411/eje.2006.014>
- Anton E, Beutel RG (2012) The adult head morphology of *Dascillus* (L.) (Dascilloidea: Dascillidae) and *Glaresis* Erichson (Scarabaeoidea: Glaresidae) and its phylogenetic implications. *Arthropod Systematics & Phylogeny* 70(1): 3–42. <https://doi.org/10.3897/asp.70.e31746>
- Antunes-Carvalho C, Gnaspini P (2016) Pretarsus and distal margin of the terminal tarsomere as an unexplored character system for higher-level classification in Cholevinae (Coleoptera, Leiodidae). *Systematic Entomology* 41(2): 392–415. <https://doi.org/10.1111/syen.12161>
- Antunes-Carvalho C, Yavorskaya M, Gnaspini P, Ribera I, Hammel JU, Beutel RG (2017) Cephalic anatomy and three-dimensional reconstruction of the head of *Catops ventricosus* (Weise, 1877) (Coleoptera: Leiodidae: Cholevinae). *Organisms Diversity and Evolution* 17(1): 199–212. <https://doi.org/10.1007/s13127-016-0305-3>
- Antunes-Carvalho C, Ribera I, Beutel RG, Gnaspini P (2019) Morphology-based phylogenetic reconstruction of Cholevinae (Coleoptera: Leiodidae): a new view on higher-level relationships. *Cladistics* 35(1): 1–41. <https://doi.org/10.1111/cla.12230>
- Assing V (2015) A new myrmecophilous species of *Eurysunius* from Turkey (Coleoptera: Staphylinidae: Paederinae). *Linzer Biologische Beiträge* 47(2): 1113–1118. https://www.zobodat.at/publikation_articles.php?id=255991
- Ball GE, Acorn JH, Shpeley D (2011) Mandibles and labrum-epipharynx of tiger beetles: Basic structure and evolution (Coleoptera, Carabidae, Cicindelidae). *ZooKeys* 147: 39–83. <https://doi.org/10.3897/zookeys.147.2052>
- Barthold S, Betz O (2020) The predatory behaviour of some Central European rove beetles (Coleoptera: Staphylinidae: Staphylininae, Paederinae). *Mitteilungen der Deutschen Gesellschaft für Allgemeine und Angewandte Entomologie* 22: 173–178. https://www.dgaae.de/files/user-upload/publikationen/mitteilungen_der_dgaae/Mitteilungen%2022/0615.pdf
- Betz O (1996) Function and evolution of the adhesion-capture apparatus of *Stenus* species (Coleoptera, Staphylinidae). *Zoomorphology* 116(1): 15–34. <https://doi.org/10.1007/s004350050006>
- Betz O (1998) Comparative studies on the predatory behaviour of *Stenus* spp. (Coleoptera: Staphylinidae): The significance of its specialized labial apparatus. *Journal of Zoology* 244(4): 527–544. <https://doi.org/10.1017/S0952836998004063>
- Betz O (1999) A behavioural inventory of adult *Stenus* species (Coleoptera: Staphylinidae). *Journal of Natural History* 33(11): 1691–1712. <https://doi.org/10.1080/002229399299806>
- Betz O (2002) Performance and adaptive value of tarsal morphology in rove beetles of the genus *Stenus* (Coleoptera, Staphylinidae). *Journal of Experimental Biology* 205(8): 1097–1113. <https://doi.org/10.1242/jeb.205.8.1097>
- Betz O (2003) Structure of the tarsi in some *Stenus* species (Coleoptera, Staphylinidae): External morphology, ultrastructure, and tarsal secretion. *Journal of Morphology* 255(1): 24–43. <https://doi.org/10.1002/jmor.10044>
- Betz O, Kölsch G (2004) The role of adhesion in prey capture and predator defence in arthropods. *Arthropod Structure and Development* 33(1): 3–30. <https://doi.org/10.1016/j.asd.2003.10.002>
- Betz O, Mumm R (2001) The predatory legs of *Philonthus marginatus* (Coleoptera, Staphylinidae): Functional morphology and tarsal ultrastructure. *Arthropod Structure and Development* 30(2): 77–97. [https://doi.org/10.1016/S1467-8039\(01\)00029-9](https://doi.org/10.1016/S1467-8039(01)00029-9)
- Betz O, Koerner L, Dettner K (2018) The Biology of Steninae. In: Betz O, Irmeler U, Klimaszewski J (Eds), *Biology of Rove Beetles*

- (Staphylinidae). Springer, Cham, Switzerland, pp. 229–283. https://doi.org/10.1007/978-3-319-70257-5_11
- Betz O, Thayer MK, Newton AF (2003) Comparative morphology and evolutionary pathways of the mouthparts in spore-feeding Staphylinoida (Coleoptera). *Acta Zoologica* 84(3): 179–238. <https://doi.org/10.1046/j.1463-6395.2003.00147.x>
- Beutel RG, Molenda R (1997) Comparative morphological study of larvae of Staphylinoida (Coleoptera, Polyphaga) with phylogenetic implications. *Zoologischer Anzeiger* 236: 37–67.
- Beutel RG, Vilhelmsen L (2007) Head anatomy of Xyelidae (Hexapoda: Hymenoptera) and phylogenetic implications. *Organisms Diversity and Evolution* 7(3): 207–230. <https://doi.org/10.1016/j.ode.2006.06.003>
- Beutel RG, Baum E (2008) A longstanding entomological problem finally solved? Head morphology of *Nannochorista* (Mecoptera, Insecta) and possible phylogenetic implications. *Journal of Zoological Systematics and Evolutionary Research* 46(4): 346–367. <https://doi.org/10.1111/j.1439-0469.2008.00473.x>
- Beutel RG, Ge SQ, Hörschemeyer T (2008) On the head morphology of *Tetraphalerus*, the phylogeny of Archostemata and the basal branching events in Coleoptera. *Cladistics* 24(3): 270–298. <https://doi.org/10.1111/j.1096-0031.2007.00186.x>
- Beutel RG, Lawrence JF (2016) 4. Coleoptera, morphology. In: Beutel RG and Leschen RAB (Eds), *Coleoptera, Beetles. Vol. 1: Morphology and Systematics*. 2nd edition. Berlin, Boston: De Gruyter, pp. 35–40. <https://doi.org/10.1515/9783110373929-007>
- Beutel RG, Luo X-Z, Yavorskaya MI, Jałoszyński P (2021) Structural megadiversity in leaf litter predators – the head anatomy of *Pselaphus heisei* (Pselaphinae, Staphylinidae, Coleoptera). *Arthropod Systematics & Phylogeny* 79: 443–463. <https://doi.org/10.3897/asp.79.e68352>
- Beutel RG, Yavorskaya MI (2019) Structure and evolution of mouthparts in Coleoptera. In: Krenn HW (Ed.), *Insect Mouthparts. Zoological Monographs* 5; Springer, Cham, pp. 387–418. https://doi.org/10.1007/978-3-030-29654-4_12
- Beutel RG, Zimmermann D, Krauß M, Randolph S, Wipfler B (2010) Head morphology of *Osmylus fulvicephalus* (Osmylidae, Neuroptera) and its phylogenetic implications. *Organisms Diversity and Evolution* 10(4): 311–329. <https://doi.org/10.1007/s13127-010-0024-0>
- Blackwelder RE (1936) Morphology of the coleopterous family Staphylinidae. *Smithsonian Miscellaneous Collections* 94(13): 1–102.
- Blanke A (2019) The early evolution of biting–chewing performance in Hexapoda. In: Krenn HW (Ed.), *Insect Mouthparts. Zoological Monographs* 5; Springer, Cham, pp. 175–202. https://doi.org/10.1007/978-3-030-29654-4_6
- Bolte KB (1996) Techniques for obtaining scanning electron micrographs of minute arthropods. *Proceedings of the Entomological Society of Ontario* 127: 67–87. <https://cfs.nrcan.gc.ca/publications?id=10333>
- Bouchard P, Smith ABT, Douglas H, Gimmel ML, Brunke AJ, Kanda K (2017) Biodiversity of Coleoptera. In: Footitt RG, Adler PH (Eds), *Insect Biodiversity*. John Wiley & Sons, Ltd, Chichester, UK, pp. 337–417. <https://doi.org/10.1002/9781118945568.ch11>
- Boudinot BE, Moosdorf OTD, Beutel RG, Richter A (2021) Anatomy and evolution of the head of *Dorylus helvolus* (Formicidae: Dorylinae): Patterns of sex- and caste-limited traits in the sausagefly and the driver ant. *Journal of Morphology* 282(11): 1616–1658. <https://doi.org/10.1002/jmor.21410>
- Boudinot BE, Fikáček M, Lieberman ZE, Kusy D, Bocak L, McKenna DD, Beutel RG (2023) Systematic bias and the phylogeny of Coleoptera – A response to Cai et al. (2022) following the responses to Cai et al. (2020). *Systematic Entomology* 48(2): 223–232. <https://doi.org/10.1111/syen.12570>
- Böving AG, Craighead FC (1931) An illustrated synopsis of the principal larval forms of the order Coleoptera. *Entomologica Americana (N S)* 11: i–viii, 1–351. <https://doi.org/10.5962/bhl.title.6818>
- Brunke AJ, Chatzimanolis S, Schillhammer H, Solodovnikov A (2016) Early evolution of the hyperdiverse rove beetle tribe Staphylinini (Coleoptera: Staphylinidae: Staphylininae) and a revision of its higher classification. *Cladistics* 32(4): 427–451. <https://doi.org/10.1111/cla.12139>
- Büsse S, Tröger H-L, Gorb SN (2021) The toolkit of a hunter – functional morphology of larval mouthparts in a dragonfly. *Journal of Zoology* 315(4): 247–260. <https://doi.org/10.1111/jzo.12923>
- Cai CY, Wang YL, Liang L [sic](should be Lü L), Yin ZW, Thayer MK, Newton AF, Zhou YL (2019) Congruence of morphological and molecular phylogenies of the rove beetle subfamily Staphylininae (Coleoptera: Staphylinidae). *Scientific Reports* 9(15137): 1–11. <https://doi.org/10.1038/s41598-019-51408-1>
- Chani-Posse MR, Brunke AJ, Chatzimanolis S, Schillhammer H, Solodovnikov A (2018) Phylogeny of the hyper-diverse rove beetle subtribe Philonthina with implications for classification of the tribe Staphylinini (Coleoptera: Staphylinidae). *Cladistics* 34(1): 1–40. <https://doi.org/10.1111/cla.12188>
- Chatzimanolis S, Cohen IM, Schomann A, Solodovnikov A (2010) Molecular phylogeny of the mega-diverse rove beetle tribe Staphylinini (Insecta, Coleoptera, Staphylinidae). *Zoologica Scripta* 39(5): 436–449. <https://doi.org/10.1111/j.1463-6409.2010.00438.x>
- Chaudonneret J (1950) La morphologie céphalique de *Thermobia domestica* (Packard) (Insecte Aptérygote Thysanoure). *Annales des Sciences Naturelles, Zoologie (ser. 11)* 12: 145–302. <https://gallica.bnf.fr/ark:/12148/bpt6k3065959h/f181.item.r=ent>
- Clarke DJ (2018) Systematics, natural history, and evolution of the saw-lipped rove beetles (Euaesthetinae): progress and prospects for future research. In: Betz O, Irmeler U, Klimaszewski J (Eds), *Biology of Rove Beetles (Staphylinidae)*. Springer, Cham, pp. 81–114. https://doi.org/10.1007/978-3-319-70257-5_6
- Clarke DJ, Grebennikov VV (2009) Monophyly of Euaesthetinae (Coleoptera: Staphylinidae): phylogenetic evidence from adults and larvae, review of austral genera, and new larval descriptions. *Systematic Entomology* 34(2): 346–397. <https://doi.org/10.1111/j.1365-3113.2009.00472.x>
- Coulcher JF, Telford MJ (2013) Comparative gene expression supports the origin of the incisor and molar process from a single endite in the mandible of the red flour beetle *Tribolium castaneum*. *EvoDevo* 4(1): 1–12. <https://doi.org/10.1186/2041-9139-4-1>
- Crowson RA (1981) *The Biology of the Coleoptera*. Academic Press, London. <https://doi.org/10.1016/C2013-0-07304-5>
- Dressler C, Beutel RG (2010) The morphology and evolution of the adult head of Adephaga (Insecta: Coleoptera). *Arthropod Systematics & Phylogeny* 68(2): 239–287. <https://doi.org/10.3897/asp.68.e31730>
- Evans MEG (1964) A comparative account of the feeding methods of the beetles *Nebria brevicollis* (F.) (Carabidae) and *Philonthus decorus* (Grav.) (Staphylinidae). *Transactions of the Royal Society of Edinburgh* 66(5): 91–109. <https://doi.org/10.1017/S0080456800023395>
- Gnaspini P, Antunes-Carvalho C, Newton AF, Leschen RAB (2017) Show me your tenent setae and I tell you who you are – Telling

- the story of a neglected character complex with phylogenetic signals using Leiodidae (Coleoptera) as a case study. *Arthropod Structure and Development* 46(4): 662–685. <https://doi.org/10.1016/j.asd.2017.06.004>
- Grebennikov VV, Newton AF (2009) Good-bye Scydmaenidae, or why the ant-like stone beetles should become megadiverse Staphylinidae sensu latissimo (Coleoptera). *European Journal of Entomology* 106(2): 275–301. <https://doi.org/10.14411/eje.2009.035>
- Gusarov VI (2018) Phylogeny of the family Staphylinidae based on molecular data: A review. In: Betz O, Irmeler U, Klimaszewski J (Eds), *Biology of Rove Beetles (Staphylinidae)*. Springer International Publishing, Cham, pp. 7–25. https://doi.org/10.1007/978-3-319-70-257-5_2
- Hammer Ø, Harper DAT, Ryan PD (2001) PAST: Paleontological Statistics Software Package for Education and Data Analysis. *Current Science* 4(1): 1–9. https://palaeo-electronica.org/2001_1/past/past.pdf
- Hansen M (1997) Phylogeny and classification of the staphyliniform beetle families (Coleoptera). *Biologiske Skrifter, Det Kongelige Danske Videnskaberne Selskab* (48): 1–339. https://www.royalacademy.dk/Publications/Low/393_Hansen,%20Michael.pdf
- Hao YN, Sun YX, Liu CZ (2020) Functional morphology of the mouthparts of lady beetle *Hippodamia variegata* (Coleoptera: Coccinellidae), with reference to their feeding mechanism. *Zoomorphology* 139(2): 199–212. <https://doi.org/10.1007/s00435-019-00474-0>
- Hörschemeyer T, Goebels J, Weidemann G, Faber C, Haase A (2006) The head morphology of *Ascioplaga mimeta* (Coleoptera: Archostemata) and the phylogeny of Archostemata. *European Journal of Entomology* 103(2): 409–423. <https://doi.org/10.14411/eje.2006.055>
- Hunt T, Bergsten J, Levkancova Z, Papadopoulou A, St. John O, Wild R, Hammond PM, Ahrens D, Balke M, Caterino MS, Gómez-Zurita J, Ribera I, Barraclough TG, Bocakova M, Bocak L, Vogler AP (2007) A comprehensive phylogeny of beetles reveals the evolutionary origins of a superradiation. *Science* 318(5858): 1913–1916. <https://doi.org/10.1126/science.1146954>
- Jaloszynski P (2012a) Adults of European ant-like stone beetles (Coleoptera: Staphylinidae: Scydmaeninae) *Scydmaenus tarsatus* Müller & Kunze and *Scydmaenus hellwigii* (Herbst) prey on soft-bodied arthropods. *Entomological Science* 15(1): 35–41. <https://doi.org/10.1111/j.1479-8298.2011.00479.x>
- Jaloszynski P (2012b) Observations on cannibalism and feeding on dead arthropods in *Scydmaenus tarsatus* (Coleoptera: Staphylinidae: Scydmaeninae). *Genus* 23(1): 25–31. http://www.cassidae.uni.wroc.pl/Jaloszynski_Behaviour%20of%20Scydmaenus.pdf
- Jaloszynski P (2014) Phylogeny of a new supertribe Cephenniinae with generic review of Eutheini and description of a new tribe Marcepianiini (Coleoptera: Staphylinidae: Scydmaeninae). *Systematic Entomology* 39(1): 159–189. <https://doi.org/10.1111/syen.12044>
- Jaloszynski P (2018) Biology of acarophagous Scydmaeninae. In: Betz O, Irmeler U, Klimaszewski J (Eds), *Biology of Rove Beetles (Staphylinidae)*. Springer, Cham, pp. 285–298. https://doi.org/10.1007/978-3-319-70257-5_12
- Jaloszynski P, Beutel RG (2012) Functional morphology and evolution of specialized mouthparts of Cephenniini (Insecta, Coleoptera, Staphylinidae, Scydmaeninae). *Arthropod Structure and Development* 41(6): 593–607. <https://doi.org/10.1016/j.asd.2012.07.002>
- Jaloszynski P, Luo X-Z, Beutel RG (2020) Profound head modifications in *Claviger testaceus* (Pselaphinae, Staphylinidae, Coleoptera) facilitate integration into communities of ants. *Journal of Morphology* 281(9): 1072–1085. <https://doi.org/10.1002/jmor.21232>
- Jenkins MF (1960) On the method by which *Stenus* and *Dianous* (Coleoptera: Staphylinidae) return to the banks of a pool. *Transactions of the Royal Entomological Society of London* 112(1): 1–14. <https://doi.org/10.1111/j.1365-2311.1960.tb00487.x>
- Karolyi F, Gorb SN, Krenn HW (2009) Pollen grains adhere to the moist mouthparts in the flower visiting beetle *Cetonia aurata* (Scarabaeidae, Coleoptera). *Arthropod-Plant Interactions* 3: 1–8. <https://doi.org/10.1007/s11829-008-9052-5>
- Karolyi F, Hansal T, Krenn HW, Colville JF (2016) Comparative morphology of the mouthparts of the megadiverse South African monkey beetles (Scarabaeidae: Hopliini): feeding adaptations and guild structure. *PeerJ* 4: e1597 [22pp]. <https://doi.org/10.7717/peerj.1597>
- Klimaszewski J, Morency M-J, Labrie P, Séguin A, Langor D, Work T, Bourdon C, Thiffault E, Paré D, Newton AF, Thayer MK (2013) Molecular and microscopic analysis of the gut contents of abundant rove beetle species (Coleoptera, Staphylinidae) in the boreal balsam fir forest of Quebec, Canada. *ZooKeys* 353: 1–24. <https://doi.org/10.3897/zookeys.353.5991>
- Klingenberg CP (2011) MorphoJ: an integrated software package for geometric morphometrics. *Molecular Ecology Resources* 11(2): 353–357. <https://doi.org/10.1111/j.1755-0998.2010.02924.x>
- Koerner L, Gorb SN, Betz O (2012) Functional morphology and adhesive performance of the stick-capture apparatus of the rove beetles *Stenus* spp. (Coleoptera, Staphylinidae). *Zoology* 115(2): 117–127. <https://doi.org/10.1016/j.zool.2011.09.006>
- Kölsch G, Betz O (1998) Ultrastructure and function of the adhesion-capture apparatus of *Stenus* species (Coleoptera, Staphylinidae). *Zoomorphology* 118: 263–272. <https://doi.org/10.1007/s004-350050075>
- Krenn HW (2019) Form and function of insect mouthparts. In: Krenn HW (Ed.), *Insect mouthparts*. *Zoological Monographs* 5; Springer Nature, Cham, Switzerland, pp. 9–46. https://doi.org/10.1007/978-3-030-29654-4_2
- Krenn HW, Pernstich A, Messner T, Hannappel U, Paulus HF (2002) Kirschen als Nahrung des männlichen Hirschkäfers, *Lucanus cervus* (Linnaeus 1758) (Lucanidae: Coleoptera). *Entomologische Zeitschrift* 112(6): 165–170.
- Kubiak M, Beckmann F, Friedrich F (2015) The adult head of the annulipalpal caddisfly *Philopotamus ludificatus* McLachlan, 1878 (Philopotamidae), mouthpart homologies, and implications on the ground plan of Trichoptera. *Arthropod Systematics & Phylogeny* 73(3): 351–384. <https://doi.org/10.3897/asp.73.e31824>
- Kypke JL (2018) Phylogenetics of the world's largest beetle family (Coleoptera: Staphylinidae): A methodological exploration. Ph.D. thesis, University of Copenhagen, vi + 106 pp.
- Lawrence JF, Newton AF (1982) Evolution and classification of beetles. *Annual Review of Ecology and Systematics*. 13: 261–290. <https://doi.org/10.1146/annurev.es.13.110182.001401>
- Lawrence JF, Ślipiński A, Seago AE, Thayer MK, Newton AF, Marvaldi AE (2011) Phylogeny of the Coleoptera based on morphological characters of adults and larvae. *Annales Zoologici* 61(1): 1–217. <https://doi.org/10.3161/000345411X576725>
- Leschen RAB, Allen RT (1988) Immature stages, life histories and feeding mechanisms of three *Oxyporus* spp. (Coleoptera: Staphylinidae: Oxyporinae). *The Coleopterists Bulletin* 42(4): 321–333. Available from: <http://www.jstor.org/stable/4008460>.
- Leschen RAB, Newton AF (2003) Larval description, adult feeding behaviour, and phylogenetic placement of *Megalopinus* (Coleoptera: Staphylinidae). *Coleopterists Bulletin* 57(4): 469–493. <https://doi.org/10.1649/586>

- Lipkow E (1997) Zur Biologie der Ernährung, Fortpflanzung, Wirtswahl und Konkurrenzvermeidung von *Oxyporus*-Arten (Coleoptera: Staphylinidae). Faunistisch-Ökologische Mitteilungen 7: 297–305. https://www.zobodat.at/publikation_articles.php?id=410656
- Liu C-T, Tong X (2023) Functional morphology of the mouthparts of longhorn beetle adult *Psacotheta hilaris* (Coleoptera: Cerambycidae) and sensilla comparisons between the sexes. Arthropod Structure & Development 77: 101312. <https://doi.org/10.1016/j.asd.2023.101312>
- Liu Z, Yu W, Wu X (2019) Ultrastructure of sensilla on the maxillary and labial palps of three species (Coleoptera: Staphylinidae: Staphylininae). Entomological Research 49(8): 386–397. <https://doi.org/10.1111/1748-5967.12389>
- Liu Y, Tihelka E, Thayer MK, Newton AF, Huang D, Tian L, Cai C (2021) A transitional fossil sheds light on the early evolution of the Staphylinine group of rove beetles (Coleoptera: Staphylinidae). Journal of Systematic Palaeontology 19(4): 321–332. <https://doi.org/10.1080/14772019.2021.1917705>
- Lü L, Cai C-Y, Zhang X, Newton AF, Thayer MK, Zhou H-Z (2020) Linking evolutionary mode to palaeoclimate change reveals rapid radiations of staphylinoid beetles in low-energy conditions. Current Zoology 66(4): 435–444. <https://doi.org/10.1093/cz/zoz053>
- Luo X-Z, Hlaváč P, Jalozyński P, Beutel RG (2021) In the twilight zone – The head morphology of *Bergrothia saulcyi* (Pselaphinae, Staphylinidae, Coleoptera), a beetle with adaptations to endogean life but living in leaf litter. Journal of Morphology 282(8): 1170–1187. <https://doi.org/10.1002/jmor.21361>
- Maddison WP, Maddison DR (2019) Mesquite: a modular system for evolutionary analysis. Version 3.61. <http://www.mesquiteproject.org>
- McKenna DD, Farrell BD, Caterino MS, Farnum CW, Hawks DC, Maddison DR, Seago AE, Short AEZ, Newton AF, Thayer MK (2015) Phylogeny and evolution of Staphyliniformia and Scarabaeiformia: Forest litter as a stepping stone for diversification of nonphytophagous beetles. Systematic Entomology 40(1): 35–60. <https://doi.org/10.1111/syen.12093>
- McKenna DD, Shin S, Ahrens D, Balke M, Beza-Beza C, Clarke DJ, Donath A, Escalona HE, Friedrich F, Letsch H, Liu S, Maddison D, Mayer C, Misof B, Murin PJ, Niehuis O, Peters RS, Podsiadlowski L, Pohl H, Scully ED, Yan E V., Zhou X, Ślipiński A, Beutel RG (2019) The evolution and genomic basis of beetle diversity. Proceedings of the National Academy of Sciences 116(49): 24729–24737. <https://doi.org/10.1073/pnas.1909655116>
- Mickoleit G (1971) Das Exoskelet von *Notiothauma reedi* MacLachlan, ein Beitrag zur Morphologie und Phylogenie der Mecoptera (Insecta). Zeitschrift für Morphologie der Tiere 69(4): 318–362. <https://doi.org/10.1007/BF00375808>
- Naomi S-I (1988a) Comparative morphology of the Staphylinidae and the allied groups (Coleoptera, Staphylinodea). III. Antennae, labrum and mandibles. Kontyû 56(1): 67–77.
- Naomi S-I (1988b) Comparative morphology of the Staphylinidae and the allied groups (Coleoptera, Staphylinodea). IV. Maxillae and labium. Kontyû 56(2): 241–250.
- Naomi S-I (1989) Comparative morphology of the Staphylinidae and the allied groups (Coleoptera, Staphylinodea). VIII. Thoracic legs. Japanese Journal of Entomology 57: 269–277.
- Newton AF (1984) Mycophagy in Staphylinodea (Coleoptera). In: Wheeler Q, Blackwell M (Eds), Fungus Insect Relationships: Perspectives in Ecology and Evolution. Columbia University Press, New York, pp. 302–353.
- Newton AF (2022) StaphBase: Staphyliniformia world catalog database (version Aug 2022): Staphylinodea, Hydrophiloidea, Histeroidea (except Histeridae). In: Bánki O, Roskov Y et al. (Eds). Catalogue of Life Checklist (Aug 2022). Species 2000: Naturalis, Leiden, the Netherlands. <https://www.catalogueoflife.org>. <https://doi.org/10.48580/dfqc-3gk>
- Okuzono M, Tokuda M (2022) Establishment of a laboratory-rearing technique for the rove beetle *Anotylus amicus* (Coleoptera: Staphylinidae) with investigations of its life cycle, behavior and morphological variations. Entomological Science 25(4): e12530. <https://doi.org/10.1111/ens.12530>
- Orousset J (1988) Faune de Madagascar, 71. Insectes, Coléoptères: Staphylinidae Euaesthetinae. Muséum National d'Histoire Naturelle, Paris. 208 pp. <https://www.biodiversitylibrary.org/item/308265>
- Posit team (2023). RStudio: Integrated Development Environment for R. Posit Software, PBC, Boston, MA. <http://www.posit.co>
- R Core Team (2023). R: A Language and Environment for Statistical Computing. R Foundation for Statistical Computing, Vienna, Austria. <https://www.R-project.org>
- Rambaut A, Drummond, AJ (2016) FigTree v1. 4.4. Institute of Evolutionary Biology, University of Edinburgh. Accessed from <https://github.com/rambaut/figtree/releases>.
- Randolf S, Zimmermann D, Aspöck U (2017) Head anatomy of adult *Coniopteryx pygmaea* Enderlein, 1906: Effects of miniaturization and the systematic position of Coniopterygidae (Insecta: Neuroptera). Arthropod Structure and Development 46(2): 304–322. <https://doi.org/10.1016/j.asd.2016.12.004>
- Remillet M (1969) Observations biologiques sur plusieurs Coléoptères hypogés de France. Annales de Spéléologie 24(1): 183–186. http://horizon.documentation.ird.fr/exl-doc/pleins_textes/pleins_textes_5/b_fdi_06-07/08054.pdf
- Richter S, Edgecombe GD, Wilson GDF (2002) The lacinia mobilis and similar structures – A valuable character in arthropod phylogenetics? Zoologischer Anzeiger 241(4): 339–361. <https://doi.org/10.1078/0044-5231-00083>
- Rohlf FJ (2015) The tps series of software. Hystrix 26(1): 9–12. <https://doi.org/10.4404/hystrix-26.1-11264>
- Schneeberg K, Beutel RG (2011) The adult head structures of Tipulomorpha (Diptera, Insecta) and their phylogenetic implications. Acta Zoologica 92(4): 316–343. <https://doi.org/10.1111/j.1463-6395.2010.00463.x>
- Schomann AM, Solodovnikov A (2017) Phylogenetic placement of the austral rove beetle genus *Hyperomma* triggers changes in classification of Paederinae (Coleoptera: Staphylinidae). Zoologica Scripta 46(3): 336–347. <https://doi.org/10.1111/zsc.12209>
- Snodgrass RE (1993) Principles of Insect Morphology. Cornell University Press, Ithaca and London, 667 pp. <https://doi.org/10.7591/9781501717918>
- Stocker B, Barthold S, Betz O (2022) Mouthpart ecomorphology and predatory behaviour in selected rove beetles of the “Staphylinine Group” (Coleoptera: Staphylinidae: Staphylininae, Paederinae). Insects 13(8): 667. <https://doi.org/10.3390/insects13080667>
- Stork NE (1980) A scanning electron microscope study of tarsal adhesive setae in the Coleoptera. Zoological Journal of the Linnean Society 68(3): 173–306. <https://doi.org/10.1111/j.1096-3642.1980.tb01121.x>
- Thayer MK (2016) Staphylinidae Latreille, 1802. In: Beutel RG, Leschen RAB (Eds), Handbook of Zoology, Arthropoda: Insecta; Coleoptera, Beetles. Vol. 1. Morphology and Systematics (Archoste-

- mata, Adephaga, Myxophaga, Polyphaga partim). 2nd edition. De Gruyter, Berlin, pp. 394–442.
- Thayer MK, Newton AF, Chatzimanolis S (2012) *Prosolierius*, a new mid-Cretaceous genus of Solieriinae (Coleoptera: Staphylinidae) with three new species from Burmese amber. *Cretaceous Research* 34: 124–134. <https://doi.org/10.1016/j.cretres.2011.10.010>
- Tihelka E, Thayer MK, Newton AF, Cai C (2020) New data, old story: Molecular data illuminate the tribal relationships among rove beetles of the subfamily Staphylininae (Coleoptera: Staphylinidae). *Insects* 11(3): 164. <https://doi.org/10.3390/insects11030164>
- Weide D, Betz O (2009) Head morphology of selected Staphylinoida (Coleoptera: Staphyliniformia) with an evaluation of possible groundplan features in Staphylinidae. *Journal of Morphology* 270(12): 1503–1523. <https://doi.org/10.1002/jmor.10773>
- Weide D, Betz O (2014) Kopfmorphologische Untersuchungen von Sporenfressern und Nicht-Sporenfressern bei Kurzflügelkäfern (Staphylinidae, Coleoptera) mittels Synchrotron-Mikrotomographie. *Mitteilungen der Deutschen Gesellschaft für allgemeine und angewandte Entomologie* 19: 173–178.
- Weide D, Thayer MK, Betz O (2014) Comparative morphology of the tentorium and hypopharyngeal-premental sclerites in sporophagous and non-sporophagous adult Aleocharinae (Coleoptera: Staphylinidae). *Acta Zoologica* 95(1): 84–110. <https://doi.org/10.1111/azo.12011>
- Weide D, Thayer MK, Newton AF, Betz O (2010) Comparative morphology of the head of selected sporophagous and non-sporophagous Aleocharinae (Coleoptera: Staphylinidae): Musculature and hypopharynx-prementum complex. *Journal of Morphology* 271(8): 910–931. <https://doi.org/10.1002/jmor.10841>
- Weihmann T, Kleinteich T, Gorb SN, Wipfler B (2015) Functional morphology of the mandibular apparatus in the cockroach *Periplaneta americana* (Blattodea: Blattellidae) – A model species for omnivore insects. *Arthropod Systematics & Phylogeny* 73(3): 477–488. <https://doi.org/10.3897/asp.73.e31833>
- Wenk P (1953) Der Kopf von *Ctenocephalus canis* (Curt.) (Aphanipitera). *Zoologische Jahrbücher Abteilung für Anatomie und Ontogenie der Tiere* 73: 103–164. [Doctoral dissertation, Eberhard-Karls-Universität zu Tübingen]
- Wheeler QD, Miller KB (2005) Slime-mold beetles of the genus *Agathidium* Panzer in North and Central America, Part I. Coleoptera: Leiodidae. *Bulletin of the American Museum of Natural History* (290): 1–95. <http://hdl.handle.net/2246/458>
- Wilhelmi AP, Krenn HW (2012) Elongated mouthparts of nectar-feeding Meloidae (Coleoptera). *Zoomorphology* 131(4): 325–337. <https://doi.org/10.1007/s00435-012-0162-3>
- Wipfler B, Machida R, Müller BR, Beutel RG (2011) On the head morphology of Grylloblattodea (Insecta) and the systematic position of the order, with a new nomenclature for the head muscles of Dicondylia. *Systematic Entomology* 36(2): 241–266. <https://doi.org/10.1111/j.1365-3113.2010.00556.x>
- Yavorskaya MI, Beutel RG, Polilov AA (2017) Head morphology of the smallest beetles (Coleoptera: Ptiliidae) and the evolution of sporophagy within Staphyliniformia. *Arthropod Systematics & Phylogeny* 75(3): 417–434. <https://doi.org/10.3897/asp.75.e31916>
- Yavorskaya MI, Hörschemeyer T, Beutel RG (2018a) The head morphology of *Micromalthus debilis* (Coleoptera: Micromalthidae) – An archostematan beetle with an unusual morphology and a unique life cycle. *Arthropod Systematics & Phylogeny* 76(3): 475–486. <https://doi.org/10.3897/asp.76.e31964>
- Yavorskaya MI, Jałoszyński P, Beutel RG (2023) A unique case of commensalism: The beaver beetle *Platypsyllus castoris* (Leiodidae, Coleoptera) and its morphological adaptations. *Journal of Morphology* 284(1). <https://doi.org/10.1002/jmor.21532>
- Yavorskaya MI, Anton E, Jałoszyński P, Polilov A, Beutel RG (2018b) Cephalic anatomy of Sphaeriidae and a morphology-based phylogeny of the suborder Myxophaga (Coleoptera). *Systematic Entomology* 43(4): 777–797. <https://doi.org/10.1111/syen.12304>
- Yin Z, Zhou D, Cai C, Huang D, Engel MS (2019) *Pangusyndicus* gen. nov.: a new mid-Cretaceous scydmaenine with reduced antennae and prothoracic gland (Coleoptera, Staphylinidae [sic]: Scydmaeninae). *Journal of Systematic Palaeontology* 17(13): 1129–1141. <https://doi.org/10.1080/14772019.2018.1504129>
- Zhang SQ, Che LH, Li Y, Liang D, Pang H, Ślipiński A, Zhang P (2018) Evolutionary history of Coleoptera revealed by extensive sampling of genes and species. *Nature Communications* 9: 205 [11 pp.]. <https://doi.org/10.1038/s41467-017-02644-4>
- Żyła D, Bogri A, Heath TA, Solodovnikov A (2021) Total-evidence analysis resolves the phylogenetic position of an enigmatic group of Paederinae rove beetles (Coleoptera: Staphylinidae). *Molecular Phylogenetics and Evolution* 157: 10759 [11 pp.]. <https://doi.org/10.1016/j.ympev.2020.107059>
- Żyła D, Solodovnikov A (2020) Multilocus phylogeny defines a new classification of Staphylininae (Coleoptera, Staphylinidae), a rove beetle group with high lineage diversity. *Systematic Entomology* 45(1): 114–127. <https://doi.org/10.1111/syen.12382>
- Żyła D, Yamamoto S, Wolf-Schwenninger K, Solodovnikov A (2017) Cretaceous origin of the unique prey-capture apparatus in mega-diverse genus: Stem lineage of Steninae rove beetles discovered in Burmese amber. *Scientific Reports* 7(45904): 1–15. <https://doi.org/10.1038/srep45904>

Supplementary Material 1

Figure S1

Authors: Spiessberger EL, Newton AF, Thayer MK, Betz O (2024)

Data type: .pdf

Explanation notes: Correlation between log-transformed PC 2 as obtained from the analysis of the geometric morphometric shape of the mandibles (cf. Fig. 13) and the log-transformed inlever/outlever ratio of the mandible (cf. Table S4). Each dot represents a different species, color-coded by subfamily or group. Species numbers are explained in Table 1. r = Pearson's correlation coefficient. $** = p < 0.01$. The positive correlation also holds true for an analysis using phylogenetic independent contrasts ($r = 0.4^*$).

Copyright notice: This dataset is made available under the Open Database License (<http://opendatacommons.org/licenses/odbl/1.0>). The Open Database License (ODbL) is a license agreement intended to allow users to freely share, modify, and use this dataset while maintaining this same freedom for others, provided that the original source and author(s) are credited.

Link: <https://doi.org/10.3897/asp.82.e114508.suppl1>

Supplementary Material 2

Tables S1–S4

Authors: Spiessberger EL, Newton AF, Thayer MK, Betz O (2024)

Data type: .pdf

Explanation notes: **Table S1.** Character matrix used in the character mapping analysis (Fig. 12). See section 3.2. for the characters and character state number codes. — **Table S2.** Principal components 1 and 2 of the species used in the analysis of the geometric morphometric shape of the mandibles. — **Table S3.** Eigenvalues, variance, and cumulative percentages of the first two principal components extracted from the analysis of the geometric morphometric shape of the mandibles. — **Table S4.** Inlever and outlever values [μm] and their quotient in ascending order of quotients.

Copyright notice: This dataset is made available under the Open Database License (<http://opendatacommons.org/licenses/odbl/1.0>). The Open Database License (ODbL) is a license agreement intended to allow users to freely share, modify, and use this dataset while maintaining this same freedom for others, provided that the original source and author(s) are credited.

Link: <https://doi.org/10.3897/asp.82.e114508.suppl2>